2018-01-01

Evaluation Of Recycled Gypsum Application Dosages To Enhance The Water Infiltration Rate At Water Retention Ponds

Jorge Luis Navarrete
University of Texas at El Paso, jorgenavarrete7257@yahoo.com

EVALUATION OF RECYCLED GYPSUM APPLICATION DOSAGES TO ENHANCE THE WATER INFILTRATION RATE AT WATER RETENTION PONDS

JORGE LUIS NAVARRETE CAMPOS

Master's Program in Civil Engineering

APPROVED :

Vivek Tandon, Ph.D., Chair

Anthony Tarquin, Ph.D.

Lixin Jin, Ph.D.

Charles H. Ambler, Ph.D.
Dean of the Graduate School

DEDICATION

Dedicated to God, parents, family, and friends.

EVALUATION OF RECYCLED GYPSUM APPLICATION DOSAGES TO ENHANCE THE WATER INFILTRATION RATE AT WATER RETENTION PONDS

by

JORGE LUIS NAVARRETE CAMPOS, B.S.C.E

THESIS

Presented to the Faculty of the Graduate School of

The University of Texas at El Paso

in Partial Fulfillment

of the Requirements

for the Degree of

MASTER OF SCIENCE

Department of Civil Engineering

THE UNIVERSITY OF TEXAS AT EL PASO

December 2018

ACKNOWLEDGMENTS

I want to express my sincere gratitude to my advisor committee chairman Dr. Vivek Tandon for granting me the opportunity to work under this research project. I give thanks to his support, confidence, mentorship, and knowledge resulting in the completion of the thesis presented herein. It was an honor and privilege to be part of his research team.

Besides my advisor, I would like to thank the other members of my thesis committee Dr. Anthony Tarquin and Dr. Lixin Jin. I am very grateful to both professors for their insight, feedback and keeping their laboratory always open for me. Also, my sincere appreciation to other UTEP professors who provided access to their laboratory and volunteered their time and knowledge including Dr. Michael Lyubchenko, Dr. Shane Walker, and Dr. Reza Ashtiani. Also, I must acknowledge other students and staff: Hans, Jose Garibay, Angel, Jesus, Ubaldo, Hector, Francisco, Madai, Shahrouz, and Daniela for their help through different phases of the project.

I gratefully acknowledge El Paso Water for their financial support on this project. Special thanks to Martin Noriega from El Paso Water and Gilbert Garcia from El Paso Recycling for their constant attention, time and many other attributions in accomplishing the project.

I would finally like to express my deepest appreciation and gratitude my parents Jose and Hortensia Navarrete and my siblings for their constant love and everlasting support. Finally, to my lovely niece Lenalee, for being the light of joy to our family.

EXECUTIVE SUMMARY

The retention ponds play central role for efficient collection, removal, and drainage of rainfall runoff from surrounding streets to minimize flooding and damage. However, low percolating retention ponds may result in an extended ponding of water, abundance bacteria accumulations, mosquito breeding, environmental hazards, among others. The presence of clayey soils and soil sodicity reduces infiltration rates of retention ponds. To enhance the infiltration rate of ponds, it is proposed to use recycled gypsum (RG), as a soil amendment in retention ponds consisting of clayey soils to enhance low infiltration rates.

To evaluate the influence of RG in clayey soils as a soil conditioner, the following approach was adopted in this study:

1. To evaluate influence of gypsum in enhancing infiltration rates, the double ring infiltrometer was utilized on the field and the falling head method in the laboratory.
2. To determine the optimum gypsum dosage, various application methods were employed to maximize benefits.
3. To identify the influence of soil and RG mineralogy, X-Ray Diffraction (XRD) technique was emplyed.
4. To identify and evaluate elements coming out at the bottom of the pond, different application cycles were employed and tests were performed using falling head permeability test protocol.
5. To evaluate the transportation of leaching metals to groundwater, the Risk-Based Corrective Action (RBCA) toolkit was used to identify movement of metals after RG application.
6. To simulate diffusion of RG in the water retention pond, a small-scale model was developed and tested.

A total of four soils were collected from the city of El Paso, TX. One soil was collected from the “Upper Valley” region, and the other three were collected from local retention ponds in

the area. These retention ponds are labeled for this study as Interchange, Westbound, Site pond, and Upper Valley soils based on their location. El Paso Water (EPW), had previously applied RG dosages to Westbound and Site pond before this study was conducted. The Upper Valley, Interchange, Westbound, and Site pond soils were classified as CL, CL, SM, and SM, respectively based on the Unified Soil Classification System (USCS). Both, Upper Valley and Interchange soil conditions were determined to be sodic and Westbound and Site soils as normal.

The double ring infiltrometer was utilized at the Interchange pond to evaluate the influence of RG using different dosages and application methods. The gypsum application methods consisted of spreading gypsum on top of the soil surface (GSS) measured in tons/acre and mixing gypsum in distilled water (DDW), measured in percent of concentrated, saturated solution dose. Each application method was performed in triplicates leading to a total of 39 test. In the GSS application method, the initial (zero RG dosage) infiltration rates for the inner and outer ring were < 0.1 in./h, and it was enhanced up to 0.35 in./h and 0.68 in./h for the inner and outer ring, respectively at 17.5 ton/acre gypsum dosage. Thus, enhancing the infiltration rate of the inner and outer ring by approximately 750 and 1,060 %, respectively. As for the DDW application method, the infiltration rate was linearly increased with dosage increase in increments of 25 %. The maximum average infiltration rate observed in the inner ring and outer ring was 0.40 in./h and 0.52 in./h, respectively. This method enhanced the infiltration rate approximately 550 % for the inner ring and 1,230 % for the outer ring.

The falling head test was used to determine the saturated hydraulic conductivity (K_{sat}) in response to different solutions. These samples were prepared at approximately 90 ± 2 lb/ft^3 dry density and infiltration solutions were prepared by dissolving gypsum in deionized water (DI) and in collected water from the Westbound pond identified as pond water (PW). These saturated solutions mixed in DI and PW are denoted as DDI100 and DPW100. Subsequently, DDI100 and DPW100 were diluted with DI and PW at different percentages by volume. For example, a dose of DD75 means that 75 % DDI100 and 25 % DI was mixed. Similarly, for a DPW25 dose, 25 % of DPW100 was mixed with 75 % PW.

Falling head permeability tests using DDI and DPW method showed a linear trend in all four soils. Interchange and Upper Valley soils K_{sat} value increased for both application methods, as higher concentrated gypsum solution dosages were applied. However, K_{sat} values of Interchange soil were higher than Upper Valley even though both soils were characterized as CL in sodic conditions. This phenomenon can be caused by factors such as lower: cation exchange capacity, specific surface area, plastic index, among others. For sandy soils (Westbound and Site pond soils), gypsum applications had minimal effect on K_{sat} values as compared to Upper Valley, and Interchange soils due to previous gypsum application and sandy soils do not have a high negatively net charge in comparison to clayey soils. The K_{sat} incremental value for the DDI and DPW methods in all four soils with increasing of RG dosages were:

Upper Valley	**Interchange**	**Westbound**	**Site**
• DDI: 693 %	• DDI: 68 %	• DDI: 1 %	• DDI: 6 %
• DPW: 443 %	• DPW: 215 %	• DPW: 6 %	• DPW: 8 %

The gypsum application method was studied using the falling head tests with leaching solutions at incrementally increased dosages as described in the previous paragraph. Additional gypsum application methods were employed to compare their influence on the saturated hydraulic conductivity obtained from DDI and DPW methods. Interchange soil was selected for analysis because the site has not been treated with gypsum and is more accessible than the Upper Valley soil in terms of higher infiltration rates and fewer complications in saturating soil samples prior to permeability measurements.

The gypsum application methods employed to determine the hydraulic conductivity were:

1. Gypsum dissolved in deionized water (DDI)
2. Gypsum dissolved in pond water (DPW)
3. Mixed gypsum in soil by weight at 10 %, 20 %, 30 %, 40 %, and 50 % (MGS)
4. Gypsum spread at the soil surface at the rate of 3.5, 6.9, 10.4, 13.9, 17.3, 20.8, 24.3 tons/acre (GSS).

The K_{sat} values in all application methods linearly incremented as higher RG applications were employed. The incremental K_{sat} value in (%) for the interchange soil for the different gypsum application approach was:

- DDI: 68 %
- DPW: 215 %
- MGS: 337 %
- GSS: 32 %

It was noticed that MGS method provided a higher incremental in K_{sat} as compared to other methods. Although, MGS K_{sat} value grew much higher due to an overall average dry density reduction of 27 %, allowing more conductive paths for water to flow through. GSS delivered the lowest increase in K_{sat} values. Since it is to expected that calcium would increase the permeability of clayey soils, GSS application approach did not have enough time for calcium to solubilize in DI water to effectively provide the calcium needed for clayey particles to flocculate and provide more spaces for water to flow through.

To evaluate contaminants that may leach with use of RG, the leached solutions were collected after "continuous ponding" application and tested to simulate retention pond experiences. Discharged leachate outflow was collected in 3 cycles: 30 mL, 80 mL, and 130 mL, and specimens were sliced in three equal parts (top, middle, and bottom) after the completion of each cycle. Collected solutions at the end of soil column, top, and bottom sliced sections were analyzed in the Inductively Coupled Plasma Spectrophotometer (ICP). As for DI applications in the upper valley soil, Ca^{2+} concentrations in collected, bottom and top sections were low (<200 mg/L) and low sodium concentrations as (< 600 mg/L). After RG applications, Ca^{2+} concentrations for the top and bottom sections increased to 350 mg/L, and sodium concentrations increased to more than 700 mg/L for both DDI100 and DPW100 application methods. This experiment showed higher calcium concentration in the top and bottom sections and higher sodium concentrations of the collected water as opposed to DI applications only. Also, the electric conductivity (EC) was measured for

the collected water for DI, DPW100, and DDI100 in cycles of 30 mL, 80 mL, and 130 mL Once DDI100 and DPW100 were applied, EC values approximately doubled compared to EC values obtained from DI applications. Also, as higher leaching cycles were applied, EC values decreased in each application method. For example, in DDI100 applications, at cycle 30 mL; the EC conductivity measured was 4.76 mS/cm, at 80 mL the EC value decreased to 4.6 mS/cm, and for 130 mL it was reduced to 4.15 mS/cm.

To identify the effects of RG on K_{sat} in highly compacted clays, the interchange soil was used to represent the low plastic clay (CL) at the bottom of the pond. A total of 9 soil specimens were compacted in a 4 in. diameter by 4.6 in. in height mold as per ASTM D698-12. The mold was coated with Rust-Oleum rust and corrosion protection before its usage. The 125 pcf moist density was achieved by compacting the specimen to an 18.5 % moisture content based on the in-situ density of the Interchange soil, subsequently saturated for approximately 30 days. The K_{sat} value was measured with the leaching solutions: DI water, DDI100, and DPW100. Permeability and leaching experiment was executed simultaneously in cycles of 48, 120 and 168 hours. Once testing was completed, the soil was sliced in three equal parts for bound cation analysis. Both collected water, and top, middle and bottom slices were analyzed for cations and heavy metals in the ICP spectrophotometer. Compared to DI water leaching solution, DDI100 and DPW100 enhanced the saturated hydraulic conductivity by an approximate average of 19 % and 29 %, respectively.

As part of analyzing the saturated hydraulic conductivity, the collected water and sliced sections (top, bottom, and bottom) were chemically analyzed for cations subsequently after the completion of the falling head permeability test. Similar to the “low density” leaching results, the Ca^{2+} concentration for DI was relatively smaller as compared to DDI100 and DPW100 for the top, middle and bottom sections. The initial average Ca^{2+} concentrations for the three sections was approximately 300 mg/L. Once DDI100 and DPW100 were leached through the specimens, the Ca^{2+} concentration increased to approximately in the range of 450 mg/L to 600 mg/L.

A theoretical metal leaching analysis was employed using the RBCA Toolkit of Chemical Releases software. It was conducted to assess the effect of simulated RG dosages in a retention pond and analyzing the migration of gypsum trace elements (arsenic, cadmium, chromium, lead, manganese, nickel, and zinc). Representative source media constituent of concern (COC) concentration was entered directly by considering the bound cations extracted from Westbound soil that have gypsum dosages in mg/kg. In the model, two off-site receptors or water wells were assumed at a distance from the source (water table under the pond soil column) of 200 and 1,000 feet. Based on the concentration dosages in the source, time, and soil permeability, an analysis was performed to determine individual COC concentrations in groundwater at x distance with respect to time. The results for all trace elements exhibited a similar trend. For example, the arsenic concentration after 6 weeks reached 6×10^{-4} mg/L. Two considerations or trends were observed, one at "one-year" trend and the other one as a "steady-state" condition. Constant arsenic concentration applications for one year resemble the "steady-state" condition and reduces to the offset of 200 feet away from the source to approximately 4.0×10^{-4} mg/L, reducing exponentially to close to 0.0 mg/L at an offset of 1,000 ft. The trend representing "one-year" represents a single RG application. Since leaching water would leach arsenic concentrations from the soil, the total arsenic would be thoroughly diluted, having zero concentration reaching to offset 200 and 1,000 ft.

Several factors contribute to the benefits of implementing RG in retention ponds. This incorporation leads to increase in the infiltration rate of clayey soils, eco-friendly, favorable to the economy, and is sustainable for the city of El Paso. The life cycle assessment for a typical drywall board is derived into paths, either material lasts to its end of life and is sent to a landfill, or material is recycled. In this analysis, a summary of environmental concerns was analyzed based on every stage of the process throughout its service life. As for the development of the drywall, its composition is made by inputs such as mining gypsum, FGD gypsum from manufacturing plants, collect facing paper, and additive during production. Although the transportation and other factors enhance CO_2 emissions, the drywall recycling allows reuse of 12 % rejected drywall material and

64 % gypsum board scraps. If this 76 % is not recycled, it would be disposed of in landfills, requiring more resources for disposal and being environmental hazard (like generation of hydrogen sulfide in the landfill).

It is recommended to **EPW** to:

- Dissolve RG in water as the most suitable application method.
- Implement an aeration system in retention ponds to reduce the probability of generating toxic gases (H_2S) when RG is applied. (see Appendix H for proposed market mixers)
- For future RG applications, it is recommended to grind particles < 0.425 mm for faster dissolution rate.
- Recommend RG supplier to remove as much as possible cellulose material.
- Maintain documentation or a log of RG application for future leaching analysis.
- Apply approximately 2.5 g/L of RG in water.
- Since Interchange pond is generally at low water levels due to its high area, it is recommended to mix RG in soil by tillage.

TABLE OF CONTENTS

LIST OF TABLES

LIST OF FIGURES

CHAPTER 1: INTRODUCTION

1.1 PROBLEM STATEMENT

The primary function of retention ponds is to mitigate flooding and efficiently drain retained water to minimize health hazards. The presence of fine soils like clay reduces infiltration rates in retention ponds. Low percolating retention ponds result in an extend ponding of water, abundance bacteria accumulation, mosquito breeding, and environmental hazards. Mosquitoes carry many diseases harmful especially children, the elderly, and individuals with the weakened immune system. The City of El Paso environmental services has established code compliances regarding standing water. For noncompliance, owners or property occupants can be fined if they fail to prevent mosquitoes breeding in pools and standing water. There have been 11 confirmed cases with West Nile virus in El Paso TX throughout history, having the highest cases in 2017 with a total of 6 new cases (Villa, 2017). Low percolating retention ponds drain the water slowly and drop monotonically with a drop in total water head. Due to a reduction in infiltration rate, the water stays in the pond for longer time triggering an environment suitable for mosquito breeding. Mosquitos' breeding main breeding habitat occurs at the stagnant water at a depth of 4 feet or less that do not experience large movements of water for at least seven days, or areas where high organic matter is flowing regardless of the water depth (U.S. Environmental Protection Agency, 2005).

In addition to a health hazard, the lower rates of infiltration may reduce overall design capacity of retention ponds. An efficient retention pond would infiltrate water into the underground aquifers and be able to accept more water during monsoon season. Depending on the rainfall intensity and runoff volume, the retention pond may fail, during monsoon season, if runoff volume is more than the retention pond capacity. The Storm Water management division of El Paso Water (EPW) oversees and maintains local retention ponds in El Paso TX, and handle overflow emergencies by employing an emergency outflow towards the Rio Grande River.

Infiltration rate in clays is also affected by seal formation, clay mineralogy, and soil structure. During wetting, the infiltration rate is higher at its initial wetting stages and decreases monotonically until a seal is formed at the upper layer of the soil profile. Seal formation is a thin layer of fines at the soil surface that is caused by mechanical aggregate breakdown (developed by rainfall drops that reduce the void size in the surface layer by increasing soil compaction). Relatively, micro soil pores are clogged by dispersed clay fine particles that transport into the soil profile. This wetting cycle causes the soil to swell and reduce the infiltration rate. In the drying process, cracks would be formed in the upper layer, even though the core mass of the soil profile remains saturated. These cracks can be >15 cm wide and may extend to a depth of 2 m (Rycroft & Amer, 1995)

To enhance infiltration rates, many researchers have identified gypsum to be a useful soil conditioner that enhances infiltration rates. On high dispersive/sodic soils in Australia, gypsum increased the water infiltration rate by flocculating and reducing the crusting associated with dispersion-induced sealing (Loveday, 1974).

Drywall is a sheet panel made of gypsum (calcium sulfate dihydrate) as the primary constituent of its composition and is mixed with additives such as fibers, starch, cellulose, and other additives to improve fire resistance capabilities. Countless demolitions of buildings occur throughout North America, and the continuous disposal of drywall waste can be a source of concern because the disposal of gypsum drywall material has been associated with the development of hydrogen sulfide (H_2S) (Yang, Xu, Townsend, Chadik, & Booth, 2016). Gypsum biodegradation occurs when gypsum drywall gets wet in landfills at which sulfate-reducing bacteria (SRB) uses the gypsum sulfate component as an electron acceptor to consequently produce hydrogen sulfide (H_2S). Hydrogen sulfide is a colorless with a unique rotten-egg odor that is characterized by a flammable and highly toxic gas.

1.2 OBJECTIVE AND APPROACHES

The primary objective of this study is to evaluate the influence of recycled drywall (gypsum) in clayey soils and to identify optimized gypsum dosages needed to enhance infiltration of retention ponds, reduce the possibility of mosquito breeding, and minimize drywall waste disposal in landfills. To achieve objectives, the following approach was followed in this study:

1. To validate and proof if gypsum applications enhance infiltration rates, the double ring infiltrometer was utilized on the field and the falling head method in the laboratory for evaluating the benefit of gypsum application.
2. Determine the optimum gypsum dosage and application method that maximizes the infiltration rate.
3. Evaluate the longevity of gypsum as an infiltration enhancer by repeating application of gypsum to identify the frequency of gypsum dosages.
4. Identify the soil mineralogy by employing X-Ray Diffraction (XRD).
5. To thoroughly evaluate the transportation of leaching metals to groundwater with Risk-Based Corrective Action (RBCA) toolkit for chemical releases.

1.3 ORGANIZATION

The contents of these report are divided into five chapters. The first chapter provides the major problem and related issues associated with low percolating retention ponds and the approach considered in this study to mitigate these problems. Chapter two focuses on background related to infiltration rates in retention ponds, chemical properties of soils, recycled gypsum and leachates, and mineralogy of the soil. The third section corresponds to the experimental design of the study to evaluate the behavior of recycling gypsum in soils. Chapter four emphasize and present the

results and discussion of the results obtained. Chapter five show a summary, conclusions, and recommendations.

CHAPTER 2: LITERATURE REVIEW

The influence of recycled gypsum can be analyzed by understanding the interaction between the three constituents: water (leachate), soil, and recycled gypsum. A brief discussion on the one-dimensional flow of water, the physical and chemical properties of the soil and gypsum is included herein. Additionally, the interaction between all three constituents along with the relevant theory on chemical analytical transport model in groundwater and soil exposure pathways is summarized in this chapter.

2.1 MOVEMENT OF WATER IN SOILS

Infiltration rate is defined as the velocity at which a fluid, in this study water, can enter the soil. Soils have different infiltration capacities that vary on physical and chemical properties of the soil. The infiltration capacity is defined as the maximum rate a fluid can enter a soil matrix (Cooperative Research Centre, 2006). Infiltration rates are also linked to the percolation rate of the

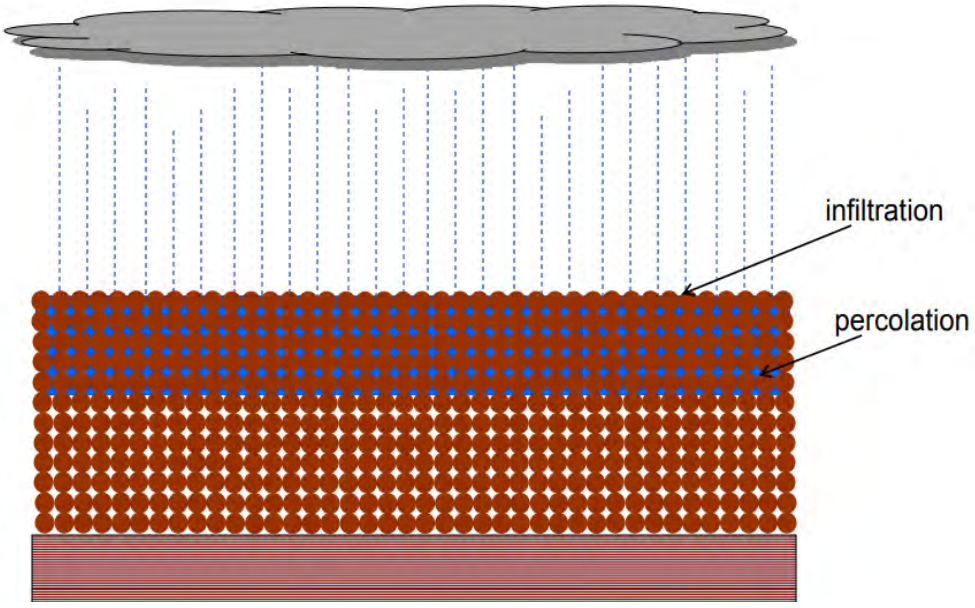

Figure 2. 1 Schematic of Water Movement (Western Washington University, 2012).

soil. Percolation is the movement of water within the soil matrix or seeps within the soil stratum under specific conditions (Figure 2.1). Infiltration rate is highly dependent on the percolation rate, and percolation rate controls the infiltration rate.

2.2 ESTIMATE THE INFILTRATION/PERCOLATION RATE

Darcy's law (1856) governs the flow of water through the soils. Darcy suggested that the average infiltration rate is proportional to the total head (Budhu, 2015). Bernoulli's principle defined the total head as the summation of elevation, pressure, and velocity heads. Since the velocity of water through the soils is less than (0.3937 in./s), the velocity head is disregarded in calculations. The infiltration rate can be estimated by the product of the saturated hydraulic conductivity and a hydraulic gradient (Equation 2.1). The hydraulic gradient is the cause of the movement of water within soils and is defined as the change in energy head per unit length measured in the direction of the flow (Massman & Allen, 2003).

$$V = Ki \tag{2.1}$$

where: K= coefficient of permeability or hydraulic conductivity, and i= hydraulic gradient $\frac{\mathrm{dh}}{\mathrm{dL}}$

Darcy's law is applicable to a) saturated and unsaturated flow (at unsaturated flow, the hydraulic conductivity is dependent on matric suction), b) steady-state and transient flow, c) flow in homogeneous and heterogeneous systems, d) flow in isotropic and anisotropic matrix and e) flow in rocks and granular material. Even though viscosity, density, and temperature of water and soil also influence the water velocity in the soil, the hydraulic conductivity is mainly dependent on the shape, size, and gradation of soil. Since soils tend to behave in a more anisotropic behavior, the vertical permeability (K_v) is very different from the horizontal permeability (K_h) because of the differences in the structure, texture, and porosity (Stibinger, 2014).

An equivalent hydraulic conductivity must be determined for the entire soil column because of the presence of different soil stratum. The hydraulic conductivities can be estimated by combining different layers at a specified depth with the harmonic mean equation (Massman &

Allen, 2003). The total depth of the soil column is considered to be from the bottom of the infiltrating pond to the water table, and all layers in-between, for estimating the equivalent hydraulic conductivity.

$$K_{equivalent} = \frac{H}{\sum \frac{h_i}{K_i}} \quad (2.2)$$

Where:

H= the total depth of the soil column

h_i= is the individual thickness of layer "i" in between total depth H

K_i= saturated hydraulic conductivity of layer "i" in the soil column

A representative hydraulic conductivity value in layered soils depends on the direction of flow of the groundwater. For example, if groundwater flows parallel to the soil layers, a representative hydraulic conductivity value is based on the summation of the hydraulic transmissivities of the layers. On the other hand, if water flows perpendicular to the layers, a representative value can be obtained by the summation of the vertical hydraulic conductivities of the layers (Oosterbaan & Nijland, 1994).

2.3 ESTIMATE THE SATURATED HYDRAULIC CONDUCTIVITY

Hydraulic conductivity can be determined by a variety of methods (a) an empirical approach based on grain size information, (b) laboratory experimental approach, and (c) in-situ

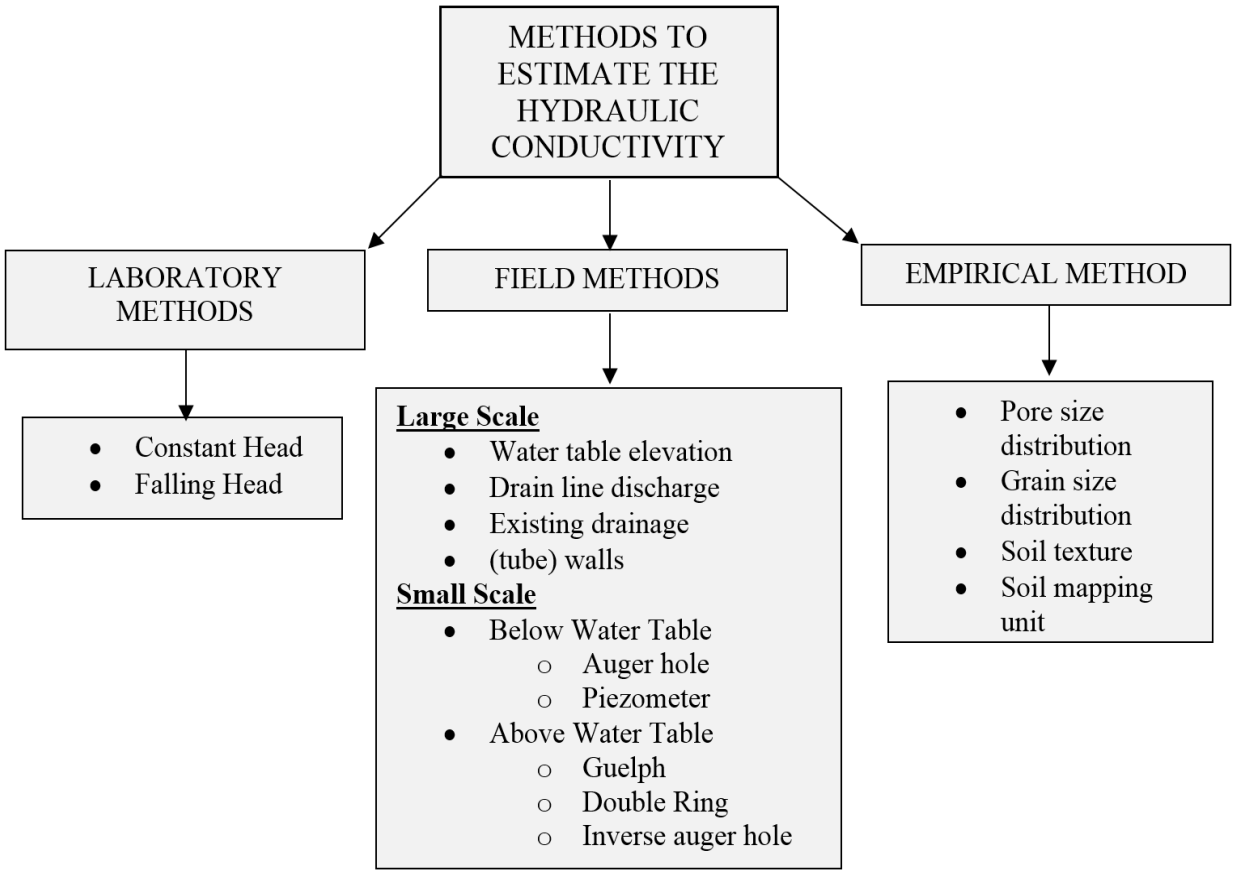

Figure 2. 2 Methods to Determine the Hydraulic Conductivity

field approach. An overview of the different methods used in practice to determine the hydraulic conductivity is shown in Figure 2.2.

2.3.1 EMPIRICAL METHOD

The empirical approach considers pore size distribution, grain size distribution, and soil texture for estimating hydraulic conductivity. Soil mapping unit is also another correlated method offered by the United States Department of Agriculture (USDA) that features drainage and saturated hydraulic conductivities of soils. Soil mapping is conducted on the essence of the soil string, at which different soil properties are amalgamated, and then correlated to obtain a range of K values (Oosterbaan & Nijland, 1994). Although the most straightforward and most commonly used approach is using values from grain size information, the empirical methods are more straightforward and quicker compared to laboratory and in-situ methods. Since these are empirical relationships, the hydraulic conductivity magnitude may not be representative of field values.

Therefore, this approach should only be used if the field and laboratory determination cannot be performed (Stibinger, 2014). Examples of standard empirical equations are shown in Table 2.1. These equations are based on grain size distribution, and the soils are expected to be relatively coarse-grained and are not suitable for fine-grained soils (Massman & Allen, 2003).

Table 2. 1 Typical Empirical Relationships for Estimation of K_{sat}

Source	Formula	Where,
Taylor (1948)	$k = {D_{50}}^2 \frac{\gamma_w}{\mu} \frac{C_1 e^3}{1+e}$	K= hydraulic conductivity C_1= constant related to shape (obtained from laboratory experiments) e= void ratio μ= Viscosity of water γ_w= unit weight of water D_{50}= grain diameter corresponding to grain size curve at 50% C= constant varying from 0.4 to 1.4 D_{10}= grain diameter corresponding to grain size curve at 10% D_{60}= grain diameter corresponding to grain size curve at 60% D_{90}= grain diameter corresponding to grain size curve at 90% f_{fines}= fraction of the soil (by weight) smaller than .074 mm
Hazen (1930)	$k = C{D_{10}}^2$	
Massmann (2003)	$log_{10}(k) = -1.57 + 0.015D_{10} + 0.015D_{60} - 0.01D_{90} - 2.08f_{fines}$	

2.3.2 LABORATORY METHODS

Two standard (falling head and constant head) methods are typically used for determination of hydraulic conductivity in the laboratory. The suitability of a test is dependent on the soil classification. According to Budhu (2015), the constant head method is used to determine the hydraulic conductivity of coarse-grained soils (like sand and gravels) while the falling head method is used to determine the hydraulic conductivity of fine-grained soils (like silt and clay) (Budhu, 2015). A schematic of the constant head method (left) and falling head method (right) is shown in Figure 2.3. In both testing methods, soil specimens are compacted to its desired density or on undisturbed soil sample obtained from the field.

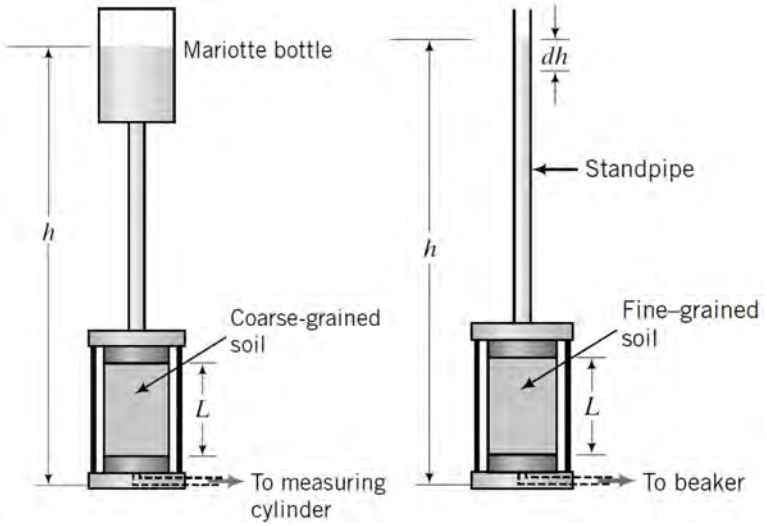

Figure 2. 3 Constant Head and Falling Head Schematic Diagram (Budhu, 2015)

2.4 SOIL PHYSICAL PROPERTIES

The movement of water through the soil depends on the physical properties (texture, structure, and bulk density) of the soil. The soil structure and texture together provide a general idea of the ability of a soil to hold and move water and air for a sustaining life with plants and natural habitats (Brady & Weil, 2008).

2.4.1 SOIL TEXTURE

The soil texture is defined as proportions of different particle size in a soil that makes up the mineral structure of the soil. The grain sizes (separates) are called boulders, gravel, sand, silt and clay in the engineering practice. There are various methods like Unified Soil Classification Systems (USCS), AASHTO Classification System, USDA Soil classification System, etc. that are used to classify soils. Classification systems differ in grain size (Table 2.2), such as USCS classifies sand in a grain size range of 4.75 mm to 0.075 mm and AASHTO from 2.0 mm to 0.075 mm. Each soil classification system is used according to the soil application. USCS applies to most geotechnical engineering applications, AASHTO is applicable for highway construction purposes, and USDA for agricultural purposes.

The coarse-grained material (sand and gravel) is composed of larger soil particles that promote relatively large pores, providing a well-interconnected conductance path for Newtonian fluids to flow. The presence of large pores prevent water to be held against the pull of gravity; thus, coarse-grained soils allow water to flow through at a faster rate in comparison to fine-grained soils (Brady & Weil, 2008). The higher percentage of particles smaller than 0.05 mm classify the soil to be fine-grained (based on the USCS) and usually suggest the presence of silts and clays. Fine-grained material is relatively smaller, providing permeable disconnected micro-pores, thus, limiting the flow of water (Schaetzl & Anderson, 2005). Although clayey soil pores are smaller, the number of pores is significantly higher that allows the soil to retain higher moisture content when fully saturated in comparison to coarse-grained soils.

Table 2. 2 Grain Size Range Based on Different Soil Classification Systems

	Size Range (mm)		
Soil Separate	**USCS**	**AASHTO**	**USDA**
Clay	Fines < 0.075	<0.002	<0.002
Silt		0.075-0.002	0.05-0.002
Sand	4.75-0.075	2-0.075	2-0.05
Gravel	76.2-4.75	76.2-2	>2

2.4.2 SOIL STRUCTURE AND BULK DENSITY

The soil structure represents cohesiveness and plasticity of the soil. The soil structure is associated with the arrangement of the separates forming peds or aggregates. Peds are naturally occurring and have a robust internal cohesion force that is difficult to break. Peds are usually held and joined by some binding agent or cohesive forces (Schaetzl & Anderson, 2005). These surface peds develop large cavities under dry conditions that physically modify the soil in the form of soil crusting. These upper-layer crusts are more compact, hard, and brittle than underlying soil material. The soil crusting reduces the number of pores leading to a reduction in permeability of

the soil (Wallace, 1998). When soils are wet, peds break down or fall apart and liberate fine fragments of soils that fall in cavities that seals the soil surface and further clogs the pores. The breakdown of this peds, or crusts creates the closing of pores and other pathways for water and air entry into a soil (De Varennes, Qu, Cordovil, & Gonçalves, 2011). The stability of peds depends on various factors such as the clay mineralogy, organic matter, and exchangeable cations. Calcium ions associated with clay generally promote aggregation, whereas sodium ions promote dispersion (De Varennes et al., 2011).

2.5 CLAY MINERALOGY

Clay is usually defined by clay mineral structure and particle size smaller than 0.002 mm. Clay minerals can be classified based on its crystal structure, chemical composition, and secondary minerals (Schaetzl & Anderson, 2005). Clay minerals have a net electrical negative charge, high surface area, and moisture susceptibility. The mineralogy of clay is an indication of soils weathering caused by the exposure to water and rocks. For example, hydrolysis is generally the most significant chemical weathering process and occurs by the reaction of ions within the feldspar mineral that is associated with hydroxyl and the dissociated hydrogen of water (Little, 1995). The reaction occurs when the hydrogen ion of water enters the lattice of feldspar and replaces the cations causing the development of tetrahedral and octahedral sheets. The clay structure can be categorized into two main components; a corner connected tetrahedral sheet and an edge connected octahedral sheet (Guggenheim, 1995). Tetrahedral sheets are typically composed of one silica and four oxygen linked together to form a network. The silica tetrahedral usually form the predominant minerals of quartz and feldspar (tectosilicate). An octahedral sheet is composed of one cation and six oxygen. Gibbsite is an octahedron sheet with one Al^{3+} as the cation and six oxygen surrounding the alumina; brucite sheet is formed by Mg^{2+} cation surrounded by six oxygen. Tetrahedral and octahedral sheets are not stable because crystal structure ion may be replaced by another ion of similar charge and radius (isomorphous substitution). In both, tetrahedral and octahedral sheets,

oxygen may be replaced by hydroxyls or can combine with oxygen to provide a positive union. Silica tetrahedral sheet and octahedral sheet combine and join in different arrangements to create dissimilar minerals.

Phyllosilicates, where one tetrahedral silica sheet is bonded to one octahedral sheet, is called 1:1 phyllosilicate, meaning that the unit cell is structured by one tetrahedral sheet jointed to an octahedral sheet (Schaetzl & Anderson, 2005). As shown in Figure 2.4, the kaolin group (kaolinite, halloysite, dickite, nacrite) and serpentinite group (chrysotile, antigorite, lizardite) are examples of 1:1 phyllosilicate minerals with an interlayer hydrogen bond and a layer charge of zero. The 2:1 layer are those with two tetrahedral silica sheets that sandwich or surround one octahedral sheet (Schaetzl & Anderson, 2005). Examples of 2:1 phyllosilicate sheets are, pyrophyllite, smectite, vermiculite, illite, chlorite and mixed layers as shown in Figure 2.4.

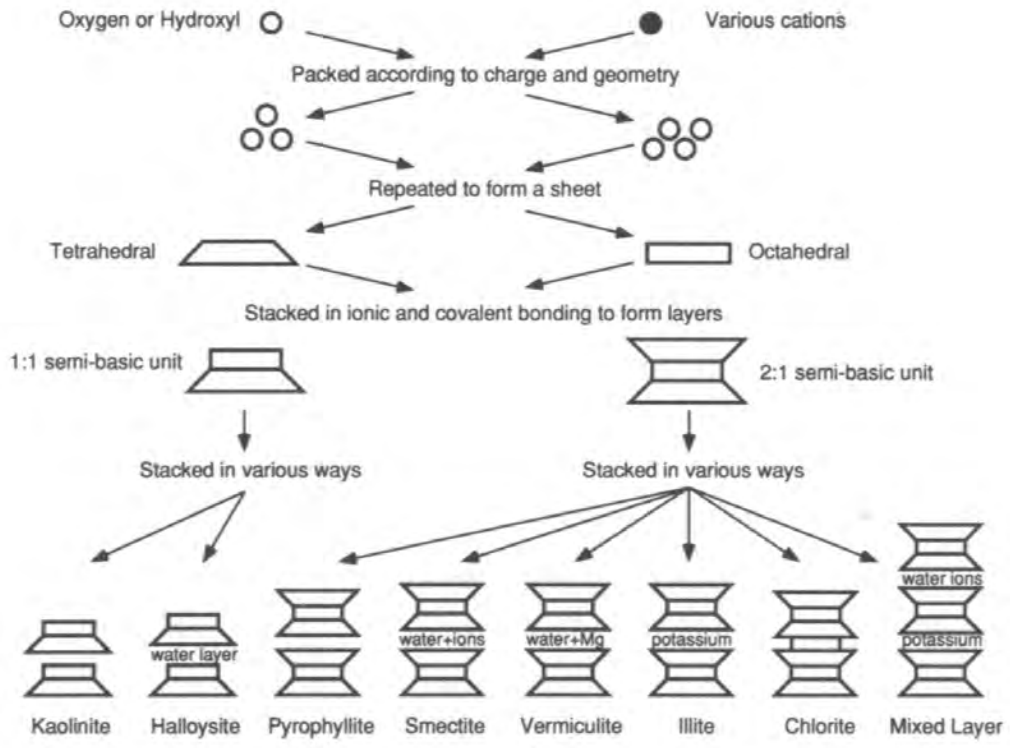

Figure 2. 4 Mineral Synthesis (Mitchell, 1993)

The configuration of *kaolinite* and *halloysite* (configuration of 1:1) is typical of the mineral to have low plasticity as opposed to smectite group whose configuration is 2:1 and can be very plastic, expansive and unstable (Little, 1995). Kaolinite and halloysites do not significantly expand when coming in contact with water. A common mineral in the smectite group is *montmorillonite*. Montmorillonite is a dioctahedral sheet and is very common in arid semi-arid soils. Montmorillonite experiences natural shrink and swell behaviors in wet-dry cycles and is sensitive to sodium since sodium causes montmorillonite particles to deflocculate. The deflocculated montmorillonite particles are then translocated through the soil depth and cause the pores to clog, thus, minimizing the availability of pores for water flow through the soil (Schaetzl & Anderson, 2005). *Vermiculite* is another expanding mineral that contains Al^{3+} or Mg^{2+} and Fe^{2+} in the structure. The hydrated ions in the vermiculite clays promote the expansion of soil in the presence of water. *Illite* is generally formed in marine environments, and K^{+} ions provide a fit in between the layers. Since illite clays have an interlayer of cations, the entrance of water is prevented within the structure making it a non-expansive clay (University of Vancouver, 2018). Another mineral type, chlorites are 2:1 phyllosilicate clays (non-expansive) that share an octahedral sheet of metal hydroxide in between, thus, minimizing expansion and contraction of layers (Schaetzl & Anderson, 2005).

2.6 SODICITY AND SALINITY OF SOILS

Common cations that are typically bound to the clay particles are calcium and magnesium that are known to be good flocculators while sodium and potassium are considered to be poor flocculators. Sodium is considered to be poor flocculator cation because it generates degradation and dispersion in the soil structure. These cations (sodium and potassium) attract water molecules because of their charge. Sodium and potassium have a single charge and a sizeable hydrated radius of 0.79 nm and 0.53 nm, respectively making them be poor flocculators. The specific amount of

sodium held in soil is known by the term sodicity (McMullen, 2000). Sodic soils have a high amount of exchangeable sodium (Lamond & Whitney, 1992).

Soil salinity depends on the extent of soluble salts present in the soil. Most common anions related to soil salinity are: chloride (Cl^-), sulfate (SO_4^{2-}), carbonate (HCO_3^{2-}) and nitrate (NO_3^-) and associated cations are calcium (Ca^{2+}), sodium (Na^+), potassium (K^+) and magnesium (Na^{2+}) (Lamond & Whitney, 1992). Even though there are scenarios under which many cations are bonded to the clay particle of the soil, the salts typically move freely in leaching solutions. The soil salinity or soluble salts are measured based on the electric conductivity (EC) of leached water, typically in units of (mS/cm). The US salinity laboratory developed a classification system (Table 2.3) to classify salt-affected soils. These soils are divided into three main classification categories, saline, sodic and saline-sodic soils. The classification depends on the EC, pH and exchangeable sodium percentage of the soil derived based on the salinity of the soil saturation extract (Rycroft & Amer, 1995).

Table 2. 3 Saline/sodic Soil Classification Table (Lamond & Whitney, 1992)

Classification	Electric Conductivity (mS/cm)	Soil pH	Exchangeable Sodium Percentage	Soil Physical Condition
Saline	> 4.0	< 8.5	< 15	Normal
Sodic (alkali)	< 4.0	> 8.5	> 15	Poor
Saline-sodic	> 4.0	< 8.5	> 15	Normal

Sodic-saline soils can be attributed to the high presence of sodium and salts content. These soils are typically found where highly saline groundwater has risen close to the soil surface caused by the capillary action effect. Under dry conditions, Franzen (2007) explained this phenomenon as “evaporation then dries the soil and pulls water by capillary flow from the wet soil zone. Because only pure water evaporates, salts are left behind”.

2.7 GYPSUM

Gypsum is a mineral, formed naturally and as a by-product of industrial processes. Gypsum is chemically known as calcium sulfate dihydrate ($CaSO_4.2H_2O$). Gypsum is used and applied to help humans, animals, plant life, and the environment because of its non-toxicity (Gypsum Association, 1992). Most of the gypsum produced in North America is used to produce drywall and building plasters, but it has many other applications as shown in Table 2.4.

Table 2. 4 Typical Uses of Gypsum in North America (Gypsum Association, 1992)

Gypsum Application:
***Soil additive*:** helps modify the soil increasing its workability, provides benefits to crops, increase infiltration rates in clayey soils, and controls the corrosive effect of alkalinity
Additive in lakes/ponds: decrease turbidity in lakes and ponds caused by dispersing clayey particles
Orthopedic uses: molded and used as surgical and orthopedic casts
Food additive: used as a dietary calcium source, water hardening treatment when making beer, reduce the acidity of wine and control clarity, and as an ingredient for foods
Color additive: additive to base drugs and cosmetics
Daily use products: gypsum is used in toothpaste, shampoos, and hair products
Gypsum board: drywall with a gypsum core and paper facing, sometimes core additives and fibers are added to increase fire resistance

Gypsum occurs naturally as well as can be produced such as: mined, Flue Gas Desulphurization, Spray-Dry Absorption materials, phosphogypsum, pickle gypsum, titanogypsum, borogypsum, fluorogypssum and others but gypsum is derived into two main types of gypsum, natural and flue-gas desulfurization (FGD). Gypsum is slightly soluble in water (2.0-2.5 g L^{-1} at 25 °C). Gypsum dissolution exhibits retrograde solubility, meaning as the temperature increases, the solubility decreases, based on Le Chatelier principle. The level of solubility plays a considerable role in the ionic strength of most soil solutions (Wallace, 1998).

2.7.1 NATURAL GYPSUM

Natural gypsum is found in sedimentary rocks. Once gypsum is mined or quarried, the rock is pulverized into fine particles. Subsequently, the fine powder is calcinated at a temperature approximately of (250 to 300 °F) to remove ¾ of the chemically bound water to form the stucco (U.S. Environmental Protection Agency, 1995). Natural gypsum is found in many countries around the world, but North America has the most significant deposits of high-quality gypsum (Gypsum Association, 1992).

2.7.2 FLUE-GAS DESULFURIZATION (FGD) GYPSUM

FGD is commonly produced as a by-product while burning coal and annual production is estimated to be 20 million tons in the United States (Natures Way Resources, 2018). The fertilizer production plants produce gypsum (FGD) as a by-product which accumulates as a waste material (Wallace, 1998). FGD gypsum provides chemical and physical benefits in agriculture because FGD produced is of high quality. Primary chemical composition, minor and trace constituents, and crystalline structure of FGD is similar to that of natural gypsum (Pflughoeft-hassett, 2007).

2.7.3 RECYCLED GYPSUM

Drywall is the predominant source of recycled gypsum, which is frequently used in the US for construction of the interior walls of many structures. The term drywall is also referred to as sheetrock, wallboard and gypsum boards. They are mainly composed of 93% gypsum and about 7% paper (Ndukwe & Yuan, 2016). Fibers are also mixed with plaster to produce a fire-resistant material. Waste gypsum material is mostly generated in three stages: 1) during the manufacturing of drywall, 2) during demolition and remodeling of structures and 3) in new construction where gypsum boards pieces are discarded (Gypsum Association, 1992). The primary source of gypsum waste (almost 64%) comes from uninstalled gypsum board scraps generated during building construction. It is estimated that 14 % and 10 % of waste is generated during demolition and

renovation, respectively (Ndukwe & Yuan, 2016). Another 12% to 4% of the total drywall waste is produced during the manufacturing of drywall due to quality control issues.

2.8 WASTE GYPSUM MATERIAL IN LANDFILLS

In the past years, the landfill disposal of gypsum has become a severe problem because of the production of toxic gases (hydrogen sulfide gas H_2S). Hydrogen sulfide gas is produced by the sulfate-reducing bacteria (SRB), which uses sulfate as an electron acceptor. Anaerobic conditions develop in the presence of moisture, stimulating sulfate-reducing bacteria to decompose the sulfate from the gypsum structure and causing high toxic levels of H_2S (Ndukwe & Yuan, 2016).

Table 2. 5 Summary of H_2S Triggers in Landfills (Tolaymat & Carson, 2015)

H_2S Formation Factor	Discussion
SO_4^{2-}	Sources such as drywall waste disposal or any other sulfate source activated sludge's, or other wastes is a sulfate source for H_2S production.
Moisture	SRB habitat is in any moist material medium such as moist soil.
Organic Matter	• H_2S may be produced by the bacterial breakdown of organic matter, although it is sufficient with the paper component of the drywall to serve as a substrate. • Organic matter is normally present in landfills (yard trimmings, the soil itself, paper, food waste, and other organic matter wastes)
Anaerobic Conditions	H_2S is also produced when the environment lacks free oxygen atoms (anaerobic conditions).
pH Conditions	SRB flourish in a pH environment ranging from 6 to 9.
Temperature Conditions	H_2S researchers have noticed that SRB can thrive in temperatures up to 176°F.

Triggers (shown in Table 2.5) are common formation factors present in landfills throughout the US. Many landfills have established new rules to landfill users concerning gypsum waste disposal quantities to regulate landfill gas production or entirely ban gypsum board disposal in landfills. A study conducted by the University of Florida consisted of analyzing the hydrogen sulfide generated by simulating construction and demolition debris. Researchers concluded that hydrogen sulfide production could be reduced with the use of concrete. H_2S is reduced by two

mechanisms 1) concrete increases the leachate pH making an unfavorable habitat for SRB and 2) concrete may react with H_2S in an “adsorptive” or “absorptive” process (Yang et al., 2016).

Additionally, to the gypsum waste disposal problems in landfills, gypsum drywall can increase the permeability of clay liners in landfills. Drywall gypsum could disintegrate the function of clay liners that waste management companies utilize to minimize toxins (from landfill wastes) movement into the groundwater (Peppin, 2015). Due to the environmental and public health hazards associated with waste drywall disposal in landfills, the industry is favorable to outreaching the goal of reducing the landfill burden and achieving maximum recyclability of drywall in the US and Canada (Gypsum Association, 1992).

2.9 RECYCLED GYPSUM AS A SOIL CONDITIONER

Recycled gypsum has important application in agriculture by enhancing the water infiltration rates. Research on recycling gypsum applications on agricultural lands has grown in the last several decades. The application of recycled gypsum in agricultural land offers a “win-win” solution for farmers/users of the recycled material and the creators because it reduces the cost of disposal and provides agronomic benefits (Wolkowski, 2003). Recycled gypsum is typically an excellent fertilizer and recognized to ameliorate water filtration, increases the calcium and sulfur nutrients in the soil, and improve soil structure. According to Ndukwe & Yuan (2016), recycled gypsum from drywall is used to ameliorate water filtration and workability of low permeable alkali soil. Due to its ability to flocculate clay particles, gypsum assists in the prevention of runoff and erosion of soils. Gypsum is known to reduce Al toxicity, and increase the Ca availability(Wallace, 1998). Gypsum added to the soil, or the leaching water will increase the calcium concentration of the infiltrated water by approximately 400 to 600 mg L^{-1}, while minimally influencing pH of the soil (Rycroft & Amer, 1995).

2.9.1 APPLICATION APPROACH

Drywall is composed of about 90% pure gypsum; the remaining 10% are typically admixtures, fibers and cellulose material that should be limited by the proper preparation and application methods. Gypsum can be applied in three different ways, 1) saturating leaching water with gypsum, 2) mixing and tilling gypsum within the soil, and 3) and sprinkling gypsum powder over soil surface (Ayers & Westcot, 1985). Usually, gypsum mixed in water requires less gypsum as compared to other application methods. The first application method is more effective than the second or third application method both in terms of cost and effectiveness (Kemper, 1975). The electrolyte conditions of gypsum in the leaching solution is fundamental in enhancing water filtrations. In addition to dissolving gypsum in leaching water, only soluble elements (major, minor, and trace element constituents) of recycled drywall would dissolve in water and would limit soil contamination from non-dissolving material (cardboard, admixtures, fibers). The recycling center should separate paper and gypsum and fracture gypsum particles into a fine powder form (Peppin, 2015).

2.9.2 GYPSUM DISSOLUTION

Rebecca J. Hintz and Kevin C. Johnson (1989), mentioned that the dissolution rate of a solute depends upon the solubility, the concentration of the solution at a specific time interval, the solute's diffusivity, and the surface area of the solute's particle size. Taking into consideration these factors, the dissolution rate of gypsum would be in fact affected and mostly by the specific surface area. Specific Surface Area (SSA) is the total surface area of particles in a sample per the total mass of the sample. Therefore, the higher amount of finer particles will enhance SSA. To determine the exact SSA of a powder is a challenging exercise, specifically for RG. RG is typically grounded and delivered to the client with different SSA dependent on the quality control of the recycler. The case might be where there are more fines than coarse gypsum particles, or vice versa, creating a vast gap between the SSA values (Figure 2.5). According to Arthur A. Noyes and Willis

R. Whitney (1897), they found the same problem stating that it is difficult to keep the surface of the dissolving substance constant.

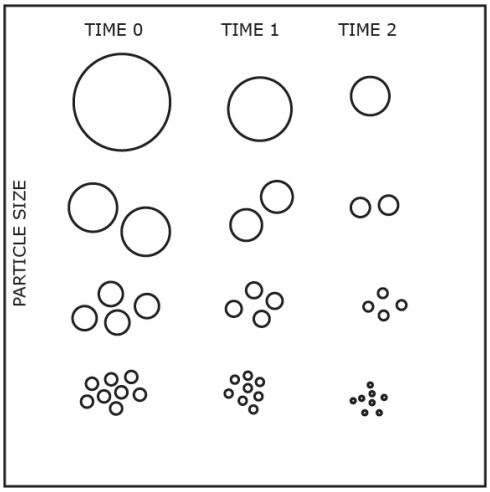

Figure 2. 5 Dissolving Particle Sizes at Different Times

2.10 CURRENT STANDARDS AND REGULATIONS

The British Standard Institution (BSI) has developed specifications regarding the production of recycled gypsum from drywall. The British standard: "PAS 109:2013 Specification for the Production of Reprocessed Gypsum from Waste Plasterboard" provides guidance and specifies the minimum requirements on production on recycled gypsum preparation. Also, the Scottish Environment Protection Agency (SEPA), have published a paper demonstrating guidance of the controls of the use of waste gypsum as a soil conditioner. If the recycled gypsum is used for agricultural purposes, it would be controlled under the "waste management licensing regime." Exemptions can be made from the requirement to hold waste management licensed.

CHAPTER 3: EXPERIMENT DESIGN

This study focused on investigating the use of RG soil amendment for enhancing infiltration rates. To better reap the benefits of RG, it is paramount to take into consideration the movement of water in response to RG dosages, mineralogy, chemical and physical properties of all three constituents. This chapter focuses on the experimental design structured, and procedures followed to comprehend and adequately achieve the goals of this study successfully.

3.1 SELECTION OF PONDS

El Paso Water (EPW) proposed studying two retention ponds with reduced percolation rates in El Paso, TX. These two retention ponds are identified in this study as Westbound Pond and Site Pond. To enhance percolation rates of Westbound and Site ponds, EPW had already utilized gypsum dosage to both retention ponds, before funding this study to explore the effectiveness of RG as a soil conditioner. Based on their feedback, percolation initially increased after gypsum dosages were applied; however, retention pond eventually remained undrained leaving behind 4 ft. of stagnant water.

Figure 3. 1 Selected Pond Location

The UTEP research team suggested performing infiltration tests using the double ring infiltrometer prescribed by ASTM D3385-18. Unfortunately, water levels remained stagnant in these ponds, limiting the accessibility to perform infiltration testing. Thus, EPW suggested a new retention pond owned and maintained by the Texas Department of Transportation (TxDOT) in the El Paso area. For this study, this retention pond is referred to as Interchange Pond. Interchanged Pond was completely dry, and RG was not used before as a soil conditioner. In the end, an additional Pond from the Upper Valley area was selected for validation of the findings. Thus, a total of four ponds were evaluated in this study. The location of the selected ponds is included in Figure 3.1.

3.2 IN-SITU TESTING

3.2.1 DOUBLE RING INFILTROMETER

Infiltration rates were measured at the Interchange Pond using the double ring infiltrometer by the ASTM D3385-18 (see Appendix A). All tests were performed with different RG application rates and two distinct methods of applications (Table 3.1). To minimize the influence of minerals present in the water, the gypsum was mixed in distilled water.

Table 3. 1 Double Ring Infiltrometer Testing Overview

RG Method of Application:	Gypsum Rates (Dosage)	Units	*Replicates
Spread on top of the soil surface (GSS)	0, 3.5, 6.9, 10.4, 13.9, 17.3, 20.8, 24.3	tons/acre	3
Mixed in distilled water (DDW)	0, 25, 50, 75, 100	%	3

*Number of replicates per each dosage

A total of 39 tests were performed at different areas in the pond. For each test, the measurements were performed at five different intervals. The first two readings were taken after 15 minutes, followed by two readings after 30 minutes and one final reading after 1 hour. Thus, each test required a testing time of 2.5 hours. Additional time of an hour is also required for apparatus setup. For GSS application method, gypsum was evenly spread throughout the inner and outer rings. To minimize the influence of particle size, gypsum was sieved, and particle size smaller than 4.76 mm were only used. Since the dosages specified in agriculture are in tons/acre,

all dosages proposed in Table 3 were applied based on the area of apparatus rings. For the DDW application method, gypsum was sieved through a 0.075 mm sieve and dissolved in the distilled water in the laboratory to form a saturated solution. The water mixed with gypsum was placed inside two 5-gallon containers and placed on top of the shaking machine (50 rpm) for One-hour, and this process was completed one day before the field experiment. Dissolved solution was extracted with a siphon pump and stored in a 10-gallon polyethylene tank at the time of testing. The laboratory prepared concentrated solution was diluted to 25, 50, 75, 100 percent solutions depending on the dosage to be tested.

3.2.2 SAND CONE TEST

Sand cone test was carried out to determine the in-place density and unit weight of the in-situ soil. Density measurements were performed at four different locations within the Interchange Pond. The measurements were then averaged and used as a reference for performing testing in the laboratory (section 3.7). The sand cone test was performed as per ASTM D1556, and the summarized procedure is included in Appendix A.

3.3 SAMPLE COLLECTION FOR LABORATORY STUDIES

Soil samples were collected from Westbound Pond, Site Pond, Interchange Pond, and the Upper Valley region of El Paso, TX and soil samples were labeled according to the pond location: Westbound soil, Site soil, Interchange soil, and Upper Valley soil, respectively. To accurately evaluate soil properties, four representative soil samples from each pond were collected from different locations within the pond and location is included in Figure 3.1. Based on the Web Soil Survey (WSS) from the United States Department of Agriculture maps, the upper valley region infiltration rates are relatively low as compared to other areas of El Paso and was the reason for selection of this pond.

3.4 IDENTIFICATION OF SOIL PROPERTIES

A series of tests were carried out to determine the physical, chemical and mineral properties of the soil. These properties would aid them in determining the effects and responses of RG applications in mitigating and enhancing infiltration rates in clayey soils.

3.4.1 PHYSICAL PROPERTIES

Soil physical properties determined in this study were: soil classifications, Atterberg limits, moisture-density curves, textures, and specific surface areas. A washed sieve analysis (AASHTO T27/T11) was performed along with Atterberg limits (ASTM D4318-17e1), and soil was classified as per the Unified Soil Classification System (USCS). Moisture density curves were determined by the Proctor compaction standard of ASTM D698-12 to find compaction characteristics of the soils for sample preparation before hydraulic conductivity measurements specified in Section 3.9. The process followed for developing moisture-density curves is included in Appendix A and obtained moisture-density curves are included in Appendix B. The specific surface area (SSA) of clay and silt particle sizes were relatively analyzed using the Mastersizer 2000 (laser diffraction particle size analyzer from Malvern Instruments) because this technique is precise and faster than the traditional hydrometer analysis. The SSA of soil particle size smaller than 0.075 mm was determined by dispersing soil sample with sodium hexametaphosphate for 24 h before the analysis. A total of three samples were evaluated for each soil, and the results were averaged and presented in Chapter Four.

3.4.2 CHEMICAL PROPERTIES

Chemical properties of the soil were determined to understand the soil chemical properties and ion exchange capacity better. The electric conductivity (EC), pH, cation exchange capacity (CEC), soluble and bound cations, sodium adsorption ration (SAR), and exchangeable sodium percentage (ESP) of the soils tests were performed. The pH and EC levels were measured in bulk saturated soil paste with an EC/pH meter. A minimum of three measurements was obtained and averaged. CEC, soluble and bound cations were determined as per the ASTM standard D7503-10.

ASTM defined “bound cations” are bounded to the mineral surface while “soluble cations” are present in the pore water of the soil. Soluble cations are typically leached when water passes through the soil. On the other hand, bound cations can remain attached to the clay particle. The CEC was measured by displacing the index ions (ammonium acetate) of soil finer than 2.0 mm with potassium chloride and measuring the amount of the displaced index ion. This mechanism is an essential factor that is fundamental to be known for the exchangeable sites when gypsum dosages are applied. Three random soil samples were collected from the four ponds for performing cation concentrations tests, and the obtained results were averaged to identify a more representative measurement. The typical output results were calcium, magnesium, sodium and potassium concentrations. These concentrations are then used to calculate the SAR and ESP values. All standards, experiment procedures and calculation formulas are included in Appendix A. All major and minor constituents, and trace elements were determined using an Optima 7200 DV ICP-OES spectrophotometer. All element concentrations are shown in Appendix C for each soil collected.

3.4.3 MINERAL PROPERTIES

3.4.3.1 X-RAY DIFFRACTION (XRD)

The XRD analysis was performed to determine detailed soil mineralogy and the atomic structure of the crystalline matter. XRD was performed on particles sizes finer than 0.42 mm. For clay identification, soils were sieved, separated from silt by decantation and treated to remove carbonates and organic matter. Treatments are essential for clay identification since XRD patterns may be affected by amorphous peaks. Approximately, only 0.5 grams of soil is required per run. A total of two runs were conducted for clay identification by mounting soil samples in a specific orientation. For soil identification in XRD analysis, it is preferred to mount the soil in a well-oriented mount as opposed to quantification, where randomly oriented mount orientation is preferred. Other treatments such as glycol and heat treatments were attempted for clay

identification; a representative sample could not be prepared for XRD analysis due to the crusting and rolling of the clay caused by cohesion forces on top of the glass slide.

Fines identification followed the same procedure as the clay identification. However, there was no separation of silts and clays. Since the number of clay particles was reduced, glycol and heat treatments were successfully achieved in fines identification. Fines identification was performed twice for each soil to limit error readings when samples were mounted. Both clays and fines phase identification were analyzed using DIFFRAC.EVA software.

For particles smaller than 0.42 mm, two representative soils were collected from each soil and were mixed and grounded with 10 % corundum and methanol in a McCrone miller for 5 minutes. The 10 % of the mixed corundum served to accommodate the orientation of the crystal structure of the soil and was used as a reference for clay quantification. Minerals were first identified using DIFFRAC.EVA then quantified using the Rietveld method for soils < 0.42 mm included in DIFFRAC.TOPAS software. Even though quartz typically overwhelms clay mineralogy as particles sizes get larger, the presence of clay mineralogy is still visible at this size. XRD studies and patterns are shown in Appendix D, sample preparation, scan speeds, and XRD analysis procedure are included in Appendix A.

3.4.3.2 SCANNING ELECTRON MICROSCOPE (SEM)

All soils were analyzed by a tabletop TM-1000 Hitachi SEM to examine the crystal structure of the soil up to 10 µm magnification. Triplicate tests were performed for all soils. SEM images can be found in Appendix D, and SEM preparation methodology is presented in Appendix A.

3.5 SELECTED RECYCLED GYPSUM (RG) PROPERTIES

RG used to execute the project was supplied by El Paso Recycling Inc (EPR), a local recycler in El Paso, TX. The main source of EPR gypsum is drywall and sheetrock from scraps produced by new constructions (leftovers). These scraps have not been painted nor installed. Based on EPR recyclers, approximately 90 % of the gypsum board received are gypsum drywall boards from the American Gypsum Company. EPR staff are familiar with the composition of the products from this company. EPR rejects the gypsum boards consisting of fiberglass since it could cause issues while grinding the material, and for most material, material safety data sheets (MSDS) are requested by EPR. Gypsum drywall is ground to powder and screened through a 12.7 mm sieve, principally for paper removal before usage.

3.5.1 CHEMICAL ANALYSIS

The major and minor trace elements of RG were determined following EPA 6010B method to trace metals using the Optima 7200 DV ICP-OES spectrophotometer, and other anions following EPA 9056 standard using the Ion Chromatography (IC). A 15 g bulk RG sample was crushed and sieved through sieve No. 200 (0.074 mm) to remove cardboard material. Out of the sieved material, three representative samples of 2.5 g were digested for dissolution of elements and filtered through a 0.45 µm pore size filter for subsequent measurement of the dissolved elements and results were then averaged. Results were then calculated from mg/L of the dissolved elements in water to mg/kg of gypsum.

3.5.2 MINERAL ANALYSIS

The mineralogy of RG was analyzed using XRD. For sample preparation, most of the cellulose material was discarded from the sample by hand sorting and sieving to minimize the presence of amorphous material in the sample. The amorphous material is non-crystalline and lacks a long-order characteristic as opposed to the crystalline that is composed of a three-dimensional molecular lattice structure. Rayed from an incidence angle of 5º2θ to 65º2θ at a step size of 0.02 with a scan speed of 0.2 s/step. A single sample was employed in XRD reading with

a total duration of approximately 10 hours. The sample was then identified using DIFFRAC.EVA and quantified computation with DIFFRAC.TOPAS.

3.5.3 ESTIMATING CELLULOSE MATERIAL CONTENT

Cellulose/paper material was determined by dissolving a bulk sample of RG in deionized water. A 35-g sample was crushed in a pestle mortar bowl to produce particle sizes smaller than sieve No. 100 (0.149 mm). Three 10 g samples were dissolved in 1 L of DI water for 1 hour at 200 rpm and allowed settlement of non-dissolved material. After 24 h, dissolved gypsum was withdrawn using a syringe to isolate the settled cellulose material. The procedure was repeated (6 times) until there was no more gypsum residuals and all cellulose material that has been isolated. The detailed experimental procedure is included in Appendix A.

3.6 COLLECTED POND WATER

Stagnant pond water (PW) was collected from the Westbound Pond location and selected to be used for infiltration experiments. Concentrated water at this location is accumulated by the runoff and drainage system of the parallel highway (IH-10). The pH and the electric conductivity was measured using a benchtop pH/EC meter, and ion concentrations were studied using the ICP spectrophotometer and Ion chromatography.

3.7 FALLING HEAD TEST

The falling head permeability test was conducted under laboratory conditions at an average temperature of 23 ± 1 °C to determine the saturated hydraulic conductivity (K_{sat}). All soils were sieved through sieve No. 4 (< 4.76 mm) as stated in ASTM D698-12 of soil using standard effort and mixed in a concrete mixer to acquire uniformity in the soils. Sieved material was filled into a 6-inch height by 2.5-inch cylindrical permeameter in three equal layers; each layer was tamped 25 times. All soil samples were packed to a bulk density of 90 ± 2 lb/ft^3 based on in-situ density obtained from the sand cone test (Section 3.2.2) performed on site. The observations were recorded

at 60, 120 and 240 s time interval, and the water temperature was measured for each soil sample. In this study, each treatment was replicated three times and averaged.

Table 3. 2 Gypsum Dosages in Leaching Solution

Dose:	Leaching Solutions			
	DDI		DPW	
	Deionized Water (DI)	*Gypsum and DI Water	Pond Water (PW)	*Gypsum and Pond Water
0 %	100 %	0 %	100 %	0 %
25 %	75 %	25 %	75 %	25 %
50 %	50 %	50 %	50 %	50 %
75 %	25 %	75 %	25 %	75 %
100 %	0 %	100 %	0 %	100 %

*Gypsum dissolved in DI water and pond water is at its 100 % saturation point.

Table 3.2 represents the proportions of water to a concentrated solution with gypsum. Gypsum was incorporated as dissolved in DI water (DDI) and pond water (DPW) in the leaching water at different saturation solutions or dosages. Subsequently, the soil was saturated with the leaching water until a constant discharge is seen at the outlet of the permeameter. Since K_{sat} is dependent on the dynamic viscosity of the leaching water, all K_{sat} measured are adjusted to a hydraulic conductivity at 20 °C. Equations and full procedures are included in Appendix A.

3.7.1 RG APPLICATION METHOD ANALYSIS EFFECTS IN K_{SAT}

As part of the falling head permeability testing, different methods of gypsum applications were evaluated using soil obtained from Interchange pond. Different gypsum application methods were evaluated to compare the saturated hydraulic conductivity obtained from method DDI and DPW to other application methods. Interchange soil was selected as the material for analysis because the site has not been treated with gypsum in the past, and its infiltration rate is higher than the upper valley. The gypsum application methods employed to determine the hydraulic conductivity were:

1. Gypsum dissolved in deionized water (DDI)
2. Gypsum dissolved in pond water (DPW)
3. Mixed gypsum in soil by weight at 10 %, 20 %, 30 %, 40 %, and 50 % (MGS)
4. Gypsum spread at the soil surface at the rate of 3.5, 6.9, 10.4, 13.9, 17.3, 20.8, 24.3 tons/acre (GSS).

Sample preparation was similar to the one included Section 3.7 (the falling head permeability test) preparation. DI Water was leached through the soil column in method MGS, and GSS and each test method was repeated three times.

3.8 LEACHING WATER THROUGH SOILS

3.8.1 LABORATORY LEACHING EXPERIMENT

To simulate leaching of gypsum through soils, the three application methods: continuous ponding, sporadic ponding, and sprinkling ponding were performed. DDI and DPW water of 100 % dose (DDI100 and DPW100) was added for continuous ponding application. Sample preparation for leaching experiment was identical to the falling head permeability test (Section 3.7).

For the leaching experiment, the hydraulic gradient was increased from 10.4 to 16 as compared to the falling head method to determine the hydraulic conductivity. The soil was saturated with DDI100 and DPW100 water solution, and pond water (PW). A graduated cylinder was placed at the outflow of the permeameter to collect the water sample. Discharged leachate outflow was collected in 3 cycles: 30 mL, 80 mL, and 130 mL.

The EC and pH of the collected water sample were measured using a pH meter and to ensure accuracy a new sample was prepared for each cycle. Once each cycle was completed, the soil sample was extracted and divided into three segments top, middle and bottom. Major-minor elements were analyzed in the top, and bottom segments for bound cations following ASTM D7503-10 standard and collected water Ca^{2+}, Mg^{2+}, K^{+}, Na^{+} while the other heavy metals

concentrations were determined using the ICP spectrophotometer. A total of 36 leaching tests were performed in this experiment.

3.8.2 THEORETICAL METAL LEACHING ANALYSIS

EPW utilize distributed water wells throughout the city as a significant source to deliver drinking water to El Paso residents. Gypsum is composed of major, minor and trace elements that can affect groundwater properties. In this section, a theoretical metal leaching analysis was employed using the RBCA Toolkit for Chemical Releases software. It was conducted to assess the effect of simulated RG dosages in a retention pond and analyzing the migration of gypsum trace elements of arsenic, cadmium, chromium, lead, manganese, nickel, and zinc. Representative source media constituent of concern (COC) concentration was entered directly by considering the bound cations extracted from the Westbound soil that have gypsum dosages in mg/kg. Westbound soil trace elements concentrations were used as input parameters because gypsum has been previously applied to this soil. The exposure pathway identification was groundwater ingestion through affected soils leaching to groundwater. The ASTM soil leachate model simulated soil to groundwater assumes that the leaching from the soil dissolves within the groundwater under the affected soils. As of the groundwater dilution, the "Domenico Model with Dispersion only (No Biodegradation)" was used assuming a steady state transport model taking in consideration the groundwater and an off-site receptor (EPW wells). In the model, two off-site receptors or water wells were assumed at a distance from the source (the pond) of 200 and 1,000 feet. Based on the concentration dosages in the source, time, and soil permeability, an analysis can be performed to determined individual COC concentrations in groundwater at x distance in respect with time. All input parameters for the RBCA Toolkit Chemical Releases software can be found in Appendix E.

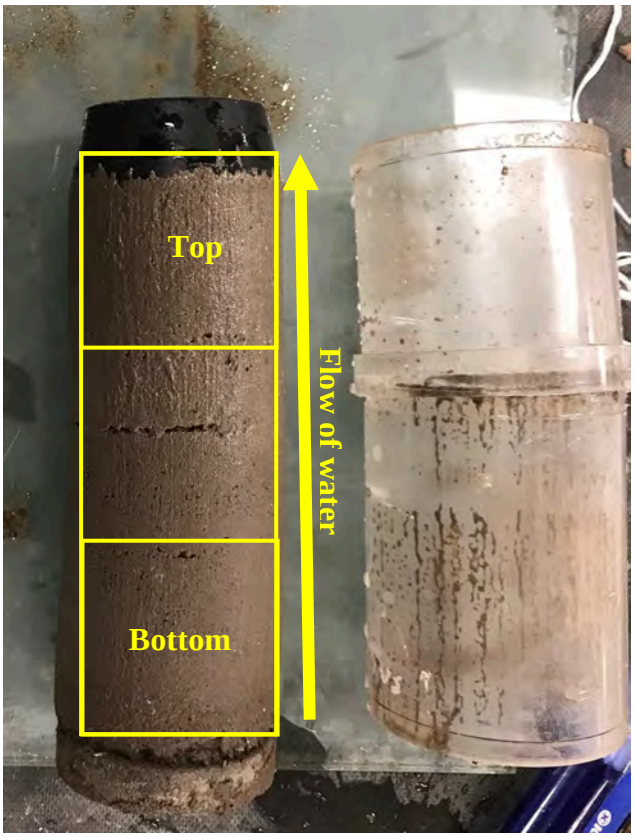

Figure 3. 2 Division of Sample for Sample Extraction

3.9 EFFECTS OF RG IN K_{SAT} IN HIGHLY COMPACTED CLAY

Due to low percolation rates in Westbound Pond, a local engineering company "CQC Testing and Engineering" performed a site investigation in the Westbound Pond area. Based on the provided boring log, approximately 5 ft under the base of the pond, a thick low plastic clay (CL) layer is present at the bottom of the pond with a wet unit weight of around 125 pcf (Appendix B).

3.9.1 SAMPLE PREPARATION

To evaluate the effects of RG in K_{sat} in highly compacted clays, the interchange soil was used to represent the low plastic clay (CL) at the bottom of the pond. A total of 9 soil specimens were compacted to a moist density of 125 pcf in a 4 in diameter by 4.6 in height mold according

to ASTM D698-12. The mold was coated with Rust-Oleum rust and corrosion protection before usage to minimize corrosion since testing was performed within the mold. The 125 pcf moist density was achieved by compacting the specimen to an 18.5 % moisture content based on the in-situ density of the Interchange soil. Weight and volume relationship characteristics of each specimen were determined such as void ratio, porosity, the degree of saturation, unit weight, dry unit weight and water required to achieve 100 % saturation. A qualitative 4 in diameter filter paper with a pore size of 2.5 µm was placed at the top and bottom of the sample followed by one porous stone at each end. All porous stones weights were recorded. Specimens were submerged in deionized water (see figure 3.3). Submerged samples were regularly weighted to identify the degree of saturation. Once the degree of saturation reached at least 98% (approximately 30 days), samples were ready for permeability testing.

Figure 3. 3 Submerged Specimens Subjected to Saturation before Falling Head

3.9.2 PERMEABILITY TESTING

3.9.2.1 FALLING HEAD PERMEABILITY & LEACHING EXPERIMENT

Once soil specimens reached 99 ± 1 % saturation level, the falling head permeability tests were performed. The K_{sat} value was measured along with the leaching solutions: DI water, DDI100, and DPW100. Permeability measurement and leachate collection were performed simultaneously. In Section 3.8 (low-density specimens), leaching cycles were measured by the

discharged leachate volume; while in this section, cycles were measured with time since a considerable discharged volume would last longer. The nine specimens were tested in three distinct leaching solutions and times (Table 3.3).

Table 3. 3 Specimen Testing Time and Leaching Solutions

Sample No.	Leaching Solution	Time tested (hours):
1	DI	48
2	DI	120
3	DI	168
4	DDI100	48
5	DDI100	120
6	DDI100	168
7	DPW100	48
8	DPW100	120
9	DPW100	168

A centrifuge tube was connected to the outflow valve of the permeameter to prevent evaporation of the collected water. Once testing was completed, the soil was sliced in three equal parts for bound cation analysis (Figure 3.4). Both collected water, and top, middle and bottom slices were analyzed for cations and heavy metals in the ICP spectrophotometer.

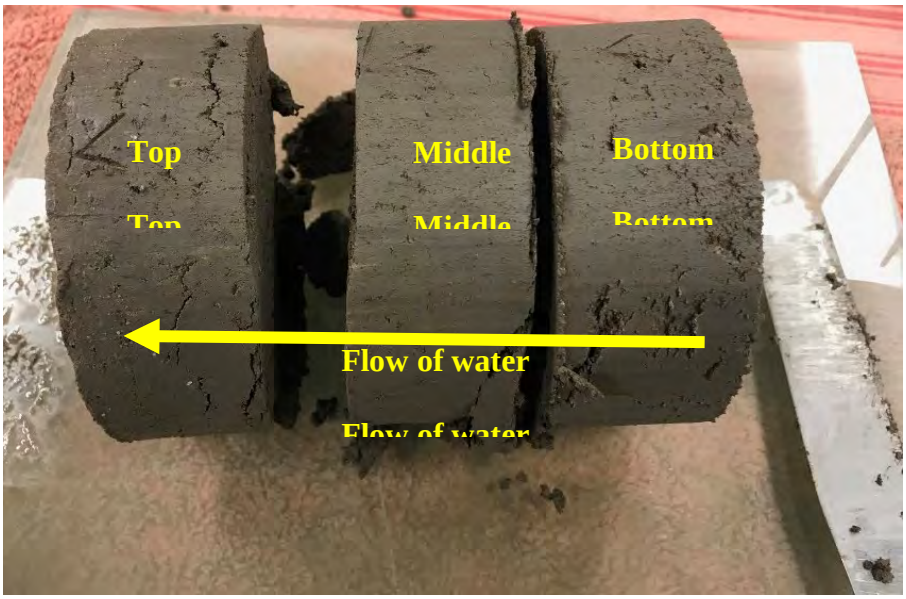

Figure 3. 4 Sliced Soil Sample after Completion of Permeability/Leaching Tests

3.10 METHOD OF APPLICATION OF RG IN RETENTION PONDS SIMULATION

Since ponds are typically filled with water, the methods like tillage, uniformly spreading gypsum on soil surface application, etc. are not practical. Therefore, the most practical method is to dissolve RG in the pond water through the mixing process. The advantages of this method are: a) it limits the presence of cardboard and cellulose material in the pond, b) maintains aerobic conditions during mixing, leached gypsum concentrations can be recorded, and c) would be cost-effective to purchase only the needed quantity of RG based on the solubility and volume of the pond filled with water. As part of the study, an experiment was designed to study the method of application of gypsum in retention ponds.

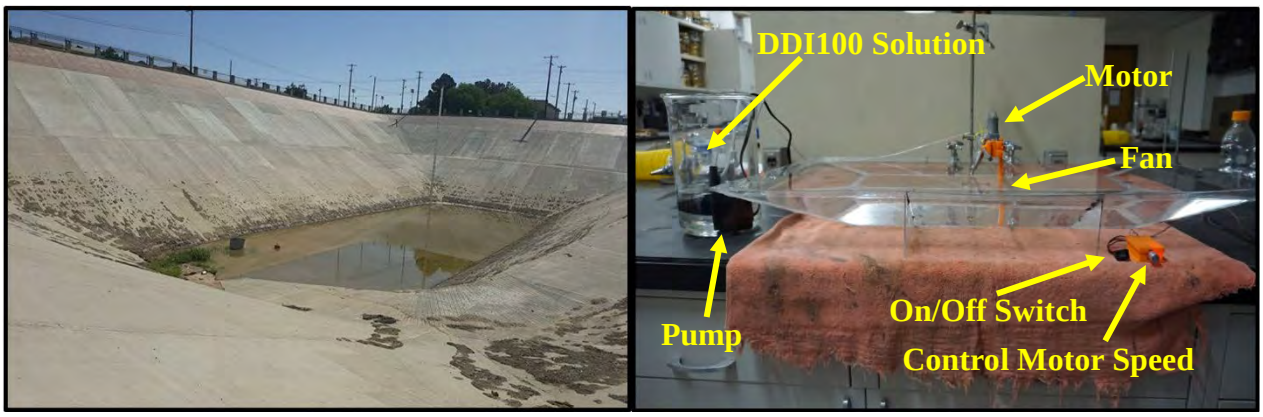

Figure 3. 5 Westbound Pond (left) and Small-Scale Pond Experiment (right)

This was achieved by simulating a small-scale retention pond similar to the Westbound Pond to 1" to 7' ratio model (Figure 3.5). Original dimensions of the rectangular bottom base of this pond are 168 ft. in length by 47 ft. in width with surrounding slopes of ½. All dimensions in the laboratory experiment were carried out proportional to the Westbound Pond. Table 3.4 summarizes the proportional dimensions used in the laboratory equivalent to a real scenario in Westbound Pond.

Table 3. 4 Small-Scale Evaluation of Westbound Pond

Dimension Category	Value	
	Westbound Pond (large-scale)	Laboratory (small-scale)
Filled Water Depth	21 ft	3 in
Depth of Fan	3 ft	7/16 in
Fans Diameter:	-	-
Fan 1	4.1 ft	0.59 in
Fan 2	5.5 ft	0.78 in
Revolutions/minute	630	630

*Westbound values are proximity values from the laboratory experiment, values were rounded up when converted.

This experiment considers only one mixer located at the middle of the pond. Two simulations were performed using one and two fans with 630 rpm. The depth of the fan is measured

from the center (point of rotation) of the fan to the top of water level in the pond. Because of the geometry, shape, and designs of different retention ponds, critical points can be scattered throughout the pond, at which gypsum is not dissolved completely. For example, a point at the center of the pond may experience a higher dissolution rate, than a point at the corner of the pond. This is due to the flow that is produced by the mixer in a confined volume. To understand the movement of water caused by a mixer positioned at the center of the pond, food coloring was dropped in front of Fan 1 and Fan 2 to visualize and determine the critical points in this rectangular shape designed ponds. Both fans demonstrated a movement of water as in Figure 3.6.

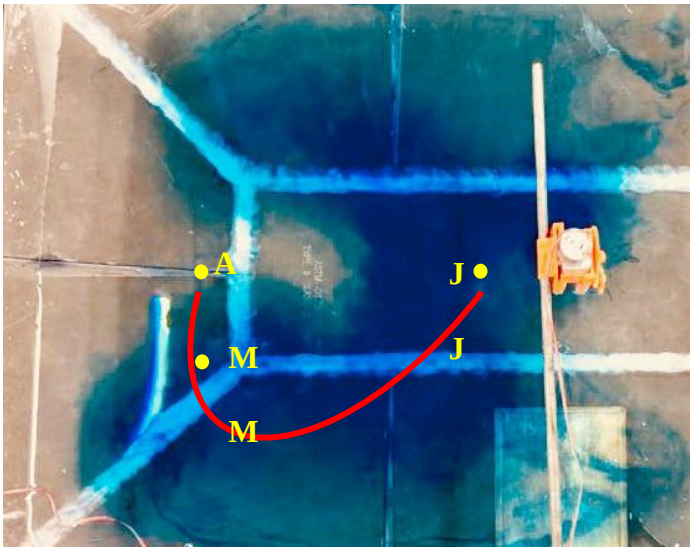

Figure 3. 6 Movement of Dye in Water

Critical points identified in this experiment were point J, A, and M. The simulation consisted of adding DDI100 solution in front of the fan at a speed of 100 mL per minute. At the critical points J, A, and M, 15 mL extractions of water samples were performed at 0.5, 1, 2, 3, 5, 10, 20, and 30 minutes using a pipette. Extraction points location is included in Figure 3.7.

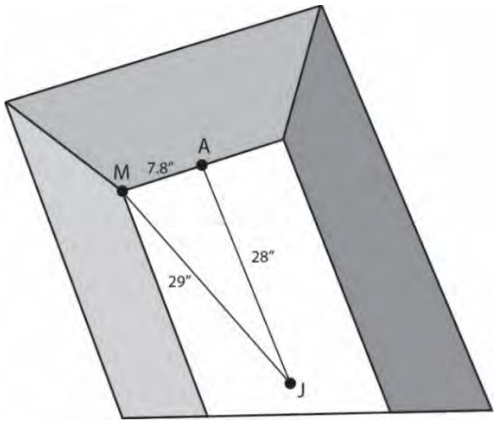

Figure 3. 7 Extraction Points

This procedure was performed one time for Fan 1 and Fan 2, with the same experimental characteristics as shown in Table 3.4. Extracted solutions were then analyzed for calcium concentrations using the ICP spectrophotometer. The dimensions and parts of the fan are included in Appendix F.

3.11 DIFFUSION RATE OF RG

Diffusion is a primary factor that contributes to the spreading of gypsum in water. Thus, it will be beneficial to identify how long will it take to disperse the gypsum fully in the water. To determine an accurate value for gypsum's diffusion, it requires to have control over specific factors that affect the diffusion of a solute in a solvent such as a temperature, volume, distance, area, the viscosity of the solvent, and among others. These contributors were controlled in the laboratory which may not be the case in the field. These contributing factors that are beyond control are debris on the pond, the change in temperature, combustibles, chemicals, and the equipment used for mixing, etc.

Taking into account the calcium concentration from the ICP results on the dissolution of gypsum, the diffusion rate at which the calcium cations disperse throughout the pond were calculated using two equations: (3.1) Lebedev and Lekhov equation and (3.2) Stokes-Einstein

equation. Each equation considers different factors, and with such, a range can be calculated to compare how the diffusion rate diverges.

$$R_s = dC/dt = k_e S' (C_m - C)^r / V \quad (3.1)$$

Where R_s is the rate of the dissolution reaction, (mg/L/sec); K_e is the diffusion coefficient, (mm^2/sec); C_m is solute concentration at equilibrium, (mg/L); C is solute concentration at time t, (mg/L); V is the solution volume, (mm^3); S' is the specific surface area, (mm^2); and r is the apparent reaction order.

$$D = kT / 6\pi\mu r \quad (3.2)$$

Where D is diffusion coefficient of the solute in solution, (mm^2/sec); k is Boltzmann Constant, (1.38064852E-23 m^2*kg/s^2*K); T is absolute temperature, (K); μ is viscosity of water at T, (mPa*s); and r is radius of the solute molecule, (mm).

Table 4.7 was developed that summarizes calcium diffusion coefficients (cm^2/sec) calculated from equations (3.1) and (3.2). Also, a referenced diffusion coefficient obtained from a peer-reviewed articles. Also, equation (3.3) Einstein's approximation equation was used to relatively calculate the time in days it takes for the calcium cation molecule to travel from the point of discharge (Point D) to each of the extraction points (Figure 3.7).

$$t = x^2 / 2D \quad (3.3)$$

where t is the elapsed time since diffusion began; x is the distance traveled by the solute in one direction, and D is the diffusion coefficient of the solute.

CHAPTER 4: RESULTS AND DISCUSSIONS

This study identified the significance of gypsum in ameliorating the hydraulic conductivity at different gypsum dosages. It is also identified the extent of cation exchange that occurs, especially the exchangeable sodium, magnesium, and calcium. Soil properties such as soil mineralogy, chemically and physical have different responses to gypsum applications.

4.1 SOIL PROPERTIES RESULTS

Table 4.1 summarizes the chemical, mineral and physical characteristics of the soil used for the experiment. Upper Valley and Interchange soils were classified as low plastic clays (CL) and west and site pond as silty sand (SM). Atterberg limits for Westbound and Site pond locations were outside the boundary in the plasticity chart and can be attributed to the presence of gypsum (Appendix B). The predominant clay mineral in these soils is montmorillonite, kaolinite, and illite (at particles <0.42 mm). All XRD patterns identifying clay fraction, influence of different treatments, soil identification and quantification (soil particles smaller than 0.42 mm) are included in Appendix D. The Upper Valley soil was observed to have the highest CEC and SSA as compared to other soils.

In terms of sodium concentration, Upper Valley soil, and Interchange soil was classified as "sodic" while westbound and site pond soil was classified as "normal" (based on Table 2.3 guidelines). Also, due to previous gypsum dosages in westbound and site pond, calcium concentrations were 17.79 and 8.98 $cmol^{+}\ kg^{-1}$, respectively in terms of soluble cations only. Bounded calcium was around the same range for all soils except for site pond soil. Since Westbound and Site pond has been already treated with gypsum, the ion concentrations may be out of bound.

Table 4. 1 Mineralogy, Chemical and Physical Properties of the Soils

Characteristic	Value			
	Upper Valley Soil	**Interchange soil**	**Westbound soil**	**Site soil**
USCS	CL	CL	SM	SM
Atterberg Limits	-	-	-	-
LL	31	25	19	18
PL	17	18	0	0
PI	14	6	Non-plastic	Non-plastic
Texture	-	-	-	-
Clay (%)	26	10	3	4
Silt (%)	30	41	22	22
Sand (%)	44	49	75	74
***SSA (m^2/g)**	2.12	1.86	1.37	1.56
EC (µs/cm)	466	209	2520	2500
pH	8.82	8.58	7.65	7.76
CEC ($cmol_+$/kg)	25	17.5	13	14
SAR (mmol $L^{-1})^{1/2}$	1.03	0.75	0.28	0.41
Soluble Cations ($cmol^+$ kg^{-1})	-	-	-	-
Ca^{2+}	1.98	2.14	17.79	8.98
Mg^{2+}	0.32	0.18	0.74	0.36
Na^+	3.82	2.71	3.03	3.05
K^+	0.35	0.18	0.25	0.19
Bound Cations ($cmol^+$ L^{-1})	-	-	-	-
Ca^{2+}	37.48	34.34	35.15	53
Mg^{2+}	4.07	2.40	1.53	0.9
Na^+	10.67	0.98	0.79	0.77
K^+	1	0.63	0.6	0.4
****Mineralogy**	-	-	-	-
Montmorillonite, %	5.28	3.17	1.37	1.43
Kaolinite, %	4.57	1.47	3.26	1.78
Illite, %	2.3	12.97	5.92	4
Other minerals, %	87.85	82.39	89.45	92.79

*Specific surface area was determined using the laser diffractometer for particles <0.074 mm
**Soil mineralogy was quantified for soil fragments <0.42 mm

The surface morphology of soil was evaluated and is included in Figure 4.1 for upper valley soil. The image is magnified to a magnification reaching 10 µm. Image to the right represents a typical surface morphology of clay rich in smectite (montmorillonite) substance (Mudzielwana, Gitari, & Msagati, 2016). Montmorillonite under SEM images can be identified because it has a more open-textured smooth surface. Individual crystal platelets cannot be seen to much in the montmorillonite because they are very tiny and dispersed, producing more cohesive films

structured of textural units (Bohor & Hughes, 1971). Based on the surface morphology, it can be concluded that upper valley soil had the highest montmorillonite mineral concentration in comparison to other soils evaluated in this study.

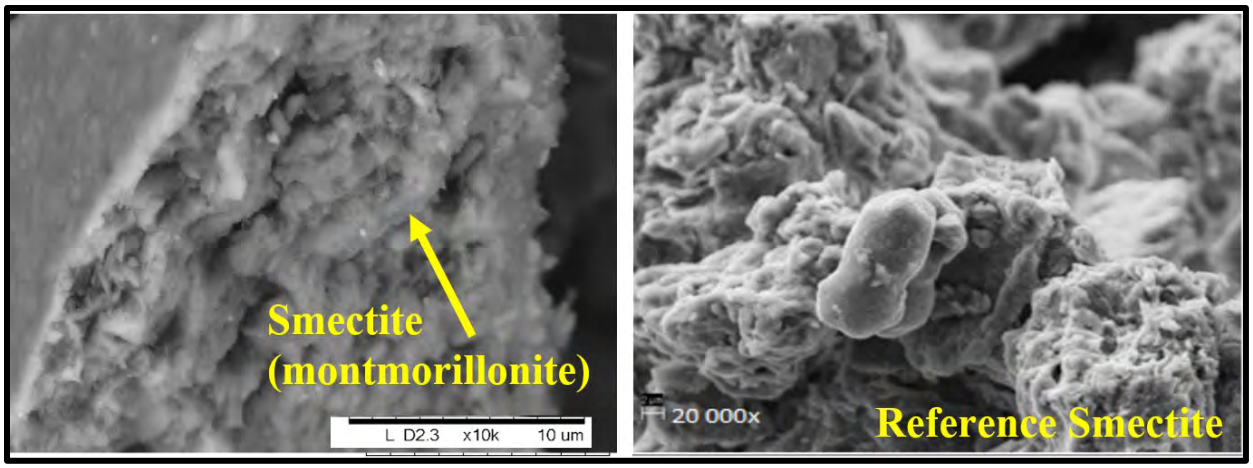

Figure 4. 1 SEM of the Upper Valley Clay Particles (left image) and Referenced Rich-Smectite Clayey soil (right image from Mudzielwana et al., 2016).

4.2 RG PROPERTIES RESULTS

The RG analytical results are summarized in Table 4.2. The major components of RG were identified to be Ca^{2+} and SO_4^{2-}. The concentration of Ca^{2+} was approximately 250,518 mg/kg while the SO_4^{2-} concentration was approximately 595,978 mg/kg. An analytical report (see Appendix C) provided by El Paso Recycler (EPR) shows the typical concentrations of mined gypsum in mg/kg based on a study report reported by KMT labs in Newton, IA. The calcium concentration of the mined gypsum is roughly 162,000 mg/kg, and the sulfur concentration is roughly 87,800 mg/kg. Other minor and trace elements were similar to the naturally mined gypsum (from the analytical report). Since the calcium concentration from the RG analysis is similar to the analytical report of mined gypsum, the use of RG is favorable because it provides a similar amount of calcium as the

mined gypsum. The use of RG also contributes to cost savings as well as conservation of natural resources.

Table 4. 2 RG Analytical Results

Constituent	Units: mg/kg	Method	Constituent	Units: mg/kg	Method
Calcium, Ca	250,518.4	*EPA 6010B*	Potassium, K	7782.84	*EPA 6010B*
Magnesium, Mg	1416	*EPA 6010B*	Sodium, Na	5816	*EPA 6010B*
Phosphorous, P	106.60	*EPA 6010B*	Arsenic, As	31.98	*EPA 6010B*
Cadmium, Cd	1.33	*EPA 6010B*	Chromium, Cr	4	*EPA 6010B*
Copper, Cu	4	*EPA 6010B*	Iron, Fe	577	*EPA 6010B*
Lithium, Li	4	*EPA 6010B*	Manganese, Mn	28	*EPA 6010B*
Nickel, Ni	6.67	*EPA 6010B*	Lead, Pb	6.67	*EPA 6010B*
Selenium, Se	4	*EPA 6010B*	Zinc, Zn	5.5	*EPA 6010B*
Inorganic Anion:			Nitrate, NO_3	458	*EPA 9056A*
Chloride, Cl	1,200	*EPA 9056A*	Sulfate, SO_4	595,978.4	*EPA 9056A*

The mineral structure of RG was evaluated using XRD, and the results are summarized in Table 4.3. The principal component of RG was gypsum with approximately 88 % of its total mineralogy, followed by calcite with 8 %, anhydrite with 2.81 %, and quartz with 1.27 %. Since mineral phases are manually identified, there could be other minerals present that may not have been not identified due to the overlapping peaks. The RG has less than 10% of the cellulose/paper material of the total weight composition with a sample standard deviation of 0.80.

Table 4. 3 X-Ray Diffraction Results for RG Composition

Recycled Gypsum Characteristic	Value (%)
Mineral:	
Anhydrite	2.81
Gypsum	88.15
Quartz	1.27
Calcite	7.77
Cellulose/Paper Material:	9.94

4.3 COLLECTED WATER ANALYSIS

Chemical characteristics of PW are shown in Table 4.4. PW has small concentrations of Ca^{2+} (24.6 mg/L) and SO_4^{2-} (17.6 mg/L). EC was measured as 267 µS/cm and a pH of 7.73 which is considered to be of good quality. EPA recommends well owners to maintain the pH levels of 6.5-8.5 and is considered to be secondary maximum contaminant levels (SMCL) for drinking water and is considered aesthetic to be in nature.

Table 4. 4 PW Chemical Characteristics

Ion Concentrations:	**Pond Water (PW)**	
Ca^{2+}	24.6	mg/L
K^{+}	11.85	mg/L
Mg^{2+}	1.8	mg/L
Na^{+}	9.42	mg/L
Cl^{-}	14.2	mg/L
SO_4^{2-}	17.6	mg/L
Electric Conductivity (EC)	267	µS/cm
pH	7.73	

4.4 DOUBLE RING INFILTROMETER RESULTS

Figure 4.2 demonstrates infiltration rates with respect to increase of gypsum dosages in RG spread on soil surface (GSS) application method. All infiltration tests were performed on soils with a moisture content of 5 ± 2 % and at a temperature of 90 ± 10 °F. Initially, the infiltration rates increased linearly as gypsum dosages are incrementally increased, until reaching a gypsum rate of 13.9 tons/acre. A subsequent increase in gypsum application rate significantly increased the infiltration rate to its maximum in both the inner (0.35 in./h) and outer rings (0.68 in./h). A further increase in gypsum dosage reduces the infiltration rates back to the linear trend. The results suggest that the optimum dosage content for this application method occurs at around 17.3 tons/acre (based on the area of influence). Factors that may contribute to the solubility during the infiltration test, and the sudden maximum peak, may be influenced by the thickness of the gypsum spread at the soil surface. Gypsum properties such as gradation, specific surface area, and temperature may

change the solubility during the testing timeframe at that specific gypsum dosage. The standard deviation for the inner and outer ring in the GSS application method was: 0.39 and 0.0255 in./h, respectively.

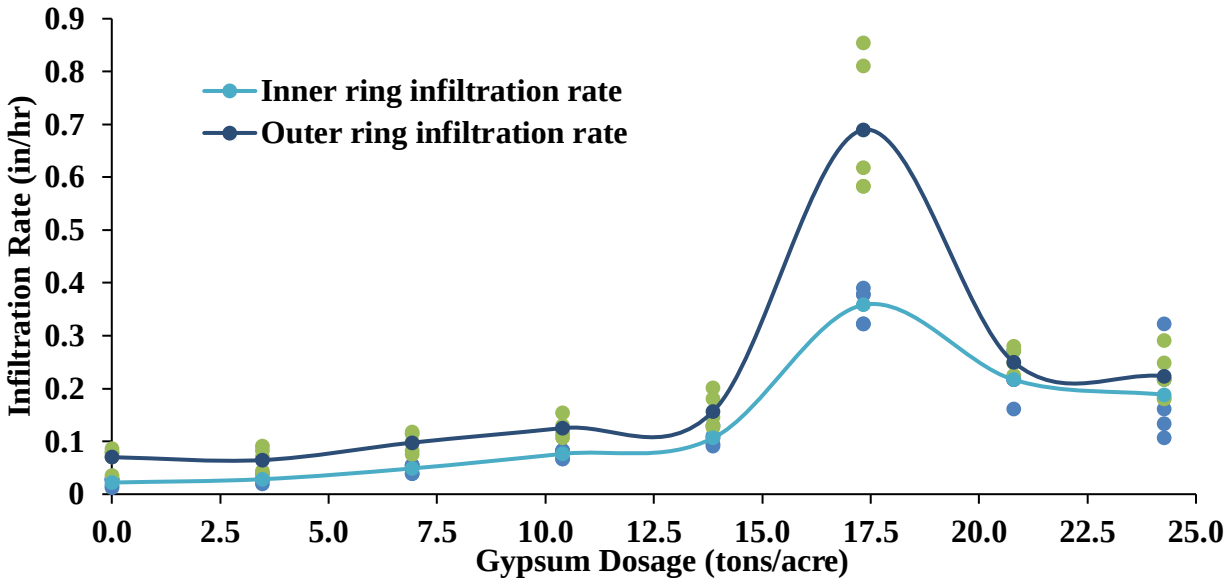

Figure 4. 2 Infiltration Rates with Gypsum Dosages by GSS Application Method

To identify the benefits of mixing gypsum in water, gypsum solutions were prepared with different concentrated dosage solutions (DDW application method), and the results are included in Figure 4.3. The behavior is relatively similar to the first application method with the only difference in terms of sudden peak. In both Figure 4.2 and Figure 4.3, the inner ring infiltration rate is slower than the outer ring. This occurs because the outer ring water flows downward in a vertical direction and horizontal towards its outer surroundings. Since the inner ring horizontal water flow is limited, the measured water flow from the inner ring will be lower in comparison to the outer ring. The maximum average infiltration rate in the inner ring was 0.40 in./h with DDW approach while 0.35 in./h infiltration rate was measured with a GSS approach. The outer ring average infiltration rate of 0.52 in./h and 0.68 in./h was measured with DDW and GSS applications methods, respectively.

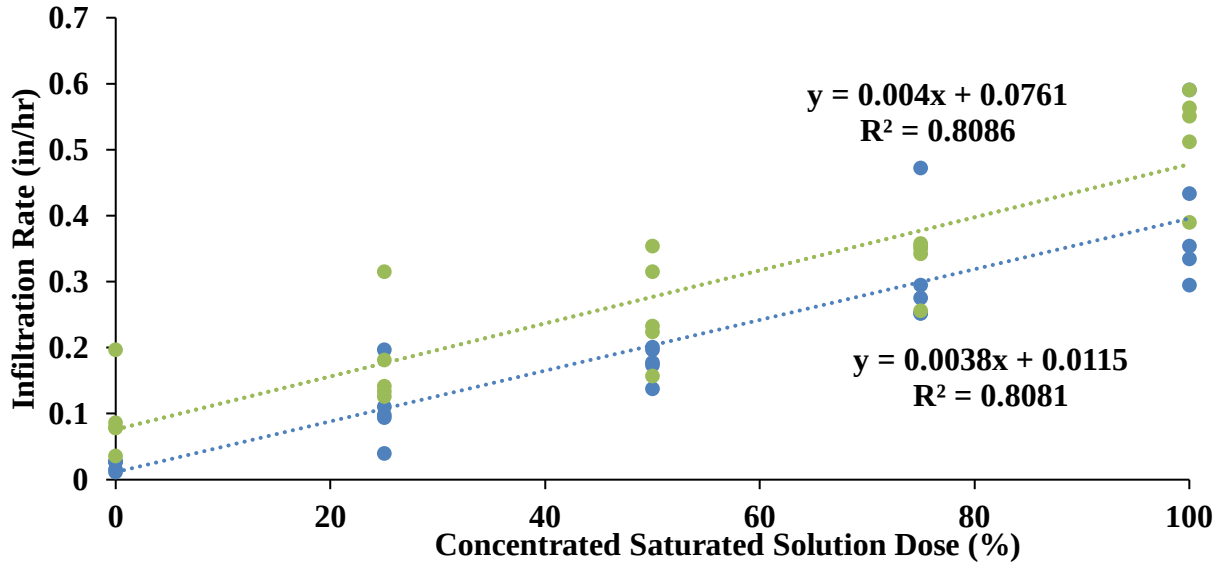

Figure 4. 3 Influence of Gypsum Dosages by DDW Application Method on Infiltration Rate

4.5 HYDRAULIC CONDUCTIVITY RESULTS

4.5.1 METHOD OF APPLICATION APPROACH RESULTS IN KSAT

The application of gypsum in all methods enhanced the hydraulic conductivity of the Interchange pond soil. Figure 4.4 presents the saturated hydraulic conductivities in the low-density specimens (90 ± 2 lb/ft^3). The hydraulic conductivity increased linearly as gypsum dosages were increased in all methods of applications. For the DDI application method, initial K_{sat} with DDI0 (DI with no RG), had a hydraulic conductivity close to 0.1 in./h as opposed to the DPW application method that had hydraulic conductivity close to 0.06 in./h.

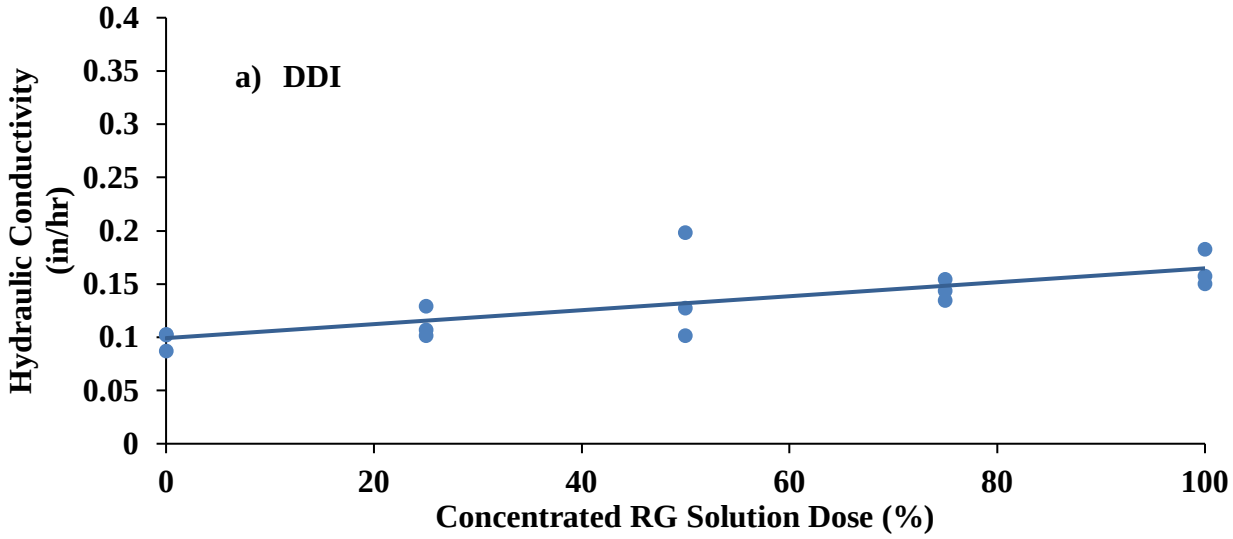
a) DDI
Hydraulic Conductivity (in/hr)
0.4
0.35
0.3
0.25
0.2
0.15
0.1
0.05
0
0
20
40
60
80
100
Concentrated RG Solution Dose (%)

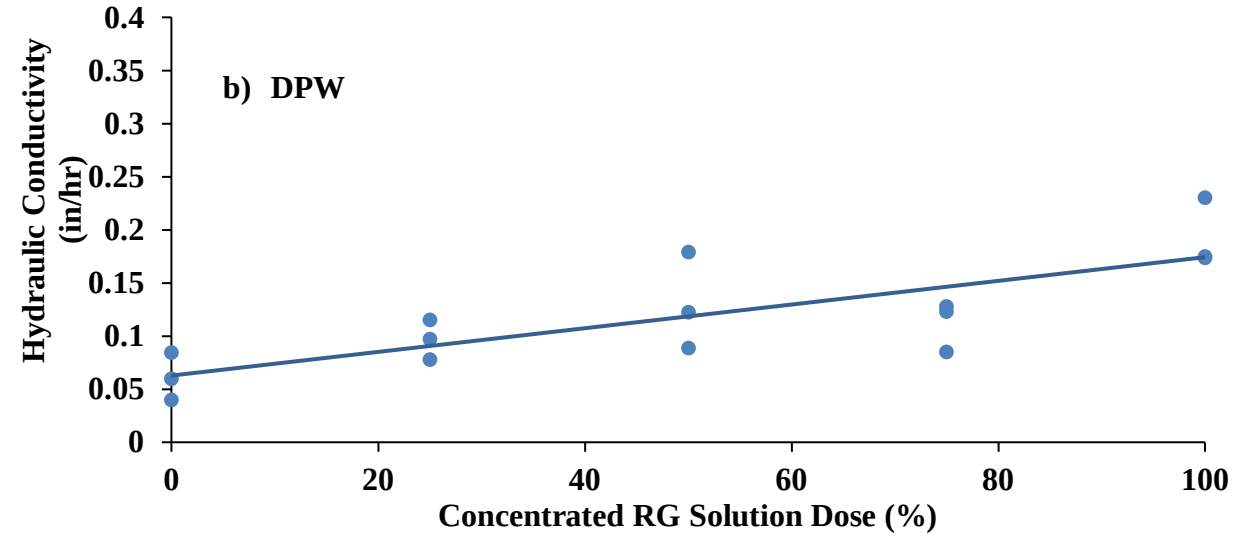
b) DPW
Hydraulic Conductivity (in/hr)
0.4
0.35
0.3
0.25
0.2
0.15
0.1
0.05
0
0
20
40
60
80
100
Concentrated RG Solution Dose (%)

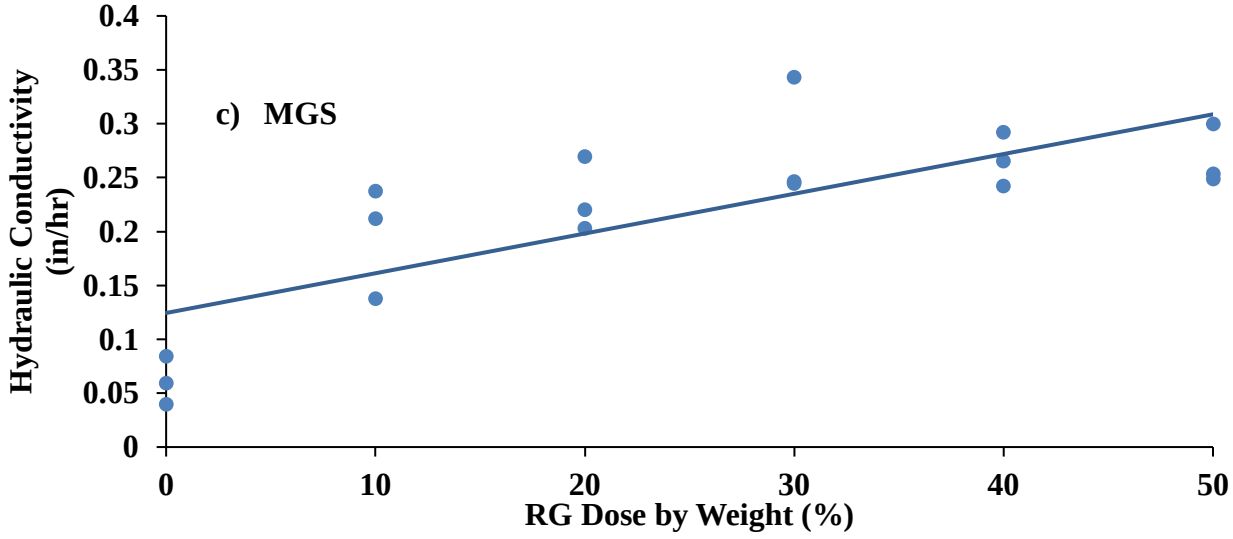
c) MGS
Hydraulic Conductivity (in/hr)
0.4
0.35
0.3
0.25
0.2
0.15
0.1
0.05
0
0
10
20
30
40
50
RG Dose by Weight (%)

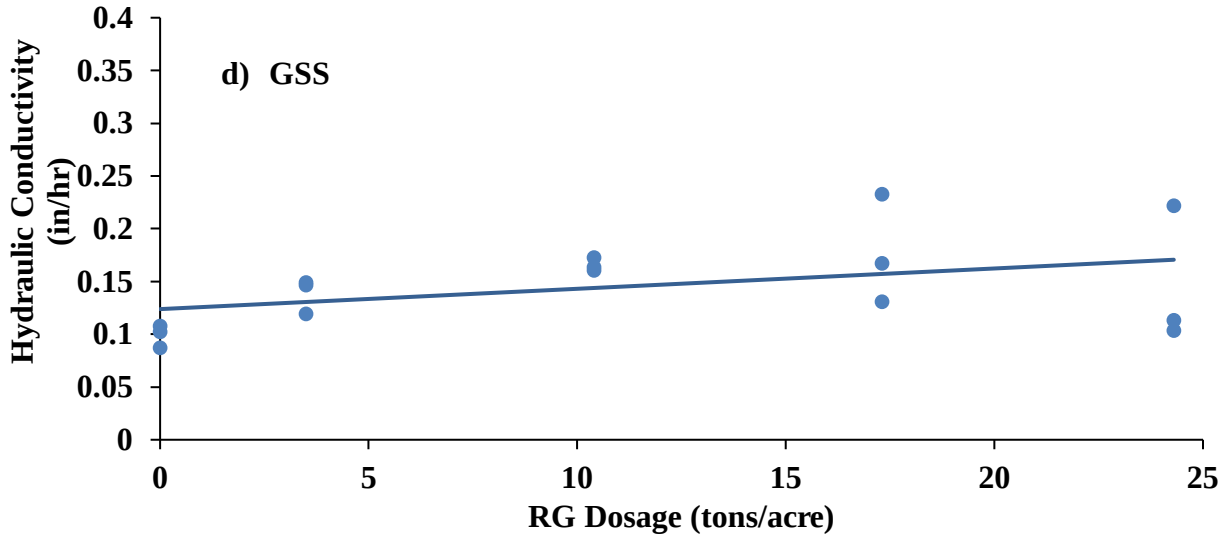

Figure 4. 4 Interchange Soil Hydraulic Conductivities with different RG Application Methods and Dosages: a) RG Dissolved in Deionized Water, b) RG Dissolved in Pond Water, c) RG Mixed in Soil, and d) RG Spread on the Soil Surface.

After continuous applications of RG solution, a maximum K_{sat} value of 0.17 in./h was reached with both DDI (with all RG concentrations) and DPW methods. The influence of saturating DI water and PW with RG would eventually deliver an approximately similar K_{sat} value. RG mixed with soil (MGS method), and DPW methods provided similar initial K_{sat} values. However, K_{sat} increased at a faster rate with MGS in comparison to DPW and DDI methods since the mixing RG in soil required mulching which reduced the density or increased the porosity of the soil. The process of mixing RG in soil decreased the density by approximately 6.5 % per increase in gypsum dosage. In the end, the total reduction in density was 27% at a maximum dosage that resulted in maximum K_{sat} value (0.15 in./h). For MGS application method, K_{sat} values increased 336 % from zero dosage to 50 % RG dosages because of reduction in density. On the other hand with GSS application method, the highest K_{sat} value was obtained with 17.3 tons/acre rate of application. Although the testing was performed at even higher dosage (24.3 tons/acre), the further increase in K_{sat} was not observed. The increase in K_{sat} value was linear and then plateaued. The peak of observed at 17.3 tons/acre was also obtained (Figure 4.2) while performing the double ring infiltration test in the field. Overall, the maximum K_{sat} enhancement of 115 % at the optimum dosages was observed with DDI, DPW, and GSS application methods.

4.5.2 FALLING HEAD RESULTS IN DDI AND DPW IN COLLECTED SOILS

Falling head permeability results are presented in Figure 4.5 for DDI, and DPW soil conditioning approaches followed on Interchange and Upper Valley soils. Although both soils were classified as CL (as per USGS classification), the permeability measured was different because of CEC, SSA, montmorillonite %, PI, and clay content being different (Interchange soil had relatively higher values in comparison to Upper Valley soil).

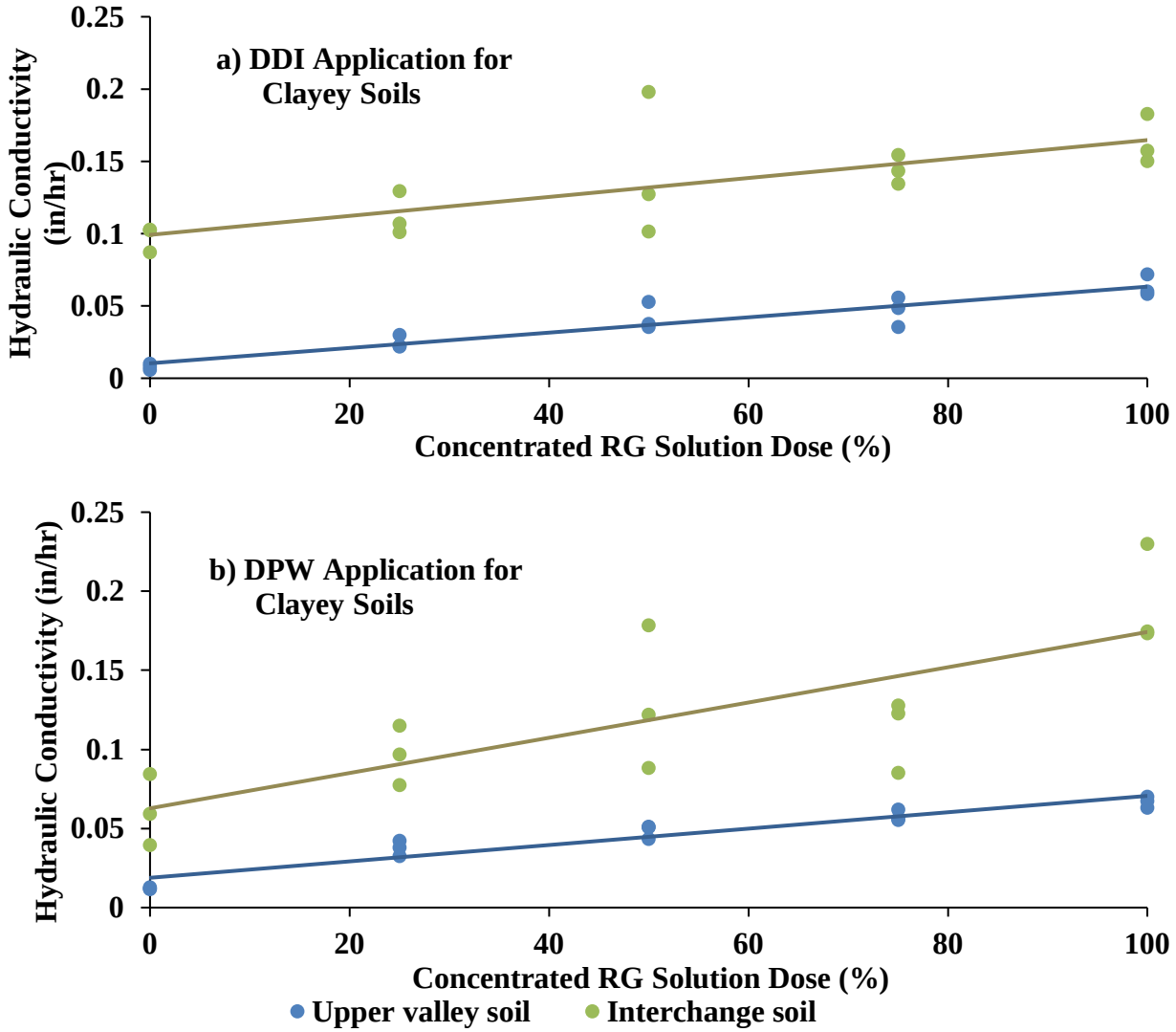

Figure 4. 5 K_{sat} of Upper Valley and Interchange Soils with Different Concentration of RG Solution Dosages (for DDI and DPW Methods of Applications).

For the DDI application method, K_{sat} of Upper Valley soil starts at an average value of 0.007 in./h (0% saturation) and then linearly increases to 0.063 in./h (at 100% saturation). The RG

significantly increased K_{sat} by approximately 693 % (from 0% saturation to 100% saturation). In the Interchange soil, the K_{sat} is roughly 0.097 in./h (for DDI0) and increases to a maximum value of 0.163 in./h (for DDI100) with an overall increase of 679 %.

The K_{sat} values, for DPW application method, behaved similarly with an increase in RG concentration. The K_{sat} value for Upper Valley soil with DPW application method was 0.012 in./h. It was observed to be slightly higher in comparison to DDI0 (K_{sat} value of 0.007 in./h) and can be attributed to the presence of Ca^{2+} ions (based on the chemical analysis of PW). With an increase in RG dosage, the K_{sat} values reached a maximum value of 0.067 in./h which is similar to the DDI method. Interchange soil in DPW application method exhibits the same linear behavior. The K_{sat} value for the Interchange soil at DPW (0% saturation) is 0.061 in./h and increased to 0.19 in./h at DPW (100% saturation). The overall increase in K_{sat} value was observed to be 215 %.

For Westbound and Site soils, the RG dosage had minimal influence on K_{sat} values. Figure 4.6 showed Westbound and Site soil response in terms of K_{sat} values when RG dosages were monotonically increased up to 100 % (DDI100). In the DDI (0% saturation) application method, Site and Westbound K_{sat} value were 0.52 and 0.70 in./h, respectively. Site soil showed a total 6 % increase, reaching a maximum K_{sat} value of 0.54 in./h (for 100% saturation) while Westbound initial K_{sat} rate remained constant with increase in RG dosage. The minimal influence of RG dosage on K_{sat} can be attributed to the soil type. Both Westbound and Site soil were classified to be sandy soil.

Similarly, in DPW application method, K_{sat} value enhancement was minimal. Site soil initial K_{sat} value was observed to be 0.45 in./h, once the saturated solution was applied, K_{sat} value increased to 0.48 in./h, with a total increase of 8 %. Westbound soil initial K_{sat} value was 0.64 in./h and was increased to 0.68 in./h, with an overall increase of 6 %.

The influence of RG dosage in sandy soils was minimal. It can be attributed to the previous application of RG dosages, minimal clay content (3 to 4 %), lower montmorillonite content (1.37 % and 1.43 %), and soils being classified as non-plastic soils.

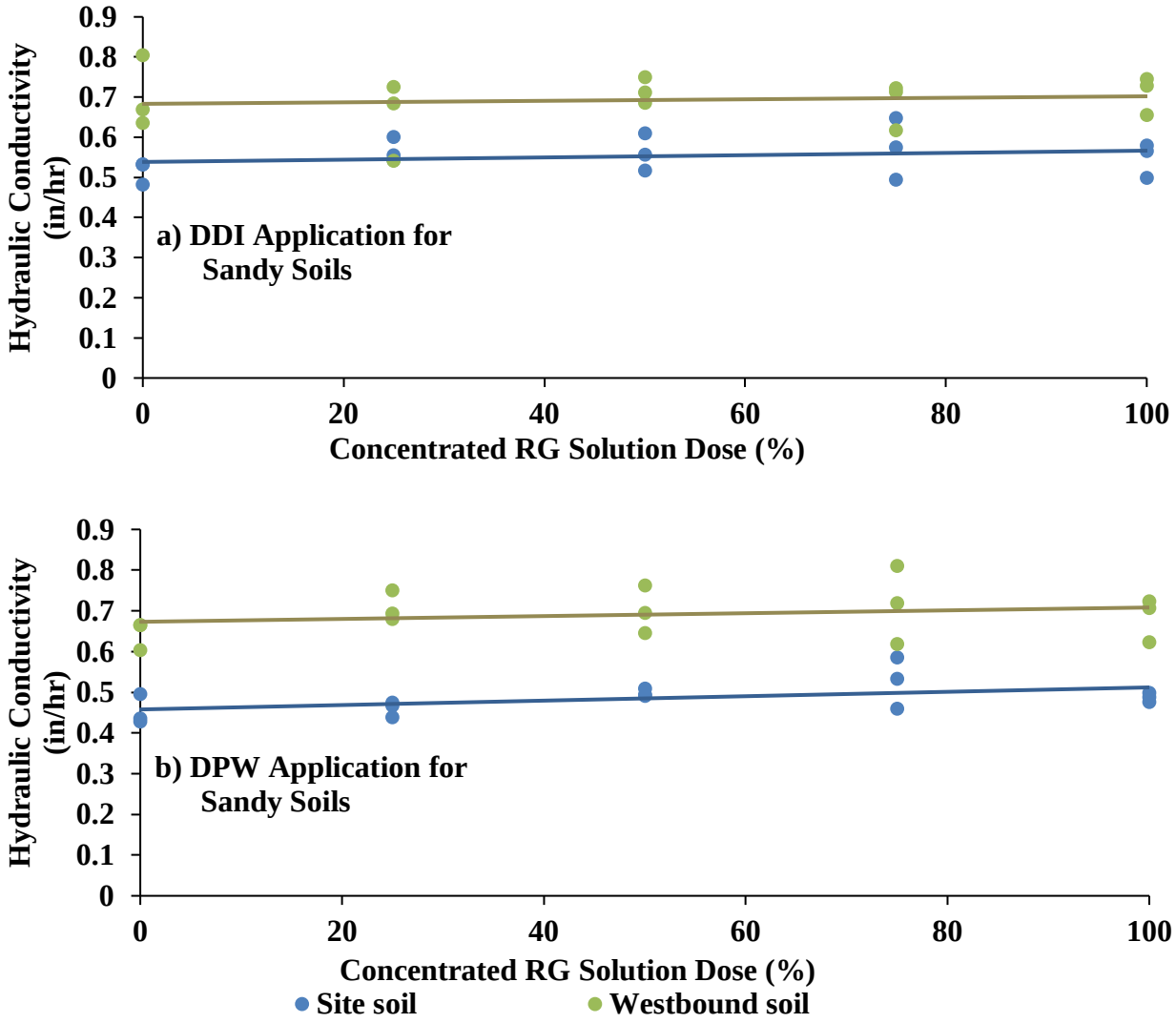

Figure 4. 6 K_{sat} of Westbound and Site Soils with different RG Dosages

4.6 LABORATORY LEACHING RESULTS

Since permeability enhancement depends on exchangeable ions, it is necessary to identify the chemical properties of solution applied (input) and solution leached (output) from the soil specimens. Table 4.5 shows the chemical properties of the applied solutions to the soil specimen. The first column summarizes the chemical properties of the PW collected from the site. The second and third column summarizes the chemical properties of the DDI100 (deionized water with 100% RG) and DPW100 (pond water with 100% RG). The electric conductivity and pH were measured for DDI100 (2.48 mS/cm and 7.37) and DPW100 (2.42 mS/cm and 7.17) before performing the leachate experiment.

Table 4. 5 Summary of Leachate Chemical Properties

Ion Concentrations:	Pond Water (PW), mg/L	DDI100, mg/L	DPW100, mg/L
Ca^{2+}	24.6	832	889
K^{+}	11.85	19.5	19.94
Mg^{2+}	1.8	3.5	0.88
Na^{+}	9.42	14.5	4.6
Cl^{-}	14.2	19	17
SO_4^{2-}	17.6	1,490	1749.1

The experiment to identify chemicals leaching out of the soil was performed on all four selected soils. The results for the Upper Valley and Westbound soils are discussed in this section while Interchange and Site pond results are included in Appendix G. The behavior of clayey and sandy soils was similar. In other words, the leachate obtained from both clayey soils was similar while the leachate obtained from both sandy soils was also similar.

Figure 4.7 summarized the calcium and sodium concentrations obtained after each test was completed corresponding to different application cycles (30 mL, 80 mL, and 130 mL) and application method for the Upper Valley soil. In Figure 4.7(a1) calcium concentration was found to be 200 mg/L on average in both the top and bottom sliced specimens from the soil. Collected water had an approximate average calcium concentration of 145 mg/L. Although high concentrations of sodium were leached from the soil (Figure 4.7 a2), the leached sodium ions reduced with an increase in application cycles (from 30 to 130 mL) and was significantly different in the leachate solution.

With increase in RG dosage, the calcium ion concentration increased from 200 to 300 mg/L with increase in RG dosage from 0 (DI) to 100% saturation (DDI100 and DPW100). The results also suggest that calcium replaced sodium ions because leachate (collected) had a higher concentration of sodium ions (Figure 4.7 a2, b2, and c2). Although higher sodium ion concentration (400 mg/L) was measured with DI application, the sodium ion concentration in the leachate also increased to 800 mg/L for DDI100 and 650 mg/L for DPW100. This can be attributed

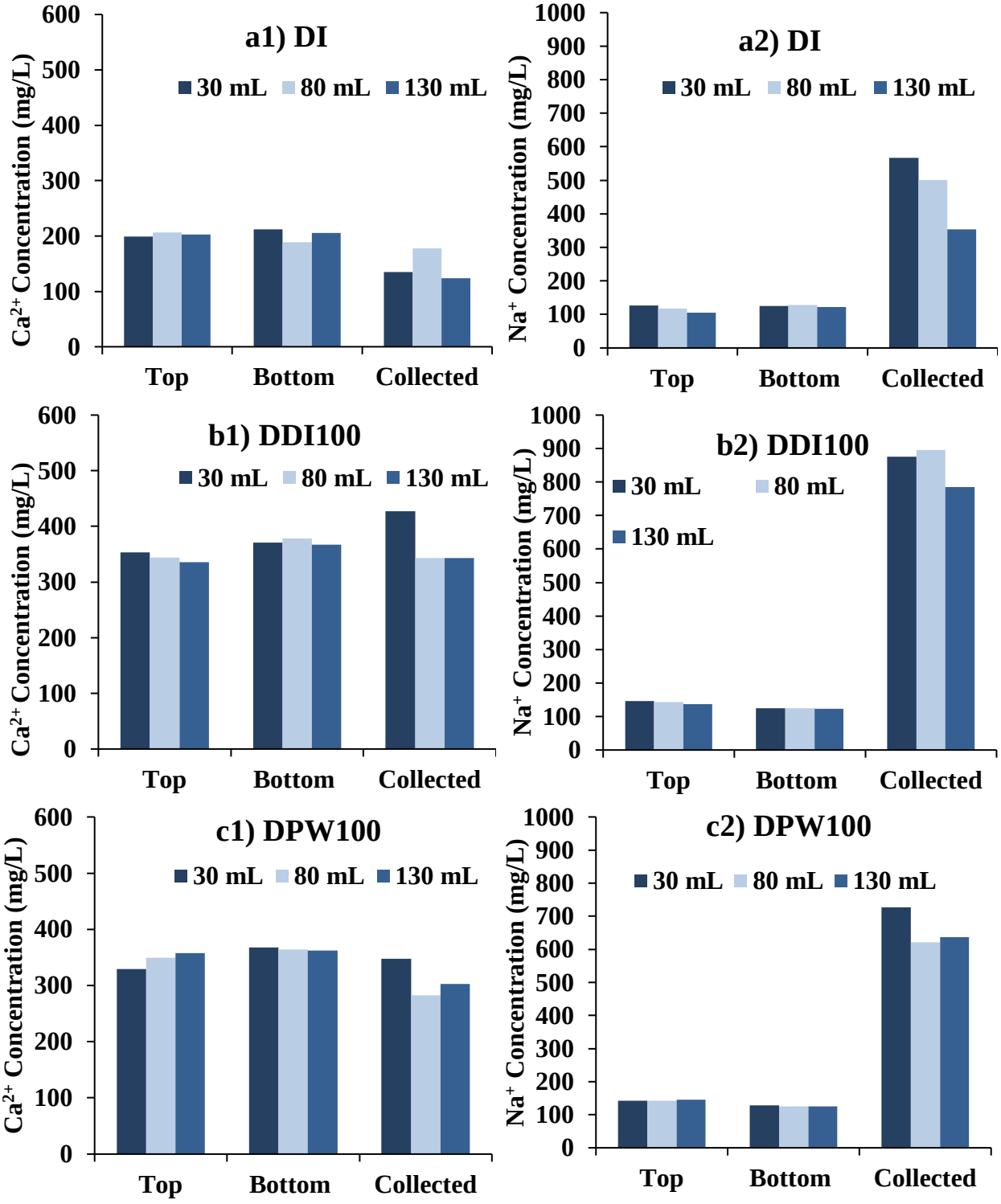

Figure 4. 7 Upper Valley Soil Calcium and Sodium Concentrations after 30, 80, and 130 mL Application Cycles with a) DI, b) DDI100, c) DPW100.

to calcium cations leaching through the soil specimen, exchanging sites with sodium, causing leaching of sodium and adsorption of calcium cations on clay particles.

In the collected solution (Figure 4.7b1) for application cycles 30, 80, and 130 mL, the calcium ion concentration was higher in the collected leachate from 50% to 40% indicating that all of applied calcium was not adsorbed by the soil. In Figure 4.7(c1), RG dissolved in DPW increased the calcium concentration similar to Figure 4.7(b1). In the collected solution (Figure 4.7c1), roughly 39 to 31 % of the calcium ions leached because of unavailability of exchangeable ions in the clayey soil.

Overall, the results presented in Figure 4.7 suggest that calcium ions replace sodium ions in the soil to enhance infiltration rates by flocculating the soil. Other cations such as magnesium and potassium may also increase or decrease the availability of exchangeable calcium ions.

Since RG enhanced K_{sat} due to exchangeable cations, the electrical conductivity (EC) of the leachate was performed to identify the presence of salts after different application cycles. The results of analyses are included in Figure 4.8. With DI water, the initial measured EC was between 2.09 and 2.8 mS/cm. The increase in RG dosage increased the EC to higher values (approximately by 1 mS/cm). The enhancement in EC was on an average higher with DD100 in comparison to DPW100. Additionally, the EC values decreased with increase in application cycles.

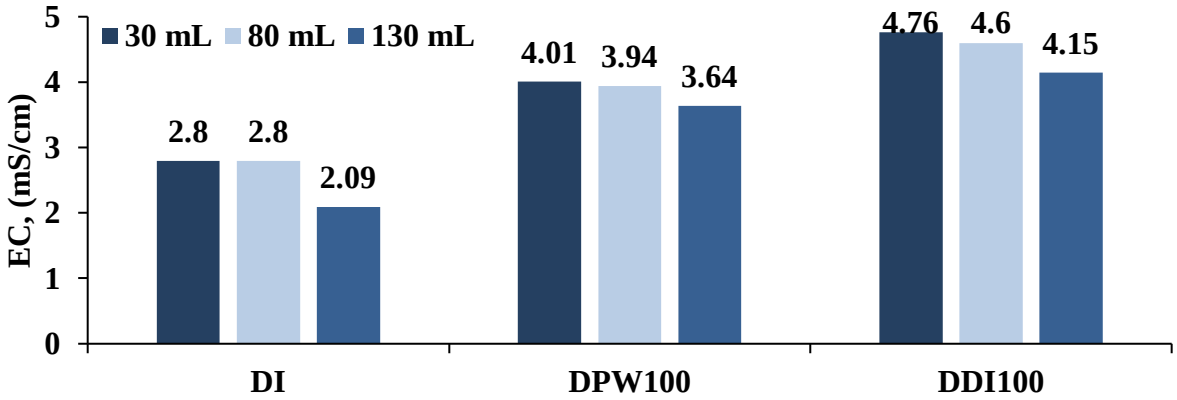

Figure 4. 8 Electric Conductivity (EC) Measurements of the Collected Solutions at different Application Cycles (for Upper Valley Soil).

DDI100 shows a higher electric conductivity comparable to DPW100 and DI. The high EC values in DPW100 and DDI10 are principally increased by the flushing of soluble salts from the soil column. DDI100 experienced a decreased rate in EC value of 0.0061 mS/cm mL^{-1} of leaching cycle as opposed to DPW100 reducing the slope of 0.004 mS/cm with a coefficient of determination of 0.93 and 0.9 respectively.

In the leaching analysis of sandy (Westbound) soil, the impacts of cation exchange are demonstrated in Figure 4.9. When DI water was leached through the soil, high concentration of calcium ions was observed in the collected solution (Figure 4.9a1). The calcium concentration remained in the range of 350 to 500 mg/L as in DI and DDI100 application methods. Collected solution calcium concentration remained in the same range as other methods (600-700 mg/L). The presence of higher calcium concentration in the leachate suggest that most of the calcium is leaching out with minimal adsorption. The trend observed in Figure 4.9 is different than Figure 4.7 indicating that there are no exchangeable ions present in the soil that can be replaced by RG. Also, EPW had already applied dosage of RG in the Westbound pond, therefore, any exchangeable ions may have already been replaced.

In terms of sodium ion concentration, the influence of RG dosage is minimal. The sodium concentration was below 40 mg/L in the top and bottom section of the soil for all three application methods (DI, DDI100, and DPW100). The collected solution analysis indicated that more sodium ions are leaching out and the concentration reduces with increasing applications cycle (from 30 to 130 mL). The presence of higher sodium concentration in the leachate can be attributed to presence of soluble salts in the soil column. Therefore, the application of deionized water the soluble cations were flushed with deionized water. A trend could not be observed because the difference in soil samples and presence of RG as well as other chemicals in the soil. The Westbound pond has a higher level of runoff water present on the top of soil columns. Since the runoff water is from various locations, it has different chemicals present in the soil as well as water that made it difficult to estimate a trend. In general, the sodium concentration was relatively lower than clayey soils indicating that RG dosage will minimally influence infiltration by flocculation.

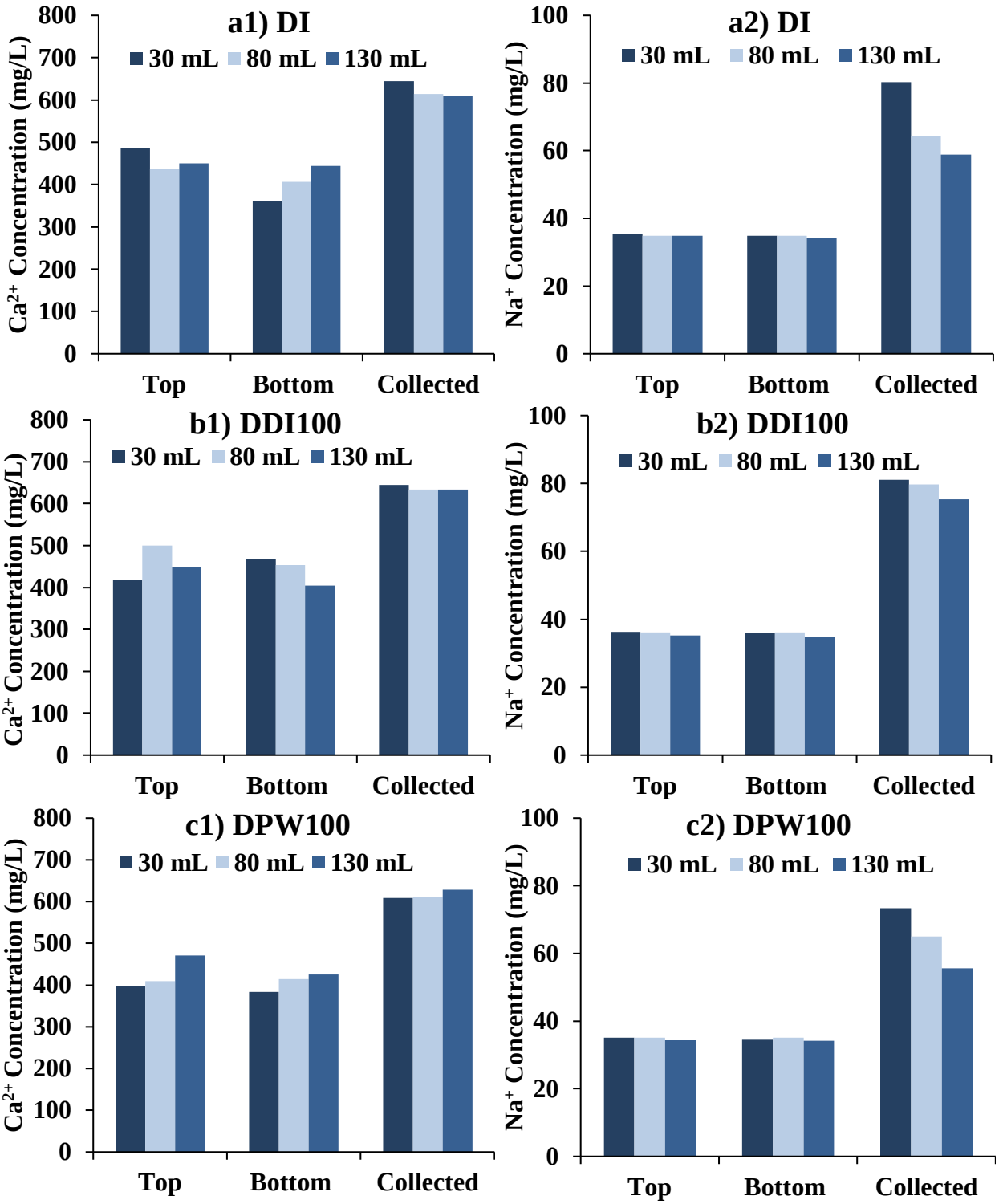

Figure 4. 9 Westbound Soil Calcium and Sodium Concentrations after 30, 80, and 130 mL Application Cycles with a) DI, b) DDI100, c) DPW100.

As of the flushed sodium that was collected, sodium concentrations decreased as higher leaching cycles would percolate, with a decreasing rate of 0.2 mg/L mL^{-1} leaching cycles. When DDI solution was leached (Figure 4.9b1)), a small concentration of calcium was adsorbed by the clay particle in the top and bottom section. In terms of the collected solution, roughly 76 % of calcium leached and 24 % remained in the soil column. The top and bottom sodium concentration remained the same regardless of application method. The measured sodium concentrations decreased with increase in application cycle from 30 to 130 mL. Sodium concentration in Figure 4.9(c2) was uniform in the top and bottom sections of the soil, and the collected solution decreased linearly at a rate of 0.2 mg/L mL^{-1} of leaching cycle with a coefficient of determination of 0.99.

The electric conductivities (EC) of the collected solutions of Westbound soil are shown in Figure 4.10. Low variation behavior is observed since westbound soil sustains RG from previous applications. The small discrepancy observed can be caused by the leaching of other salts.

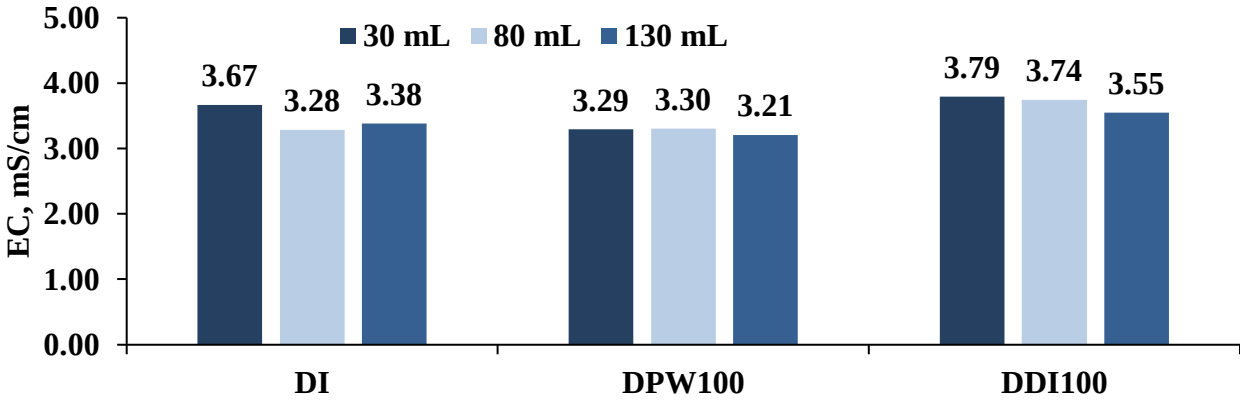

Figure 4. 10 Electric Conductivity Measurements of the Collected Solutions at different Application Cycles and Leaching Solutions (for the Westbound Soil).

4.7 RBCA TOOLKIT FOR CHEMICAL RELEASES

The transient groundwater modeling result using the RBCA Toolkit for chemical releases is discussed in this section. Since RG is composed of various trace elements, this study consisted of analyzing the leaching pathways that may contaminate groundwater. The source is considered

from the point at which water has left the infiltrated the soil column and reached the groundwater table. Although various trace elements were evaluated, the arsenic trace element is discussed in this section only for the sake of brevity while remaining trace elements are included in Appendix E. The analysis was performed using the steady-state Domenico analytical solute transport model that assumes an infinite aquifer. The simulation was performed for "affected soils leaching to groundwater" with a rainfall intensity of 200 in./year to resemble stagnant water in the pond. Two receptors (wells) were simulated at 200 and 1,000 ft. away from the center of the pond, collinearly to the direction of the groundwater flow.

Figure 4.11 demonstrates the leaching concentrations as a.) *concentration vs. distance from the source for a given time* and b.) *concentration vs. time for the given distance from the source.* In Figure 4.11a, the leaching of arsenic was analyzed for a year and the maximum concentration of 6×10^{-4} mg/L was measured. In the steady state trend, it simulates as if the RG concentration is maintained constant throughout the year (input concentration values), meaning, water will leach the same concentration of arsenic throughout the year. In contrast, trend line "t=1.0 yr." water leaches RG from soil considering just the initial concentrations (input values) and dwindles as the ponding water passes through the soil column.

Figure 4.11b demonstrates the increase of arsenic concentration at the source. Initial arsenic concentration at the start was 3.0×10^{-4} mg/L and increased linearly to a maximum of 6×10^{-4} mg/L after approximately six weeks. After six weeks, the arsenic concentration minimally changed for the remainder of the year.

Constiuent: Arsenic
Source Medium: Affected Soils Leaching to Groundwater
Biodegredation: None

a) Concentration vs. Distance from source (for given time) Time (yr) 1.0

Distance (ft)		0	120	240	360	480	600	720	840	960	1080	1200
t = 1.0 yr	Conc. (mg/L)	5.9E-4	0.0E+0	0.0E+0	0.0E+0	0.0E+0	0.0E+0	0.0E+0	0.0E+0	0.0E+0	0.0E+0	0.0E+0
Steady-state		5.9E-4	5.3E-4	2.9E-4	1.6E-4	9.7E-5	6.4E-5	4.6E-5	3.4E-5	2.6E-5	2.1E-5	1.7E-5

Off-site1	Off-site2
MCL	MCL
200	1000
0.0E+0	0.0E+0
3.6E-4	2.4E-5
POE Concentration Limit (mg/L) 1.0E-2	1.0E-2

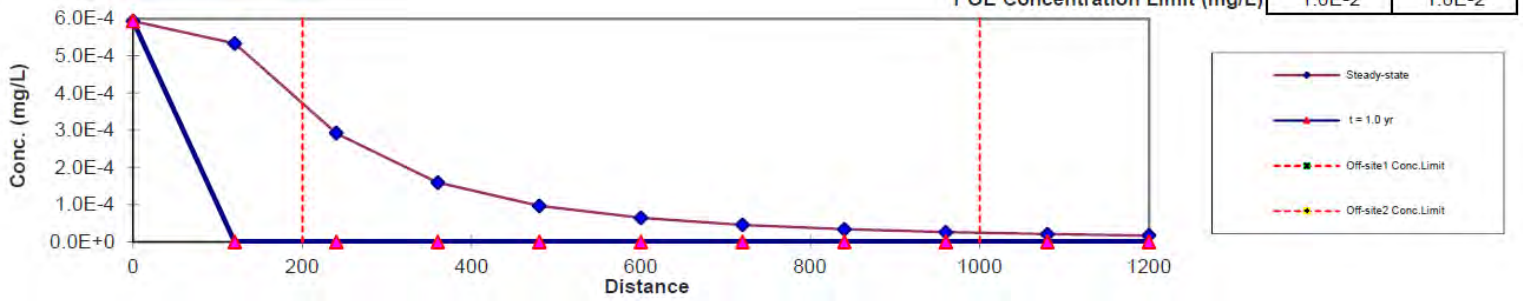

b) Concentration vs. Time (for given distance from source) Distance (ft) 0

Time (yr)		0	0.1	0.2	0.3	0.4	0.5	0.6	0.7	0.8	0.9	1
x = 0 ft	Conc. (mg/L)	3.0E-4	5.9E-4	5.9E-4	5.9E-4	5.9E-4	5.9E-4	5.9E-4	5.9E-4	5.9E-4	5.9E-4	5.9E-4
Off-site1 (200 ft)		0.0E+0	0.0E+0	0.0E+0	0.0E+0	0.0E+0	0.0E+0	0.0E+0	0.0E+0	0.0E+0	0.0E+0	0.0E+0
Off-site2 (1000 ft)		0.0E+0	0.0E+0	0.0E+0	0.0E+0	0.0E+0	0.0E+0	0.0E+0	0.0E+0	0.0E+0	0.0E+0	0.0E+0

Time to Reach Conc. Limit (yr)	
Off-site1	NA
Off-site2	NA

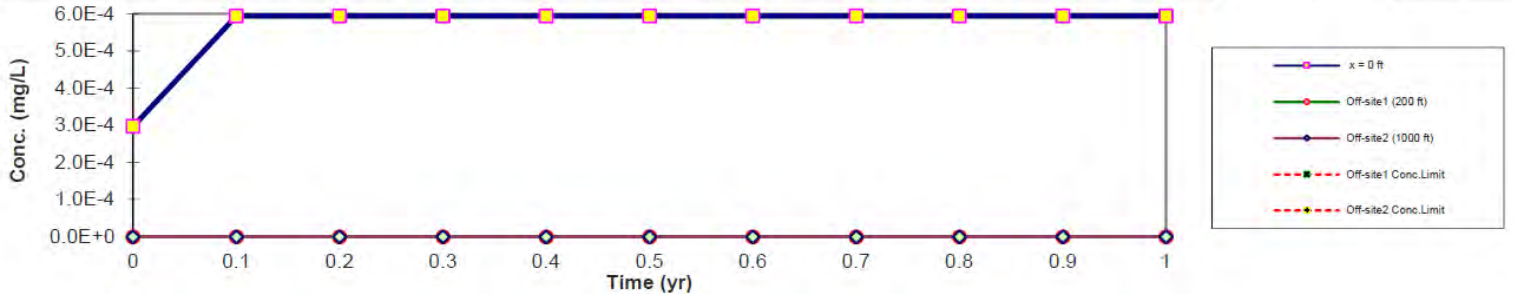

Figure 4. 11 Arsenic Leaching into Groundwater

4.8 HIGHLY COMPACTED CLAY RESPONSE TO RG APPLICATIONS

The influence of RG dosage on hydraulic conductivity (K_{sat}) depends on soil type. Therefore, the influence of RG on highly compacted clay (soil from Interchange pond) was evaluated, and the results are summarized in Table 4.6.

Table 4. 6 Interchange Soil Compacted Specimen Properties before Saturation

	RG Application Method:								
	DI			**DDI**			**DPW**		
Sample No.	1	2	3	4	5	6	7	8	9
Measure-ment Cycle, h	48	120	168	48	120	168	48	120	168
Void Ratio, e	0.66	0.65	0.676	0.69	0.67	0.69	0.8	0.68	0.67
Porosity, n (%)	39.9	39.6	40.3	40.8	40.4	40.8	44.5	40.3	40.2
Saturation, S (%)	79.5	80.7	78.17	76.6	78.0	76.7	65.8	78.2	78.7
Moist Unit Wt., γ (lb/ft^3)	126.9	127.7	126.1	125.0	126	125.1	117.2	126.1	124.4
Dry Unit Wt., γ_{dry} (lb/ft^3)	107.1	107.7	106.4	105.5	106.3	105.6	98.2	106.4	106.7
Saturated Unit Wt., γ_{sat} (lb/ft^3)	132.0	132.4	131.5	131	131.5	131.0	126.7	131.6	131.8
*Volume, V (mL)	76.9	72.0	83.1	90.3	83.7	89.9	143.7	82.9	80.9

*Volume required to fill air voids with water (achieve 100% saturation)

All samples were saturated before testing; therefore, densities and volume of voids may be slightly altered after saturation due to the induced pore water pressure. The dry density of most of the samples was within 106 ± 2 lb./ft^3 with the exception of Sample No. 7 that had a dry density of 98.2 lb./ft^3. Additionally, Sample No. 7 was porous with the highest void ratio of 0.8 while remaining soil samples had a void ratio of roughly 0.6.

Saturated hydraulic conductivities (K_{sat}) in response to DI, DDI100, and DPW100 are shown in Figure 4.12 at an interval of 48, 120, and 168 h after deionized water is allowed to enter in the specimen. An average K_{sat} value of 4.86 x 10^{-5} in./h is achieved with a standard deviation of 1.22 x 10^{-6} in./h. Overall, the K_{sat} value is enhanced by 24 % (Figure 4.12b) when RG dosage was increased from 0 to 100% saturation (DDI100). DDI100 solution boosts the K_{sat} value to an average of 5.98 x 10^{-5} in./h with a standard deviation of 4.48 x 10^{-6} in./h.

The K_{sat} of soil was slightly higher (Figure 4.12c) when the testing was performed using DPW100 (100 % saturation) in comparison to DDI100 water. Additionally, the standard deviation was also higher for in comparison to DDI100. The average K_{sat} value measured was 7.68 x 10^{-5} in./h with a standard deviation of 1.54 x 10^{-5} in./h. This standard deviation was the highest value obtained from the three different methods of RG applications. The maximum K_{sat} value of 0.9 x 10^{-5} in./h was obtained after 48 h in comparison to other cycles (120 or 168 h) even though the soil specimen had a similar density as compared to other samples. The only reason for higher conductivity can be attributed to the presence of more exchangeable ions in DPW in comparison to DDI.

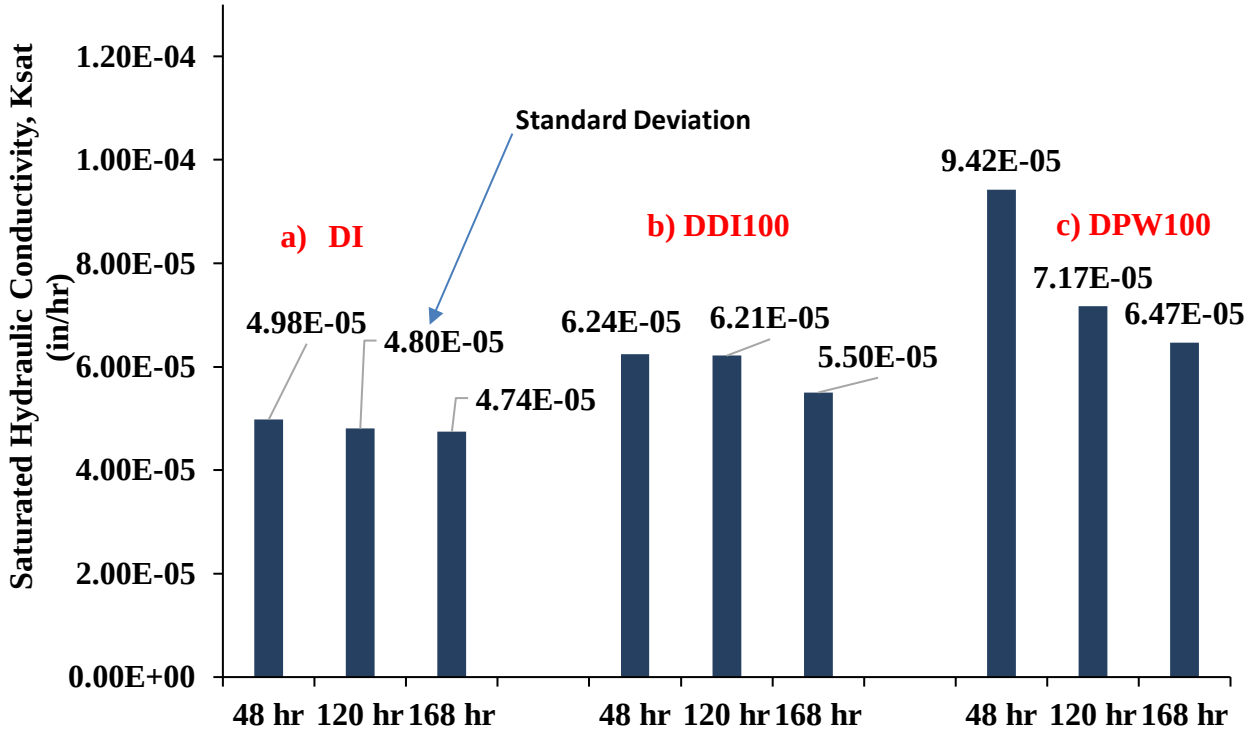

Figure 4. 12 K_{sat} for Interchange Soil with Increase in Leaching Times

As part of analyzing the saturated hydraulic conductivity summarized in Figure 4.12, the collected water and sliced sections (top, bottom, and bottom) were chemically analyzed for cations after the completion of the falling head permeability test. After completion of test, the specimen was cut in three equivalent portion and the soil fluid was analyzed along with concentration of ions in the collected leachate. The results of the chemical analyses are summarized in Figure 4.13. The parts a1, b1, and c1 shows the calcium ion concentration while a2, b2, and c2 show the sodium ion concentration.

With use of DI (zero dosage of RG), the ca ion concentration is roughly 300 mg/L and increases to roughly 500 mg/L when the RG dosage is increased to 100% (DDI100). However, the influence of RG dosage with pond water (DPW100) was lower (below 500 mg/L of calcium ion concentration). In terms of sodium ion concentration, the influence of RG dosage was minimal.

.

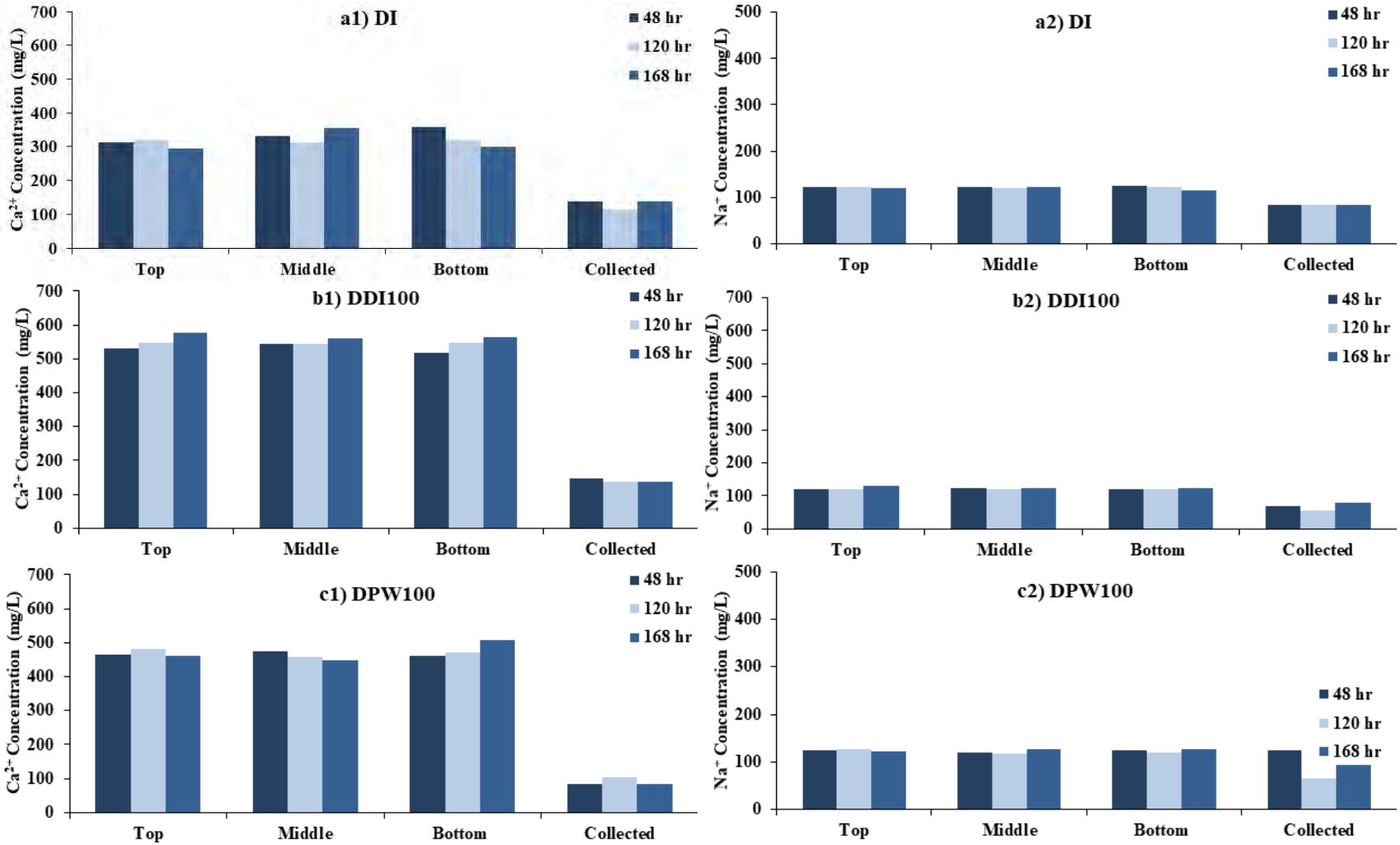

Figure 4. 13 Chemical Determination of Calcium and Sodium Concentrations with a) DI, b) DDI100 and c) DPW100 RG Dosages.

The soils calcium concentrations in the bottom, middle and top are linearly increasing as higher time cycles are employed as shown in Figure 4.13(b1) and Figure 4.13(c1). This occurs because as higher time leaching cycles are incremented, the higher the clay aggregate surface is available for absorbtion of the calcium cations. The total calcium in the soils with DDI100 and DPW100 applications is approximately 584 mg/L with a standard deviation of 19 mg/L and 470 mg/L with a standard deviation of 17 mg/L, respectively. The sodium concentration in DDI100 and DPW100 application methods was very similar to Figure 4.13(a2) and can be attributed to lower hydraulic conductivity hindering the draining of the sodium concentrations in the soil.

4.9 APPLICATION METHOD APPROACH IN PONDS

4.9.1 DISSOLUTION RATE OF RG

The evaluation of RG dissolution rate was performed at a solution temperature of 24 ± 1°C with two different sizes of RG. The tests were performed for a total of 1,200s and results are summarized in Figure 4.14. The test results suggest that the calcium concentration increases with time as well as reduction in particle size and thereafter plateaus. The reduction in particle size increases the specific surface area allowing more dissolution of calcium. The dissolution steadily increases from time 0 s to 120 s. After 120 s, the calcium concentration dissolution rate decreases until a steady state is achieved. The results summarized in Figure 4.14 suggest that maximum dissolution is achieved after 300 s. After 300 s no further dissolution occurs indicating that a maximum concentration is reached depending on the particles size and further dissolution doesn't occur because RG settles at the bottom due to gravity. The reduction in particle size enhances the dissolution but dissolution stops after 100% saturation. Therefore, it can be concluded that just dumping the RG in the pond water may provide some benefit but will much of RG will be wasted if it is not thoroughly distributed. To maximize the benefits, it will be appropriate to distribute the RG with a pump to optimize the benefits of RG on enhancing infiltration rates.

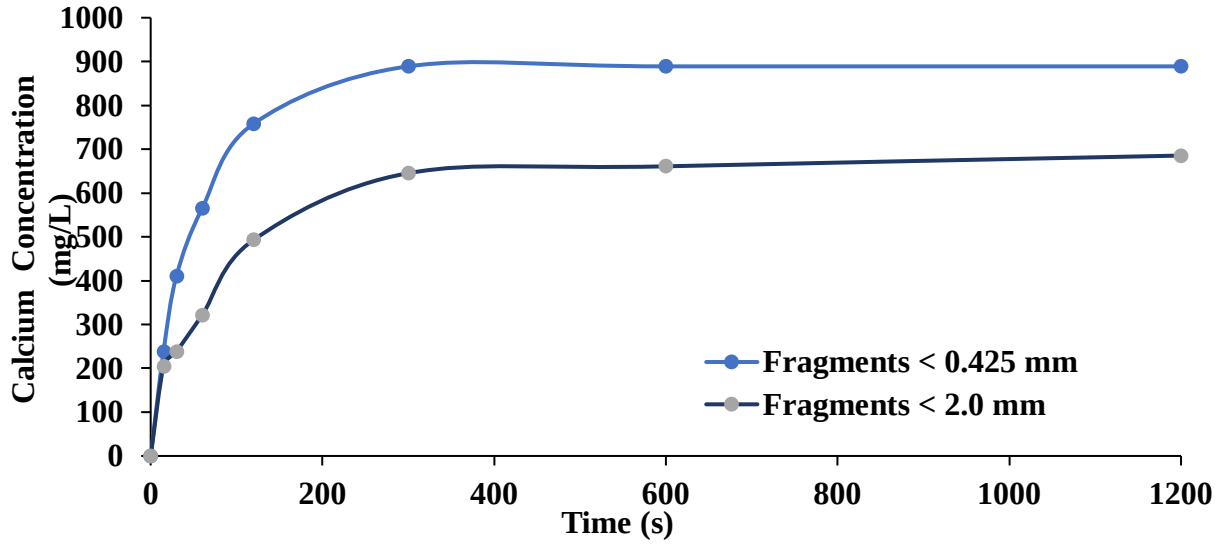

Figure 4. 14 RG Dissolution Rate

4.9.2 SMALL SCALE RETENTION POND SIMULATION

This section focuses on the propagation of gypsum in a simulated retention pond with a scale of 1" to 7' ratio model. Since the diffusion rate of gypsum is relatively measly, DDI100 was used in this section to analyze the diffusion rate of a saturated solution in a pond filled with DI water. Fan 1 and 2 with a diameter of 0.59 and 0.78 in, respectively were used to diffuse the gypsum solution to points A, M, and J at a speed of 630 rpm Figure 3.7.

The siphon extractions were performed at points A, M and J to identify calcium concentrations and results are summarized in Figure 4.15 at different times with respect to Fan 1 and 2. In Figure 4.15 at point A and M, higher calcium concentrations were achieved by the 0.78 in. blade fan. Both points showed an incremental calcium concentration as time passed by, except for point J. In Figure 3.6, the dispersion of dye curved from point J (beneath the gypsum solution source) to point M and spread towards point A. Similar behavior is observed with the dissolution of gypsum regarding calcium concentrations. At point J, a discrete scatter calcium concentration is observed as time increases, not following a linear, or algorithmic trend. This occurs because the point J is collinear to the saturated solution source underneath the fan. A certain percentage of saturated calcium solution is sedimented towards point J, and another portion is distributed in a winding path to point M. Point M shows the highest calcium concentrations than point A and J.

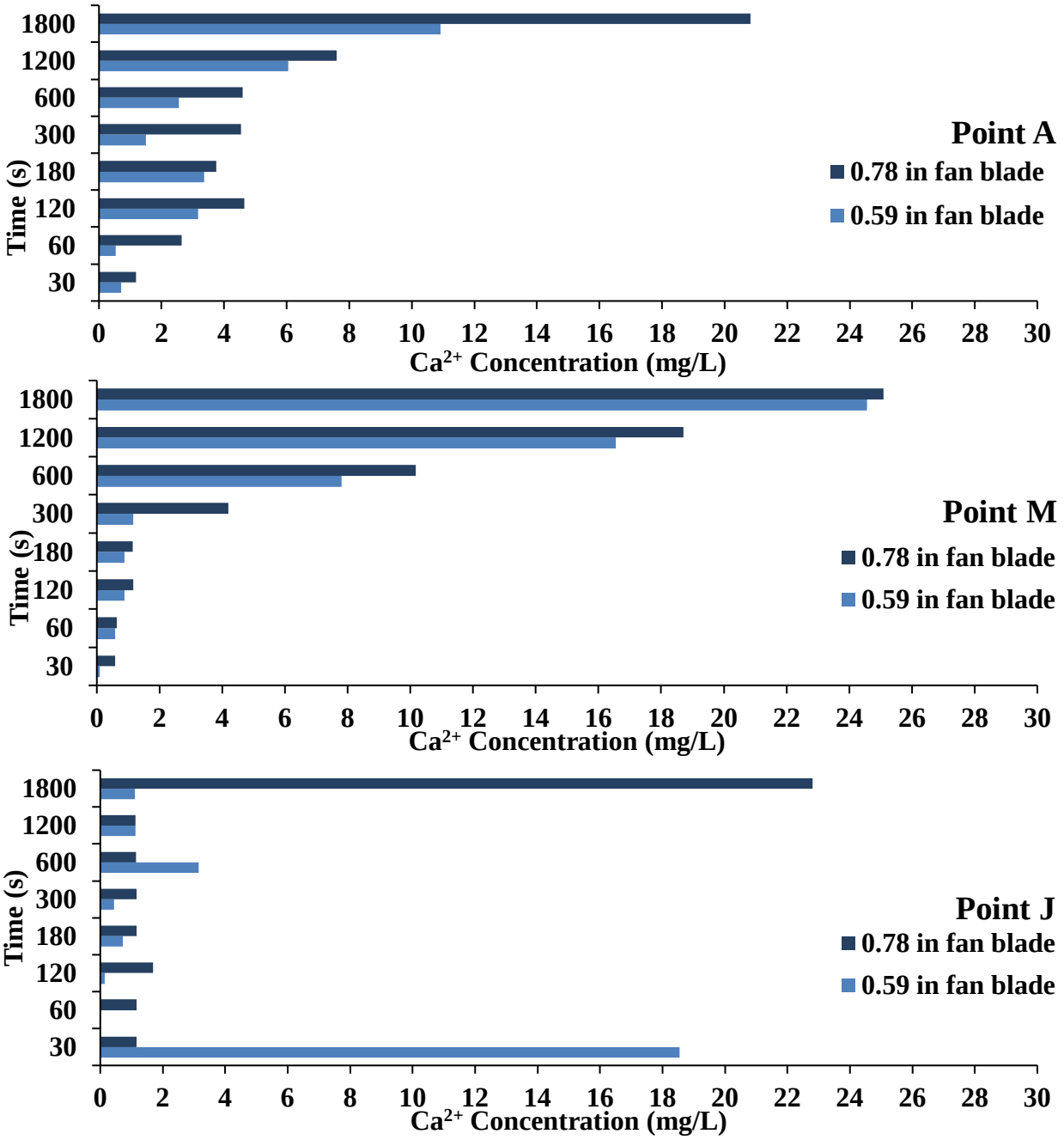

Figure 4. 15 Calcium Concentrations at points: A, M, and J

At the time 1800 s, the calcium concentration achieved is 25 and 24.6 mg/L for Fan 1 and 2, respectively. From point M to A depicted in Figure 3.6, the concentration was spread in a circular motion, wrapping, closing the low concentration area in point A. This behavior in Figure

4.15 at point A is also observed, calcium concentrations are distributed at a lower rate as compared to path J-M.

4.9.3 DIFFUSION COEFFICIENTS BASED ON CALCIUM CONCENTRATIONS

Table 4.7 shows the coefficient of diffusion calculated using equation (3.1) and (3.2) based on the data obtained in Figure 4.15. These results are measured for the diffusion of RG at the inflow source (Point D), and diffused to points: A, M, and J. These values are compared to a reference value acquired from the web.

Table 4. 7 Calcium Diffusion Coefficients

Source	Diffusion Coefficient (cm^2/sec)	Time from Point *D to Point J (Days)	Time from Point D to Point M (Days)	Time from Point D to Point A (Days)
Equation (3.1)	4.97E-04	1	63	102
Equation (3.2)	1.06E-05	32	2961	4768
Web	7.90E-06	43	3983	6414

* D means Discharge point

There is a considerable difference between the calculated diffusion rates and the reference value obtained from the web. The diffusion coefficient from the web was determined using molecular weight, temperature, the viscosity of median, and ion charge along with other unspecified parameters. Since temperature and viscosity are also used in equation (3.2), it can be said that this is the reason for both values to be closer as compared to equation (3.1). The high discrepancy is observed in equation (3.1) when calculated the results from equation (3.2) and the web. To calculate the diffusion rate in equation (3.1) other parameters were contemplated such as the change of calcium concentration (before and after), the volume of the median, and the specific surface area. These parameters resulted in a larger coefficient value, due to the experimental setup; at which the mixer influenced the outcome in the change of calcium concentrations; by increasing the RG to disperse quicker and dissolve faster. With the aid of the mixer, the calcium diffusion

coefficient resulted in a faster time compared to the other two values. Since the diffusion time is dependent on the diffusion coefficient, it is safe to state both values are proportional to one another.

4.10 RG LIFE CYCLE ASSESSMENT (LCA)

This section focuses on the LCA study on the local RG provided by El Paso Recycling Inc. Several factors contribute to the benefits of implementing RG in retention ponds. This incorporation leads to increase in the infiltration rate of clayey soils, eco-friendly, favorable to the economy, and is sustainable for the city of El Paso. Figure 4.16 shows the life cycle assessment for a typical drywall board. Drywall path is typically derived into paths, either material lasts to its end of life and is sent to a landfill, or material is recycled. In this analysis, a summary of environmental concerns is analyzed based on every stage of the process throughout its service life. As for the development of the drywall, its composition is made by inputs such as mining gypsum, FGD gypsum from manufacturing plants, collect facing paper and produce additive production. The extraction and processing of raw materials, crushing and drying in furnace takes place as for the plasterboard fabrication. These consume energy and produce CO_2 caused by the transportation and usage of the furnace. In terms of electricity, diesel, fuel oil, and natural gas consumptions to produce natural gypsum, requires roughly: 0.00102 kWh/kg, 0.0211 MJ/kg, 0.00246 MJ/kg and 0.045 MJ/kg respectively (Suarez, Roca, & Gasso, 2016). For example, mined gypsum involves the drilling and blasting of the rock at which material is then hauled to the drywall manufacturers. Once the drywall board is manufactured, approximately 12 % of the material is rejected due to the quality control regulations and the rest is stock in retailing companies. Usually, the rejected material would be sent to a recycler for recycling. Material that meets the requirements and is in stock ready for its consumption, for the most part, it is applied to construction sites. The life of the plasterboard may fulfill its term and reach its end of life, at which material is demolished and sent to the landfill (24 %) characterized as the path I in Figure 4.16. This material usually is not recyclable due to toxic element that might be inherent in the material such as asbestos, mercury,

and lead. Contrarily, Path II, during construction new drywall gypsum board scraps (64 %) may be used in a recycler.

As for Path II, its input source material is from uninstalled scraps and rejected material from quality control requirements. Regarding the consumption of diesel in recycling plants, considering the efficiency of 60% to 80%, diesel consumption is roughly 0.036 MJ/kg of gypsum recycled (Gypsum Recycling International, 2015). Some RG applications include agricultural soil conditioner, new drywall, cement, paper products, and composting. These materials could not be generated if the 76 % would have been disposed to landfills. Some of the benefits of recycling gypsum are: lower cost of waste disposal, the material is 100% traceable, the recycling rate is increased, 200 kg and 2.5 tons of CO_2 saved of recycled gypsum and recycled paper saved, and plasterboards are 100% recyclable (Gypsum Recycling International, 2015). Also, hydrogen sulfide toxic gas can be minimized in landfills because waste gypsum has been found to produce toxic gas in the landfill.

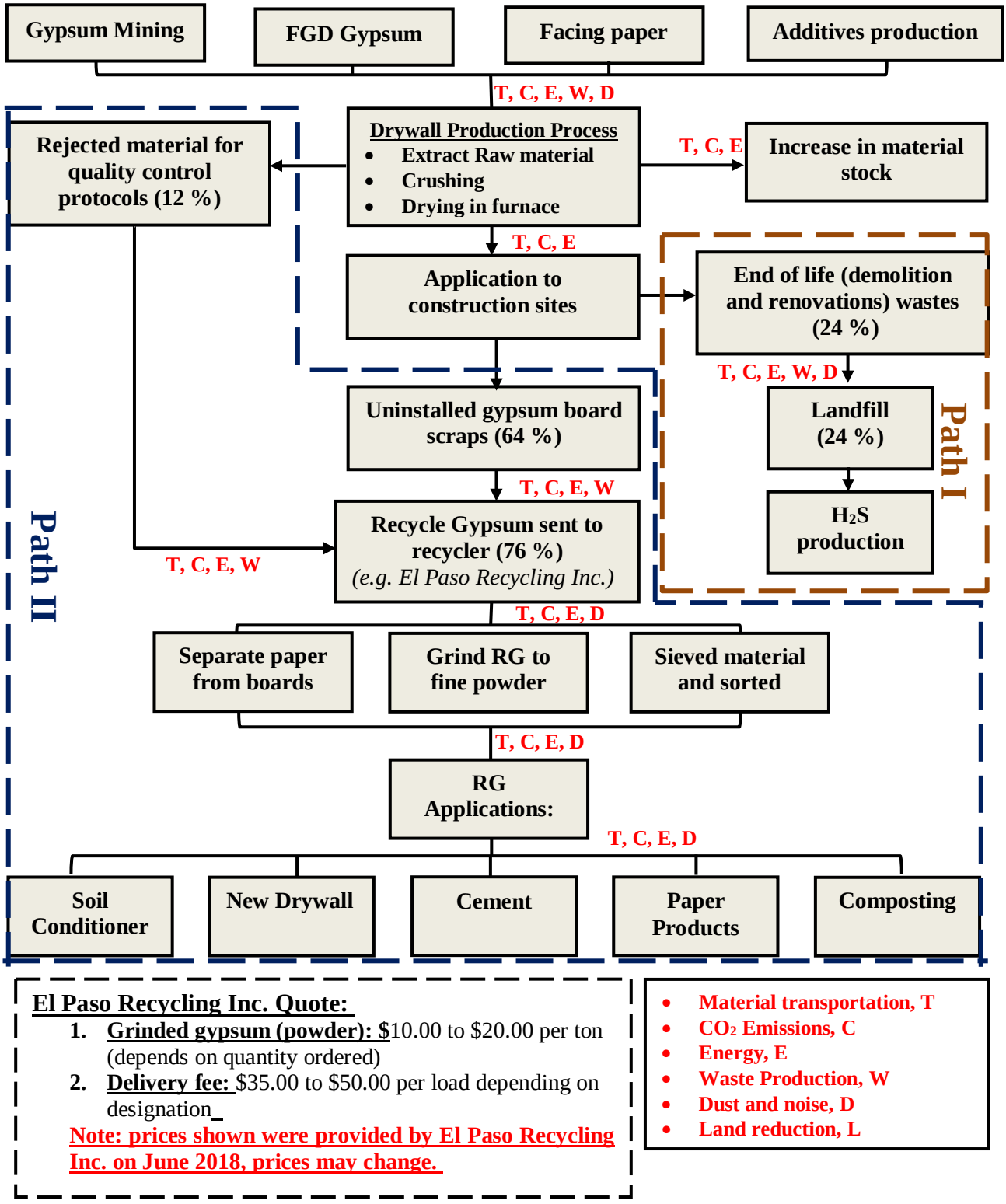

Figure 4. 16 LCA of RG

CHAPTER 5: SUMMARY, CONCLUSIONS, AND RECOMMENDATIONS

In summary, to mitigate problems with low percolating retention ponds has a clayey soil layer at the bottom of the pond, it was proposed to apply RG dosages to enhance water infiltration rates. This study focused on evaluating the influence of RG on infiltration and to identify gypsum dosages needed to enhance infiltration rates that would cooperate in the sustainability aspects of retention ponds and its environment. A total of four soils were chosen for this study: two silty grains of sand (SM) and two low plastic clays (CL). Site and westbound soils had traces of previous RG dosage applications.

RG was observed to increase the infiltration rate using the double ring infiltrometer and an increased in K_{sat} values in low dry density dry density compaction efforts (90 ± 2 lb/ft^3) and high density compaction efforts (106 lb./ft^3). As for the application methods using the double ring infiltrometer, the infiltration rate was increased in the inner and outer ring at 17.3 ton/acre for the GSS method of application. For the DDW application method, the inner ring was less enhanced in comparison to GSS method.

In laboratory permeability testing, the averaged saturated hydraulic conductivity for all soils was enhanced with DDI and DPW methods by approximately:

Upper Valley	**Interchange**	**Westbound**	**Site**
DDI: 693 %	DDI: 68 %	DDI: 1 %	DDI: 6 %
DPW: 443 %	DPW: 215 %	DPW: 6 %	DPW: 8 %

- The K_{sat} values linearly incremented as higher RG applications were employed using various methods of application.
- The incremental K_{sat} value in (%) for the interchange soil for the different RG application approach was; DDI: 68 %, DPW: 215 %, MGS: 337 %, GSS: 32 %.
- RG studied is composed of approximately 250,518 mg/kg of Ca^{2+}

- RG for this study was considered as recycled drywall or sheetrock. Based on the X-ray diffraction mineral analysis, RG was composed of anhydrite, gypsum, quartz, calcite and cellulose material with 2.81, 88.15, 1.27, 7.77, and 9.94 % respectively.
- Not much of an increase in Ca^{2+} concentrations were observed between cycles.

Based on the results of this study, the following conclusions were developed:

- The higher enhancement was observed in clayey soils in % due to the presence of higher net negative charge, where calcium cations are adsorbed to flocculate soil.
- The permeability of the soil is dependent on density, chemical and mineral properties such as high SSA, montmorillonite content, sodicity condition, plasticity, and CEC.
- Calcium concentrations in leaching DDI100 and DPW100 approximately doubled in all three cycles.
- K_{sat} value improvements were minimal in sandy soils.
- Based on the analysis, RG would not affect groundwater caused by trace elements found in its composition in a one-year term.
- Application of RG to retention ponds may produce hydrogen sulfide (H_2S) if the current pond state is in anaerobic conditions.

It is recommended to <u>EPW</u> to:

- Dissolve RG in water as the most suitable application method.
- Implement an aeration system at retention ponds to reduce the probability of generating toxic gases (H_2S) when RG is applied. (see Appendix H for proposed market mixers)
- For future RG applications, it is recommended to grind particles < 0.425 mm for faster dissolution rate.

- Recommend RG supplier to minimize the presence of cellulose material.
- Maintain documentation or a log of RG application for future leaching analysis.
- Apply approximately 2.5 g/L of RG in water.
- Since Interchange pond is normally at low water levels, it is recommended to mix RG in soil by tillage.
- Table 5.1 presents an approximation of the volume of the pond that would aid RG dosage applications at different water levels.

Table 5. 1 Application Dosages of Studied Ponds

Interchange			**Westbound**			**Site**		
Water Level (ft)	**Volume (gal)**	**RG dosage (tons)**	**Water Level (ft)**	**Volume (gal)**	**RG dosage (tons)**	**Water Level (ft)**	**Volume (gal)**	**RG dosage (tons)**
0.5	1936109	20	0.5	26307	0.3	0.5	75805	0.8
1	3888413	41	1	52613	0.5	1	151611	1.6
1.5	5840716	61	1.5	79505	0.8	1.5	228422	2.4
2	7798428	81	2	106789	1.1	2	305907	3.2
2.5	9761555	102	2.5	134469	1.4	2.5	384067	4.0
3	11730106	122	3	162544	1.7	3	462904	4.8
3.5	13704086	143	3.5	191018	2.0	3.5	542419	5.7
4	15683505	164	4	219892	2.3	4	622615	6.5
4.5	17668369	184	4.5	249168	2.6	4.5	703494	7.3
5	19658686	205	5	278848	2.9	5	785057	8.2
5.5	21654464	226	5.5	308934	3.2	5.5	867307	9.0
6	23655709	247	6	339427	3.5	6	950244	9.9
6.5	25662430	268	6.5	370330	3.9	6.5	1033872	10.8
7	27674633	289	7	401645	4.2	7	1118191	11.6
7.5	29692327	310	7.5	433373	4.5	7.5	1203205	12.5
8	31715519	331	8	465515	4.8	8	1288914	13.4
8.5	33744216	352	8.5	498075	5.2	8.5	1375320	14.3
9	35778425	373	9	531054	5.5	9	1462426	15.2
9.5	37818155	395	9.5	564453	5.9	9.5	1550233	16.1
10	39863413	416	10	598275	6.2	10	1638743	18.0
10.5	41914206	437	10.5	632522	6.6	10.5	1727959	18.0

Future recommendations and limitations on the study:

- For better results, longer application cycles should be employed like 30 mL, 1,000mL, 5,000 ml.
- Evaluate different soils to evaluate and document benefits of RG dosage on enhancing rate of infiltration.
- Perform longer analyses to identify and document movement of trace metals and salts to the groundwater.
- Obtain RG from different suppliers at different intervals to document variability in RG supplied to EPW.
- Develop a prototype model in the field and document change in infiltration rates.

REFERENCES

Ayers, R. S., & Westcot, D. W. (1985). Water quality for agriculture. Rome: FAO. Retrieved from http://www.fao.org/DOCReP/003/T0234e/T0234e00.htm

Bohor, B. F., & Hughes, R. E. (1971). Scanning electron microscopy of clays and clay minerals. *Clays and Clay Minerals*, *19*(1), 49–54. Retrieved from http://www.clays.org/journal/archive/volume 19/19-1-49.pdf

Brady, N. C., & Weil, R. R. (2008). *The Nature and Properties of Soils* (14, illust ed.). Prentice Hall.

Budhu, M. (2015). *Soil Mechanics and Foundations* (3rd ed.). Chichester, West Sussex: John Wiley & Sons, Ltd.

Cooperative Research Centre, C. (2006). VitiNotes. *Vineyard Activities 8: Measuring the Infi Ltration Rate of Water into Soil*, 1–3. Retrieved from www.crcv.com.au%5Cnwww.winetitles.com.au

De Varennes, A., Qu, G., Cordovil, C., & Gonçalves, P. (2011). Soil quality indicators response to application of hydrophilic polymers to a soil from a sulfide mine. *Journal of Hazardous Materials*, *192*(3), 1836–1841. https://doi.org/10.1016/j.jhazmat.2011.07.020

Guggenheim, S. (1995). Structural Aspects, 18. https://doi.org/10.1002/9783527615292.ch6

Gypsum Association, G. A. (1992). Treatment and Disposal of Gypsum Board Waste - Part 2. *Construction Dimensions*, (March), 58–62. Retrieved from http://www.awci.org/cd/pdfs/9202_a.pdf

Gypsum Recycling International, G. (2015). Recycling Gypsum. Retrieved from http://cmslogin.dk/Customers/Gypsum Recycling Int/Archive/747/Gips brochure global.pdf

Kemper, W. (1975). Dissolution rate of gypsum in flowing water. *Soil Science Society of …*, *39*(3), 458. https://doi.org/10.2136/sssaj1975.03615995003900030026x

Lamond, R. E., & Whitney, D. A. (1992). Management of Saline and Sodic Soils, 1–4. Retrieved from https://www.bookstore.ksre.ksu.edu/pubs/mf1022.pdf

Little, D. N. (1995). *HANBOOK FOR STABILIZATION OF PAVEMENT SUBGRADES Dubuque, IA: Kendall/Hunt Pub*.

Loveday, J. (1974). Methods for analysis of irrigated soils. Commonwealth Agricultural Bureaux.

Massman, J. W., & Allen, T. (2003). A Design Manual for Sizing Infiltration Ponds, (October), 72. Retrieved from https://www.wsdot.wa.gov/research/reports/fullreports/578.2.pdf

McMullen, B. (2000). SOILpak for vegetable growers, 1–8. Retrieved from http://www.dpi.nsw.gov.au/__data/assets/pdf_file/0007/167533/soipak-vegetable-prelim.pdf

Mitchell, J. K. (1993). *Fundamentals of Soil Behavior* (2, illustr ed.). Wiley.

Mudzielwana, R., Gitari, M. W., & Msagati, T. A. M. (2016). Characterisation of smectite-rich clay soil: Implication for groundwater defluoridation. *South African Journal of Science*, *112*(11–12), 1–8. https://doi.org/10.17159/sajs.2016/20150442

Natures Way Resources, R. (2018). Gypsum (CaSO4). Retrieved from http://www.natureswayresources.com/infosheets/gypsum.html

Ndukwe, I., & Yuan, Q. (2016). Drywall (Gyproc Plasterboard) Recycling and Reuse as a Compost-Bulking Agent in Canada and North America: A Review. *Recycling*, *1*(3), 311–320. https://doi.org/10.3390/recycling1030311

Oosterbaan, R. J., & Nijland, H. J. (1994). Determining the Saturated Hydraulic Conductivity. *Drainage Principles and Applications. International Institute for Land Reclamation and Improvement*, (m), 435–456. Retrieved from http://edepot.wur.nl/183180

Peppin, C. (2015). Gypsum Recycling International. Retrieved from http://feeco.com/gypsum-recycling/

Pflughoeft-hassett, D. F. (2007). A Comparison of Properties of FGD & Natural Gypsum Products What is Gypsum ? *October*. Retrieved from https://www.acaa-usa.org/Portals/9/Files/PDFs/FGDproducts/2-A_Comparison_of_Properties_of_FGD_and_Natural_Gypsum_Products.pdf

Rycroft, D. W., & Amer, M. H. (1995). *Prospects for the Drainage of Clay Soils, Issues 51-53*. Rome: Food & Agriculture Org., 1995.

Schaetzl, R. J., & Anderson, S. (2005). *Soils: Genesis and Geomorphology*. Cambridge University Press.

Stibinger, J. (2014). *Examples of Determining the Hydraulic Conductivity of Soils. Theory and Applications of Selected Basic Methods*. Retrieved from http://envimod.fzp.ujep.cz/sites/default/files/skripta/16e_final_tisk.pdf

Suarez, S., Roca, X., & Gasso, S. (2016). Product-specific life cycle assessment of recycled gypsum as a replacement for natural gypsum in ordinary Portland cement: Application to the Spanish context. *Journal of Cleaner Production*, *117*, 150–159. https://doi.org/10.1016/j.jclepro.2016.01.044

Tolaymat, T., & Carson, D. (2015). Best Management Practices to Prevent and Control Hydrogen Sulfide and Reduced Sulfur Compound Emissions at Landfills That Dispose of Gypsum Drywall. Retrieved from https://cfpub.epa.gov/si/si_public_record_report.cfm?dirEntryId=310622

U.S. Environmental Protection Agency, E. (1995). Mineral Products Industry 11.16-1, *93*, 1–9. Retrieved from http://www.epa.gov/ttnchie1/ap42/ch11/final/c11s16.pdf

U.S. Environmental Protection Agency, E. (2005). Stormwater Structures & Mosquitoes. Retrieved from https://www3.epa.gov/npdes/pubs/sw_wnv.pdf

University of Vancouver, U. (2018). Clay Minerals Soils to Engineering Technology to Cat Litter. Retrieved from https://web.viu.ca/earle/geol312/USC-anderson-clays.pdf

Villa, P. (2017). www.elpasotimes.com. Retrieved from https://www.elpasotimes.com/story/news/health/2017/09/11/el-paso-health-officials-confirm-6-new-cases-west-nile-virus/655945001/

Wallace, T. (1998). *Handbook of Soil Conditioners: Substances That Enhance the Physical Properties of Soil: Substances That Enhance the Physical Properties of Soil*. Taylor & Francis.

Western Washington University, W. (2012). Lecture 8 : Soils and Percolation Infiltration is the movement of water INTO the soil surface. Retrieved from http://kula.geol.wwu.edu/rjmitch/L8_soils_percolation.pdf

Wolkowski, R. P. (2003). Using recycled wallboard for crop production, 8. Retrieved from http://www.soils.wisc.edu/extension/pubs/A3782.pdf

Yang, K., Xu, Q., Townsend, T. G., Chadik, P., & Booth, G. (2016). Hydrogen Sulfide Generation in Simulated Construction and Demolition Debris Landfills: Impact of Waste Composition. Retrieved from https://www.tandfonline.com/doi/pdf/10.1080/10473289.2006.10464544

APPENDIX A: PRELIMINARY PROTOCOLS

Sand Cone Test
(ASTM D1556)

Scope

This test method is used to determine the in-place density and unit weight of soil using a sand cone apparatus. It is only effective for particle size smaller than 1.5 in. diameter. It is not suitable for soil containing organics, water content near saturation, or highly plastic soils that would deform during the excavation of the test hole.

Apparatus

Sand-Cone Density Apparatus
Sand Container
Sand Cone
Base Plate
Sand
Scale
Drying Equipment
Miscellaneous Equipment
Pick
Bucket
Cloth

Procedure

Steps	Procedure
1	Select a plane and even surface on the field and place the base plate to ensure it is flat and even.
2	Dig a test hole without disturbing the surroundings through the base plate center hole.
3	Place the Sand-Cone Apparatus on top of the base plate.
4	Allow the sand to fill the excavated hole and the funnel.
5	Record the remaining mass of the sand in the container and collect excavated soil.

Calculations

The volume of the test hole:

$V = (M_1 - M_2)/\rho_1$

V = volume of the test hole, ft^3 [cm^3],
M_1 = mass of the sand used to fill the test hole, funnel, and base plate, lbm [g],
M_2 = mass of the sand used to fill the funnel and base plate, lbm [g], and
ρ_1 = bulk density of the sand, lbm/ft^3[g/cm^3].

Dry Mass of Material Collected:

$M_4 = 100*M_3/(w+100)$

w = water content, %,
M_3 = moist mass of the material collected, lbm [g], and
M_4 = dry mas of the material collected, lbm [g].

In-Place Wet and Dry Density of the Material Collected:

$\rho_m = M_3/V$

$\rho_d = M_4/V$

ρ_m = wet density of the tested material, lbm/ft^3 [g/cm^3], and

ρ_d = dry density of the tested material, lbm/ft^3 [g/cm^3].

Double Ring Infiltrometer Infiltration Testing
(ASTM D3385-18)

Scope

This test method describes a procedure for field measurement of the rate of infiltration of liquid (typically water) into soils using double-ring infiltrometer. This test method is particularly applicable to relatively uniform fine-grained soils, with an absence of very plastic (fat) clays and gravel-size particles and with moderate to low resistance to ring penetration. This test method may be conducted at the ground surface or at given depths in pits, and on bare soil or with vegetation in place, depending on the conditions for which infiltration rates are desired. However, this test method cannot be conducted where the test surface is below the groundwater table or perched water table.

Apparatus

Infiltrometer Rings
Steel tape
Shovel
Tamper
Stopwatch
Level
Rubber Hammer
Thermometer
Mariotte tubes
Cover for the rings

Procedure

Steps	Procedure
1	Drive the outer ring about 6 in. deep into the soil. Place the inner ring in the center of the outer ring and drive it between 2 in. to 4 in. deep into the soil. Ensure to keep the soil undisturbed. If so, tamper it to make it firm.
2	Place the Mariotte tubes so that the reference head is between 1 in. to 6 in. Fill both rings to the desired depth. Ensure that when filling them up, the soil does not get disturbed.
3	Start flow of water from the Mariotte tubes. When the fluid level becomes constant, determine the depth in both rings using the steel tape. If the depths between the inner ring and annular space varies more than 5 mm (1⁄4 in.), raise the Mariotte tube having the shallowest depth. Maintain the liquid level at the selected head in both the inner ring and annular space between rings as near as possible throughout the test, to prevent the flow of fluid from one ring to the other.
4	Record the ground temperature at a depth of about 300 mm (12 in.), or at the mid-depth of the test zone. Determine and record the volume of liquid that is added to maintain a constant head in the inner ring and annular space during each timing interval by measuring the change in elevation of the liquid level in the Mariotte tube. Also, record the temperature of the liquid within the inner ring.
5	For average soils, record the volume of liquid used at intervals of 15 min for the first hour, 30 min for the second hour, and 60 min during the remainder of a period of at least 6 h, or until after a relatively constant rate is obtained.

6	The appropriate schedule of readings may be determined only through experience. For high-permeability materials, readings may be more frequent, while for low-permeability materials, the reading interval may be 24 h or more. In any event, the volume of liquid used in any one reading interval should not be less than approximately 25 cm3
7	Place the driving cap or some other covering over the rings during the intervals between liquid measurements to minimize evaporation. Upon completion of the test, remove the rings from the soil, assisted by light hammering on the sides with a rubber hammer

Calculations

Inner Ring calculation:

$V_{IR} = \Delta V_{IR} / (A_{IR} * \Delta t)$

V_{IR} = inner ring incremental infiltration velocity, cm/h,

ΔV_{IR} = volume of liquid used during the time interval to maintain the constant head in the inner ring, cm^3

A_{IR} = internal area of the inner ring, cm^2, and

Δt = time interval, h.

Annular Space Between Rings Calculations:

$V_A = \Delta V_A / (A_A * \Delta t)$

V_A = annular space incremental infiltration velocity, cm/h,

ΔV_A = volume of liquid used during the time interval to maintain the constant head in the annular space between the rings, cm^3, and

A_A = area of annular space between the rings, cm^2.

Laboratory Compaction Characteristics of Soil
(ASTM D698-12)

Scope

This test method covers laboratory compaction method used to determine the relationship between molding water content and dry unit weight of soils (compaction curve) compacted in a 4 in. (101.6 mm) diameter by 4.6 in. (116.8mm) height mold with a 5.50-lbf (24.5-N) hammer dropped from a height of 12.0 in. (305 mm) producing a compactive effort of 12 400 ft-lbf/ft^3 (600 kN-m/m^3).

Apparatus

4 in. diameter Mold
Rammer
Sample Extruder (Jack)
Balance
Drying Oven
Straightedge
Mixing Tools

Procedure

Steps	Procedure
1	Prepare 4 to 5 cylindrical soil samples with increasing water content. For example: 8%, 10%, 12%, 14%, and 16%.
2	The soil must be compacted into three equal layers with 25 blows each layer.
3	After compacting the last layer, remove the collar from the mold and trim the excess soil with a straightedge to even the soil surface to the top of the mold.
4	Record the weight of the soil plus the mold and collect a portion of the material to find the density.
5	Repeat the process for all samples and follow the calculations to plot the MD Curve.

Calculations

Dry Mass of the Test Fraction:

$$M_{d,tf} = \frac{M_{m,tf}}{1 + \frac{w_{tf}}{100}}$$

$M_{d,\,tf}$ = Dry Mass of test fraction, nearest g,
$M_{m,\,tf}$ = Moist mass of test fraction, nearest g, and
w_{tf} = Water content of test fraction, nearest 0.1%.

Moist Density:

$$\rho_m = K \times \frac{(M_t - M_{md})}{V}$$

ρ_m = moist density of compacted sub specimen, g/cm^3,
M_t = Mass of moist soil in mold and mold, g,
M_{md} = Mass of compaction mold, g,
V = Volume of compaction mold, cm^3, and
K = Conversion constant depends on density units and volume units.
1 for g/cm^3 and volume in cm^3, or 1000 for g/cm^3 and volume in m^3

Dry Density:

$$\rho_d = \frac{\rho_m}{1 + \frac{w}{100}}$$

ρ_d = Dry density of compaction point, g/cm^3, and
w = molding water content of compaction point, nearest 0.1%.
Dry Unit Weight:

$$\gamma_d = K_1 \times \rho_d$$

γ_d = Dry unit weight of compacted specimen in lbf/ft^3 or kN/m^3,
K_1 = Conversion constant depends on density units and dry unit weight units.
62.428 for density in g/cm^3 and γ_d in lbf/ft^3, or 9.8066 for density in g/cm^3 and γ_d in kN/m^3.

Washed Sieve Analysis
(AASHTO T27/T11)

Scope

Sieve analysis determines the gradation or distribution of aggregate particle sizes within a given sample by washing the soil through No. 200 sieve.

Apparatus

Balance

Sieves

Mechanical sieve shaker

Drying equipment, such as an Oven

Containers and utensils

Washing device

Procedure

Method A

Steps	Procedure
1	Record the total dry mass of soil sample before washing.
2	Wash the soil through a No. 200 sieve until the water passing through sieve becomes clear.
3	Dry the washed soil and record the total dry mass washed soil sample.
4	Pour the dry material in the sieves and place it on the mechanical sieve shaker for approximately 10 minutes.
5	Determine the individual or cumulative mass retained on each sieve and the pan to the nearest 0.1 g.

Calculations

Check to make sure that sum of the total mass of material after sieving must agree with a mass before sieving to within 0.3 percent.

$$\frac{dry\ mass\ after\ washing - total\ mass\ after\ sieving}{dry\ mass\ after\ washing} \times 100$$

Percent Retained:

$$IPR\frac{IMR}{M} \times 100 \qquad or \qquad CPR = \frac{CMR}{M} \times 100$$

IPR = Individual Percent Retained,
CPR = Cumulative Percent Retained,
M = Total Dry Sample mass before washing,
IMR = Individual Mass Retained, and
CMR = Cumulative Mass Retained

Percent Passing:

$$IPR\frac{IMR}{M} \times 100 \qquad or \qquad CPR = \frac{CMR}{M} \times 100$$

PP = Percent Passing, and
PPP = Previous Percent Passing.

Laser Diffraction

Scope

Laser diffraction measures particle size distributions (gradation of soil finer than No. 200 sieve) and fine's specific surface area (SSA) by measuring the angular variation in the intensity of light scattered as a laser beam passes through a dispersed particulate. Large particles scatter light at small angles relative to the laser beam and small particles scatter light at large angles. The angular scattering intensity data is then analyzed to calculate the size of the particles responsible for creating the scattering pattern on Malvern Mastersizer 2000. The particle size is reported as a volume equivalent sphere diameter.

Apparatus

50 ml centrifuge tubes

Deflocculating agent, Sodium Hexametaphosphate.

Balance

Weighting dish

DI Water

No. 200 sieve

Malvern Mastersizer 2000

Procedure

Steps	Procedure
1	Sieve soil sample through No. 200 sieve.
2	Add 0.25 g of sieved soil in a centrifuge tube plus 40 mL of DI water.
3	Mix the sample with the deflocculating agent. Use 5 g of Sodium Hexametaphosphate per 125 mL of DI Water. In this case 1.6 g.
4	After leaving the mixture for 24 hours, the sample is ready to be analyzed with the Malvern Mastersizer 2000.

Particle Density
(ASTM D854)

Scope

This test method covers the determination of the specific gravity of soil solids passing through the 4.75-mm (No. 4) sieve, using a water pycnometer.

Apparatus

Pycnometer

Balance

Thermometric Device

Funnel

Squirt bottle

Procedure

Steps	Procedure
1	Record the Pycnometer mass (empty).
2	Record the Pycnometer mass full of water.
3	Record the Pycnometer mass with 50 g of soil sample and water.
4	Dispose of the material, use the squirt bottle to remove any excess of the material left on the pycnometer.

Calculations

Mass of Pycnometer and water at test temperature:

$$M_{\mathrm{pw,t}} = M_{\mathrm{p}} + (V_p \cdot \rho_{w,t})$$

$M_{\rho w,\,t}$ = mass of the pycnometer and water at the test temperature (T), g,

M_p = the average calibrated mass of the dry pycnometer, g,

V_p = the average calibrated volume of the pycnometer, mL, and

$\rho_{w,\,t}$ = the density of water at the test temperature (Tt), g/mL

Specific Gravity of soil at test temperature:

$$G_t = \frac{\rho_s}{\rho_{w,t}} = \frac{M_s}{\left(M_{\rho_{w,t}} - \left(M_{\rho ws,t} - M_s\right)\right)}$$

ρ_s = the density of the soil solids Mg/m^3 or g/cm^3,

$\rho_{w,\,t}$ = the density of water at the test temperature (Tt), from Table 2, g/mL or g/cm^3,

M_s = the mass of the oven dry soil solids (g), and

$M_{\rho ws,\,t}$ = the mass of pycnometer, water, and soil solids at the test temperature, (T), g.

Determination of Solute Cations, Bond Cations, and the Cation Exchange Capacity (ASTM D7503-10)

Scope

This test method describes the procedures for measuring the soluble and bound cations as well as the cation exchange capacity (CEC) of fine-grained inorganic soils. Clay minerals in fine-grained soils carry a negative surface charge that is balanced by bound cations near the mineral surface. These bound cations can be exchanged by other cations in the pore water, which are referred to as soluble cations. The cation exchange capacity is a measure of the negative surface charge on the mineral surface. The CEC generally is satisfied by calcium (Ca), sodium (Na), magnesium (Mg), and potassium (K) although other cations may be present depending on the environment in which the soil exists.

In this test method, the soluble salts from the mineral surface are washed off with DI water, and then the concentration of soluble salts within the extract is measured. The bound cations of the clay are measured by using a solution containing an index ion that forces the existing cations in the bound layer into solution. The total concentrations of bound and soluble cations in this solution are measured. The CEC is measured by displacing the index ion with another salt solution and measuring the amount of the displaced index ion.

Apparatus

Oven
No. 10 U.S. Standard Sieve
Desiccator
Balance
Weighting Paper
Shaker
Cap Containers
500 mL Filtering Flask
Flexible Tubing
Bucher Funnel
Wash Bottle
Squirt Bottle
Graduated Cylinder
2.5 µm Ashless Filter Paper
250 mL Volumetric Flasks
Reagent Water
Ammonium Acetate, 1M
Isopropanol
Potassium Chloride, 1M
Ammonium Sulfate
Personal Protective Equipment

Procedure

Determination of Soluble Cations

Steps	Procedure
1	Add the mass of air-dry soil corresponding to 2 g of soil solids and 100 mL of Type II DI water to a covered container that fits tightly into the shaker (Use only air-dry soil that passes the No. 10 US Standard Sieve).
2	Place the containers in an end-over-end shaker and shake for 1 h at 30 rpm.
3	Vacuum filter the mixture in each container using 2.5 µm ashless filter paper.
4	Transfer the extract to a 100-mL acid washed volumetric flask, preserve it with 1 mL HNO_3, and fill to the specified volume.
5	Analyze each extract for cation concentration (in mg/L) using inductively coupled plasma spectrometry, atomic absorption, or another suitable method.

Determination of Bound Cations

Steps	Procedure
1	Add the determined mass of air-dried soil corresponding to 10.0 g of soil solids and 40 mL of 1 M NH4OAc (Ammonium Acetate) into 100 mL covered container (Use only air-dry soil that passes the No. 10 US Standard Sieve)
2	Shake the covered containers for 5 min in an end-over-end shaker at 30 rpm. Agitate the container to rinse the particles from the side of the container and let the mixture stand for 24 h. After 24 h, shake the container with the mixture for 15 min at 30 rpm in the end-over-end shaker.
3	Rinse the 500-mL filtering flask, and Buchner funnels with NH4OAc. Place the Buchner funnel over the 500-mL filtering flask and line the Buchner funnel with 2.5 µm ashless filter paper.
4	Transfer the contents of the shaken container to the Buchner funnel. Rinse the container and cap into the Buchner funnel using a squirt bottle containing 1 M NH4OAc. Apply low suction to the filtering flask (<10 kPa).
5	Wash the soil in the Buchner funnel with four 30 mL portions of 1 M NH4OAc. Add each 30-mL portion slowly and allow the entire 30 mL portion to drain before adding the next 30 mL portion. Do not allow the soil to dry between additions of NH4OAc. Turn the suction off to the filtering flask after the last washing. Leave the NH4OAc washed soil in the Buchner funnel; this soil is to be used for determining the cation exchange capacity (CEC).
6	Rinse the 250-mL volumetric flask with 1 M NH4OAc. Transfer the filtered aqueous solution into the 250-mL volumetric flask. Preserve the solution to pH of 2 with ICP-grade nitric acid and fill the volumetric flask to volume with NH4OAc.
7	Analyze the cation concentration (in mg/L) in the aqueous solution using inductively coupled plasma spectrometry or atomic absorption.

Cation Exchange Capacity

Steps	Procedure
1	Rinse an acid washed 500 mL filtering flask with isopropanol. Place the Buchner funnel with the 1 M NH4OAc washed sample onto the 500-mL filtering flask. Apply low suction (<10 kPa) to the filtering flask. Do not allow the soil to dry when suction is applied.
2	Wash the soil with three 40 mL portions of isopropanol. Allow each 40-mL portion to drain before adding the next portion. Washing with isopropanol removes residual NH4OAc. Turn off the suction to the filtering flask when free liquid is no longer visible.
3	Separate the Buchner funnel from the filtering flask. Discard the isopropanol collected in the 500-mL filtering flask and rinse the flask with Type II DI water three times. Return the Buchner funnel containing the isopropanol washed soil to the rinsed filtering flask.
4	Apply suction to the filtering flask and wash the soil with four 50 mL portions of 1 M KCl solution. Allow each portion of the 1 M KCl solution to drain before adding the next portion. Do not allow the soil to dry between additions of KCl solution.
5	Rinse a 250-mL volumetric flask with 1 M KCl. Transfer the extract into the 250-mL volumetric flask. Rinse the filtering flask with Type II DI water and transfer the contents into the volumetric flask. Fill the volumetric flask to volume with water
6	Analyze the KCl extract for nitrogen concentration (mg/L) using a spectrophotometer.

Calculations

Concentration of Soluble Cations:

$$S = C \times \frac{0.100L}{M_o(g)} \times 1000\frac{g}{kg}$$

S = concentration of soluble cations ($cmol^+$ /kg) in the soil,
C = concentration of cations ($cmol^+$ /L) in the DI water, and
M_o = oven-dry mass of soil.

Concentration of Bond Cations:

$$M^+ = C \times \frac{0.25L}{M_o(g)} \times 1000\frac{g}{kg} - S$$

M^+ = concentration of adsorbed cation ($cmol^+$ /kg) in soil, and
C = concentration of cation ($cmol^+$ /L) in the NH4OAc.

Cation Exchange Capacity:

$$CEC = N \times \frac{1cmol^+}{140mg} \times \frac{0.25L}{M_o(g)} \times 1000\frac{g}{kg}$$

CEC = concentration of cation exchange capacity ($cmol^+$ / kg), and
N = concentration of nitrogen (mg/L).

Sodium Absorption Ratio (SAR)

$$SAR = \frac{[Na^+]}{([Ca^{2+}] + [Mg^{2+}])^{1/2}}$$

SAR = Sodium Absorption Ratio (mmol/L), and

[] = Concentration expressed as mmol/L.
Exchangeable Sodium Percentage (ESP pH>4.8)
ESP = ($[Na^+]$/CEC) x 100
ESP = Exchangeable Sodium Percentage, %,
[] = Concentration expressed as cmol/kg, and
CEC = concentration of Cation Exchange Capacity, cmol/kg.
Exchangeable Sodium Percentage (ESP pH<4.8)
ESP = ($[Na^+]$/ECEC) x 100
ESP = Exchangeable Sodium Percentage, %,
[] = Concentration expressed as cmol/kg, and
ECEC = concentration of Effective Cation Exchange Capacity, cmol/kg.

X-Ray Diffraction
(Multiple Methods)

Scope

X-ray diffraction (XRD) relies on the dual wave/particle nature of X-rays to obtain information about the structure of crystalline materials. The primary use of the technique is the identification and characterization of compounds based on their diffraction pattern.

Apparatus

Sieve No. 200 and No. 40
Acetic Acid
Hydrogen Peroxide
Sonic Prove
2.5 µm pore size ashless filter papers
0.45 µm pore size ashless filter papers
Glass slides
Methanol
Aluminum Oxide
McCrone Micronizing Mill
Personal Protective Equipment
Beakers

Procedure

Clay Identification

Steps	Procedure
1	Sieve soil through sieve No. 200.
2	Remove Carbonates and Organic matter (acetic acid and hydrogen peroxide methods).
3	Separate Silts and Clays (Decantation method) using a sonic probe.
4	Filter through 2.5 µm pore size ashless filter paper.
5	Mount in a glass slide (Oriented Aggregate Mount Method)
6	Analyze in Rigaku X-Ray diffraction system operated at 30 kV, 15 mA, and X-Rayed from an incidence angle of 5º2Ø at a step size of 0.02 with a scan speed of 0.2 s/step.
7	Analyze data for identification with Diffrac. EVA evaluation software.

Fines Identification

Steps	Procedure
1	Sieve soil through sieve No. 200.
2	Remove Carbonates and Organic matter (acetic acid and hydrogen peroxide methods).
3	Mount in a glass slide (Randomly Oriented Method).
4	Treat sample (Air dried, Ethylene Glycol Method, heated to 550ºC)
5	Analyze in Rigaku X-Ray diffraction system operated at 30 kV, 15 mA, and X-Rayed from an incidence angle of 5º2Ø to 65º2Ø at a step size of 0.02 with a scan speed of 0.2 s/step.
6	Analyze data for identification with Diffrac. EVA evaluation software.

Soil Quantification
(Eberl Method - U. S. Geological Survey Open-File Report 03-78)

Steps	Procedure
1	Sieve soil through sieve No. 40.
2	1g of sample mix with 0.11g of Al_2O_3 and grind with 4 mL of methanol in a McCrone micronizing mill for five minutes using corundum grinding element.
3	Mount in a glass slide (Randomly Oriented Method).
4	Analyze in Rigaku X-Ray diffraction system operated at 30 kV, 15 mA, and X-Rayed from an incidence angle of 5º2Ø to 65º2Ø at a step size of 0.02 with a scan speed of 0.5 s/step.
5	Analyze data for identification with Diffrac. EVA evaluation software.
6	Quantify data with Diffrac.TOPAS software.

Gypsum Mineral Analysis

Steps	Procedure
1	Sieve 1g of gypsum through sieve No. 200.
2	Mount in a glass slide (Randomly Oriented Method).
3	Analyze in Rigaku X-Ray diffraction system operated at 30 kV, 15 mA, and X-Rayed from an incidence angle of 5º2θ to 65º2θ at a step size of 0.02 with a scan speed of 0.2 s/step.
4	Analyze data for identification with Diffrac.EVA evaluation software.
6	Quantify data with Diffrac.TOPAS software.

Acetic Acid Treatment to Remove Carbonates
(U. S. Geological Survey Open-File Report 01-041)

Scope

It may be necessary to dissolve the carbonates in some limestones and sediments before the clay minerals can be identified. However, treatment with strong acids to remove carbonate can modify the structure of clay minerals (e.g., trioctahedral minerals are often destroyed by such treatment), and even dilute acid can attack the silicate layers via interlayer regions and exposed edges. Generally, dilute acetic acid is preferred over hydrochloric acid because it is less likely to affect clay crystallinity.

Apparatus

glacial acetic acid
distilled water
glass graduated cylinder
glass rod
marking pencil
300-ml glass beakers
glass pipette with a rubber bulb
siphon or centrifuge

Procedure

Steps	Procedure
1	Add 1-part acid to 4 parts distilled water in the graduated cylinder and mix thoroughly with the glass rod. Caution: acetic acid can cause burns. Wear safety goggles, plastic gloves, and an apron while working with this chemical.
2	Label 300-ml beakers and add a sample.
3	Add 50-75 ml of the acetic acid solution slowly to avoid foaming and overflow of the beaker. A glass pipette may be used to transfer the acid solution. When effervescence subsides, add another 50-75 ml of acid. Stir and allow to stand overnight. Repeat until suspension no longer effervesces.
4	Allow the suspension to settle and carefully siphon or pour off the supernatant liquid or wash sample by centrifuging. Dispose of acid waste properly. We place it in a 20-liter container of ground-up mollusk shells until neutralized.

Removal of Organic Matter with Hydrogen Peroxide
(U. S. Geological Survey Open-File Report 01-041)

Scope

The presence of organics, which causes a broad hump on X-ray powder diffraction patterns, can obscure the diffraction maxima of mineral species. Unfortunately, just about any treatment to clays involves some risk. With hydrogen peroxide, the danger is oxidizing octahedral iron and changing the layer charge with chlorite and vermiculite. However, one has to do something to resolve clay peaks in some organic-rich samples. The general rule (if there is one) is to go ahead with the peroxide treatment, but if you see some strange diffraction patterns that defy interpretation, suspect that iron oxidation has occurred. This is rarely the case under normal circumstances.

Apparatus

hydrogen peroxide (3%)
glass graduated cylinder
distilled water
300-mL glass beakers
glass rod
pencil
squeeze bottle of distilled water
lab tissues
siphon
safety equipment

Procedure

Steps	Procedure
1	If the hydrogen peroxide is laboratory grade (30%), prepare a dilute solution of 3% using a graduated cylinder and distilled water. Caution: hydrogen peroxide is a strong oxidizer that can cause severe burns. Wear goggles, plastic gloves, and an apron while working with this chemical.
2	Label the beakers with a pencil or marker.
3	Place a sample in each beaker and add about 50-100 mL of dilute hydrogen peroxide. Stir each beaker with the glass rod to suspend the sample. Rinse the glass rod between each sample and dry with a lab tissue. When bubbling stops or slows, add another 50-100 ml of dilute hydrogen peroxide and re-stir the suspension.
4	When the addition of hydrogen peroxide to the samples no longer causes bubbling, the organics have been removed. Allow the suspension to settle and carefully siphon or pour off the supernatant liquid, or wash the sample by centrifuging.

Separation of Silt and Clay by Decantation
(U. S. Geological Survey Open-File Report 01-041)
Scope

Decantation is the gravity settling of particles in a suspension. Although more time consuming than centrifugation, decantation can also be used to separate the clay- and silt-sized fractions for X-ray powder diffraction. For this technique, it is assumed that the coarse fraction (sand and gravel) has been removed and that the fine fraction (silt and clay) has been retained as a suspension. After a muddy suspension is dispersed and allowed to settle, aliquots of clay suspension may be withdrawn from above 5 cm in depth at the times and temperatures shown in Table 1.

Table 1. Withdrawal time and temperature table for the separation of silt and clay (<2 micrometers) fractions by decantation (Folk, 1974; Poppe and others, 2000). All depths are assumed to be 5 cm; temperatures are in degrees C. Hours: h; minutes: m; seconds: s.

TEMPERATURE	TIME
20	4h 6m
24	3h 54m
32	2h 58m

Apparatus

wide-mouth glass jars with lids
plastic centrifuge tubes with caps
centrifuge tube rack
measuring tape or ruler
marking pen
labeling tape
dispersant (sodium hexametaphosphate)
spatula
squeeze bottle with distilled water
ultra-sonic probe
lab tissues
thermometer
timer
plastic syringe

Procedure

Steps	Procedure
1	Label the jars with 0 and 5-cm depths. Sample identifiers should be labeled on the jars and centrifuge tubes with labeling tape for easy removal later.
2	Add the suspension to be separated to the jar, fill each jar up to the 0-cm water-depth line with distilled water, and add a small amount of dispersant with the spatula (Note: the amount of dispersant should not exceed 0.5% of the suspension by weight). Seal the jar, and shake vigorously to homogenize the suspension.
3	Disperse the sample with the sonic probe for 15-20 seconds. Rinse off the tip of the probe with distilled water and dry between samples.
4	Start the timer and check the temperature of the suspension to determine the settling time. If more than one sample is to be separated, record the start and calculated withdrawal times for each sample.
5	After the appropriate time has elapsed (e.g. 4 hours, 6 minutes at 20 C) and the silt has settled past the 5-cm mark, use the syringe to withdraw the clay suspension from the interval above this depth and inject it into the centrifuge tube for storage until mounting as an oriented aggregate (any convenient container will suffice). Repeat withdrawals until an adequate amount of clay has been isolated, or, if a complete separation is necessary, use larger containers as receptacles for the clay fraction and repeat the analysis until the supernatant liquid is clear after settling. Remember to rinse out the syringe with distilled water between withdrawals to prevent cross-sample contamination.

Randomly Oriented Power Mounts for X-Ray Powder Diffraction
(U. S. Geological Survey Open-File Report 01-041)

Scope

X-ray diffraction can determine the bulk mineralogy of a sediment sample with a randomly oriented powder mount. The random orientation ensures that the incident X-rays have an equal chance of diffracting off any given crystal lattice face of the minerals in the sample. The use of a powder press to make randomly oriented powder mounts is undesirable because excessive force could cause the preferred orientation of the crystallites. Although some orientation is inevitable (platy minerals tend toward some preferred orientation), the method described below is sufficient for most applications. Sample splits are commonly dried at 60 °C before the preparation of randomly oriented powder mounts. The mounts are typically X-rayed between the angles of 2 and 70 degrees two theta using copper K alpha radiation at a scanning rate of 2 degrees per minute.

Apparatus

plastic tape
weighing paper (4"x4")
mortar and pestle
ASTM number 230 (.062 mm mesh) sieve stiff brush
spatulas
pencil
sample holders and clips (the ones pictured here are for a Phillips diffractometer)
glass microscope slide
a piece of glass slide cut to size sufficient to cover the sample holder opening

Procedure

Steps	Procedure
1	Tape the glass slide over the opening of the sample holder. Leave tabs on each side for later removal of this cover, but fold the extra tape against itself so that it will not stick to other objects or the sample. Place the holder glass side down on a piece of weighing paper.
2	Grind the dried sample thoroughly so that it is easily brushed through the sieve. The particles should be much finer than .062 mm to avoid fractionation of the minerals. The sieve is used only to achieve even distribution and to ensure that the grinding is complete.
3	Place a second holder over the first as a mask. This enables the buildup of a thick enough layer of the sample for later packing while maintaining a clean metal surface on the final holder.
4	Place the sieve over the sample holder and brush the sample from the mortar. (Note: the sample may become contaminated from the sieve and utensils. These contaminants will not affect the X-ray diffraction analysis, but do not plan to reuse this cut of the sample for sensitive chemical analyses.)
5	Use the spatula to loosen any sample that has stuck to the mortar and brushed the material into the sieve.
6	Brush the sample through the sieve into the cavity of the sample holder. The purpose of the brushing is to obtain an even distribution and to minimize preferred orientation of the particles.

7	Remove the sieve and mask. Place the sample holder on a clean piece of weighing paper, tap the powder remaining on the mask onto the first weighing paper, and replace the mask over the sample holder.
8	Pour the excess powder onto first weighing paper into the sample holder. Distribute the powder evenly.
9	Use a glass slide to pack the sample into the cavity firmly enough so that it will not fall out, deform, or slide, but not so firmly that preferred orientation will be produced on the opposite surface (which will later become the top surface). The glass slide can also be used to scrape any sample that has flattened onto the holder surface during packing back over the holder opening.
10	The additional sample can be used as a filler if necessary to create a firm pack. This part of the sample need not be as finely ground, as it will become the bottom surface and will not be exposed to the X-ray beam.
11	Pack as above and then attach a clip to the back of the holder. Alternately, if a generic holder is being used, another cut-glass slide can be attached with tape to cover the holder's opening.
12	Turn the sample holder over and lift the tab of tape. The glass cover is carefully lifted with a slight twisting motion to break and surface adhesion. This will be the surface exposed to the X-rays. It should be smooth, uniform, and flush with the metal surface of the holder. If not remake the mount.
13	Label the sample holder with the pencil.

Ethylene Glycol Treatment
(U. S. Geological Survey Open-File Report 01-041)
Scope
Organic liquids, primarily ethylene glycol and glycerol, are extensively used as an auxiliary treatment to expand swelling clays. Whether or not a mineral expands and the amount of expansion can provide essential supplementary information aiding clay-mineral identification. Swelling clays include smectites (e.g., montmorillonite, nontronite, and beidellite), some mixed-layer clays, and vermiculite.

Apparatus
ethylene glycol
glass rod
lab tissue

Procedure

Steps	Procedure
1	Apply a drop of ethylene glycol directly to the surface of the oriented aggregate mount with the glass rod. Spread the ethylene glycol if necessary.
2	Mounts are ready to be X-rayed as soon as the liquid is uniformly absorbed. Excess ethylene glycol may be gently mopped up with lab tissue.

Oriented Mounts
(U. S. Geological Survey Open-File Report 01-041)
Scope
The clay fraction can be separated from the bulk sample by centrifugation or decantation and mounted as an oriented aggregate mount for clay-mineral identification. The oriented aggregate mounts force the clay mineral particles, usually plate-shaped phyllosilicates, to lie flat, allowing the operator to direct the incident X-ray beam down the Z-axis of the minerals and to record the diagnostic basal diffractions. It is the Z-axis that shows the extent of d-spacing expansion and (or) contraction indicative of certain clay minerals during subsequent treatments. These treatments include air drying, glycation with ethylene glycol, heating to 400 ℃, and heating to 550 ℃. The material from the randomly oriented powder mount may be used for this analysis.

Apparatus
glass slides cut to fit diffractometer
carbide or diamond glass scriber
lab tissues
vacuum pump
Millipore filtration apparatus vacuum tubing
Millipore HA, 47-mm, 0.45-micron
nominal pore opening cellulose filters
pipette or 20-25 cc syringe
single-edge razor or metal spatula
cylinder with a 2.5 - 5 cm outside diameter

Procedure

Steps	Procedure
1	Cut the glass slides to fit the sample holder and label them with a scriber. Rinse and dry the slides to remove any remaining glass shards.
2	Assemble the filtration device with the cellulose filter in place. Pour approximately 20 ml of the clay suspension into the assembled filtration device. The exact amount will depend on the density of the suspension, mineralogy, presence of organics, and grain size of the particles.
3	If the filter clogs, use the pipette or a syringe with a needle attached to remove the excess clay suspension from the filtration device.
4	As soon as the remaining suspension has been completely drawn into the filter, remove the glass funnel and use a single-edge razor or metal spatula to remove the moist filter from the filtering device.
5	Wrap the filter membrane tightly around the cylinder with the clay film up and held firmly with the thumb and forefinger.
6	Membrane filter and clay film are center-positioned near the glass slide and then quickly and smoothly lightly rolled across the slide to transfer the clay film to the slide. Any hesitation or jerky motion during the transfer may cause rippling of the film and disrupt the preferred orientation.
7	The mounts dry in a few minutes and are then ready for X-ray diffraction analysis. The specimens are subsequently exposed to glycol or heat treatments

Heat Treatment
(U. S. Geological Survey Open-File Report 01-041)
Scope
Heat treatments at various temperatures are commonly used to help identify clay minerals by revealing changes in crystal structure spacings or loss of the structure. Depending on the temperature and the mineral species, these treatments can collapse the structure by dehydration, or in the case of other minerals destroy the crystal structures. However, it is essential for the analyst to remember that some of the changes caused by the heat treatments may be temporary and that partial or complete rehydration may occur during cooling.
Apparatus
furnace
tongs
wire hook
Procedure

Steps	Procedure
1	Preheat the oven to 400 ℃.
2	Place the oriented aggregate mount in the furnace using the tongs. Leave sample in the furnace not less than one-half hour at 400 ℃.
3	Remove mount by pulling it forward with the wire hook until the edge of the mount can be grasped with the tongs. Do not remove mounts until they are ready to be run on the diffractometer.
4	X-ray the sample and repeat the above procedure at 550 ℃.

Scanning Electron Microscope (SEM)
Scope
The scanning electron microscope (SEM) uses a focused beam of high-energy electrons to generate a variety of signals at the surface of solid specimens. The signals that derive from electron-sample interactions reveal information about the sample including external morphology (texture), chemical composition, and crystalline structure and orientation of materials making up the sample. In most applications, data are collected over a selected area of the surface of the sample, and a 2-dimensional image is generated that displays spatial variations in these properties.
Apparatus
Air dried samples used on XRD clay identification
Hitachi stub
Carbon Conductive Cement (CCC)
TM-1000 Hitachi SEM microscope
Procedure

Steps	Procedure
1	Use air-dried samples used on XRD clay identification.
2	Mount the air-dried sample to a Hitachi stud with CCC.
3	Use a tabletop TM-1000 Hitachi SEM microscope to examine the crystal structure of the soil intensified to 10 μm magnification.

Siphon Supernatant Liquid

Scope

To find the residual mass in recycled gypsum.

Apparatus

Bulk recycle gypsum
Tamper and pan
Magnetic stirrer
1000 mL beaker
Siphon

Procedure

Steps	Procedure
1	Shatter 10 g of bulk gypsum in a pan with the tamper (to increase the dissolution rate of gypsum in water).
2	Mix the 10 g on DI Water in the magnetic stirrer for an hour at 200 rpm.
3	Keep it undisturbed for 24 hours and extract the supernatant with a siphon to remove the dissolved gypsum.
4	Wash off soluble material from the sample with DI Water
5	Repeat steps 2 to 4, six times.
6	Oven dry the remaining at 40 °C

Solubility of Gypsum

Scope

To find the solubility of Gypsum in DI Water and Pond Water from Westbound Pond. Also, to analyze the ions on the dissolved water on the Ion Chromatography (IC) machine.

Apparatus

Sieve No. 200
Magnetic Stirrer
Siphon
Beaker

Procedure

Steps	Procedure
1	Sieving gypsum through No. 200 and mix 10 g with 1000 mL of DI Water.
2	Mix it using a magnetic stirrer at 400 rpm for an hour.
3	Keep it undisturbed for 24 hours and siphon for ion analysis in the Ion Chromatography machine.
4	Repeat the procedure with Pond Water.

Dissolution Rate of Gypsum

Scope

To find and analyze the dissolution rate of Gypsum with size fragments of < 0.45 mm and < 2.00 mm.

Apparatus

Sieve No. 40
Sieve No. 10
Magnetic Stirrer
Mechanical Pipette
4000 mL Beaker
Stopwatch
0.45 µm pore size high-quality nylon membrane
15 mL centrifuge tubes

Procedure

Steps	Procedure
1	Sieve 20g of gypsum through sieve No. 40 and mixed 500 mL of DI Water in a magnetic stirrer at 600 rpm.
2	Collect 15mL of the dissolved sample for 15 secs, 30 secs, 1 min, 2 min, 5 min, 10 min, and 20 min.
3	Filter the 15-mL collected through a 0.45 µm pore size membrane to remove non-dissolved particles
4	Analyze in ICP for Calcium concentrations
5	Repeat the procedure but now sieved gypsum through sieve No. 10.

Falling Head Permeability

Scope

Falling head permeability test is used to determine the time it takes for water to flow through fine grain soils such as silts and clays.

Apparatus

Falling Head Apparatus
Sieve No. 4
Soil sample
Tamper
Temperature meter
Flask
Squirt bottle

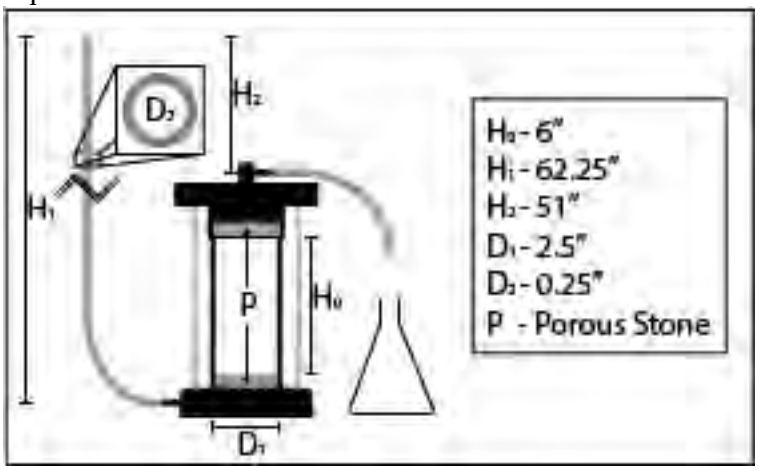

Falling Head Apparatus Set up (Not to Scale)

Procedure

Steps	Procedure
1	Sieve soil through sieve No. 4.
2	Fill the Falling head apparatus with the soil sample in three layers with 25 blows each layer. Record the apparatus weight before and after filling it with the soil sample.
3	Connect the in-house on the bottom of the apparatus and the out-hose on the top. Place a flask at the end of the out-hose to collect the water.
4	Saturate the soil with the desired water until it comes constantly from the out-hose.
5	Fill the in-hose to H_1 and record the height at 60, 120, and 240 seconds. Refill the in-hose to H_1 for each time.
6	Record the water temperature.

Calculations

Hydraulic Conductivity:

$$k = \frac{\alpha L}{A(t_2 - t_{1)}} \ln(\frac{h_1}{h_2})$$

k = vertical hydraulic conductivity

α = cross-sectional of the tube
L = length of the soil sample
A = cross-sectional area of the soil sample
t_2-t_1 = difference in the end of test time and initial test time
h_1 = initial head of water at time t_1
h_2 = end of test head water at time t_2
Temperature Correction Factor:
$R_T = 2.42 - 0.475\ln(T)$
R_T = Temperature correction factor in °C
T = Temperature at which the measurement was made
Reported Hydraulic Conductivity at 20 °C, $K_{20°C}$
$K_{20°C} = k \times R_T$

Water Leaching Test

Scope

To find metals (Ca^{2+}, Mg^{2+}, K^{+}, Na^{+} and other heavy metals) that passes through the soil, 30 mL, 80 mL, and 130 mL of water leaching needs to be collected for the ICP analysis.

Apparatus

Sieve No. 4
Falling Head Apparatus
Graduated Cylinder
Soil Sample
Tamper
Squirt Bottle

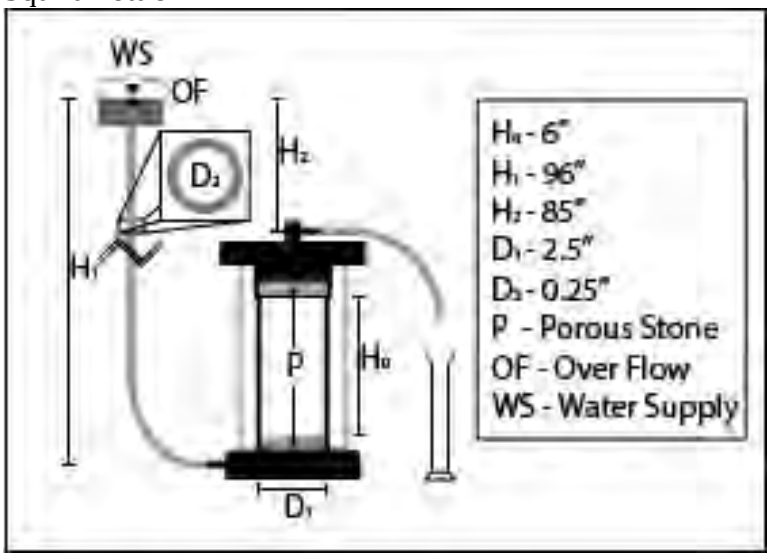

Leaching Apparatus (Not to Scale)

Procedure

Steps	Procedure
1	Sieve sample soil through sieve No. 4.
2	Fill the Leaching apparatus with the soil sample in three layers with 25 blows each layer. Record the apparatus weight before and after filling it with the soil sample.
3	Connect the in-hose on the bottom of the apparatus and the out-hose on the top. Place a graduated cylinder at the end of the out-hose to collect 30 mL of water.
4	Saturate the soil with the desired water until it comes constantly from the out-hose.
5	Fill the in-hose to H_1 and keep a constant head. Collect 30 mL of water.
6	Cut the saturated soil in three parts (Top, Middle, and Bottom) to also analyze it on the ICP.
7	Redo the procedure for 80 mL and 130 mL

APPENDIX B: SOIL PHYSICAL/CHEMICAL CHARACTERISTICS AND CQC BORING LOGS

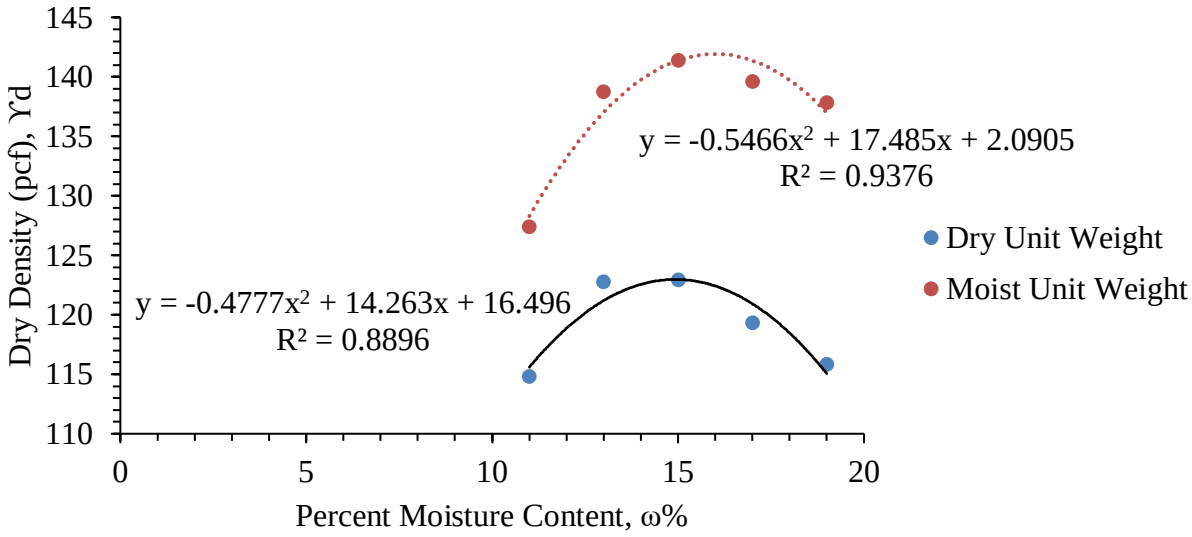

Figure B. 1 Upper Valley Soil MD Curve

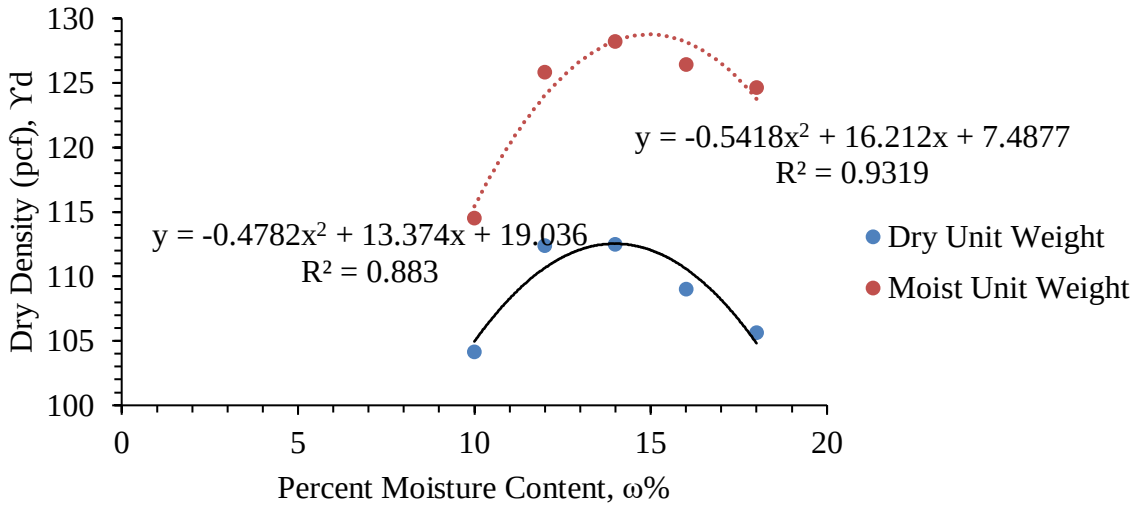

Figure B. 2 Interchange Soil MD Curve

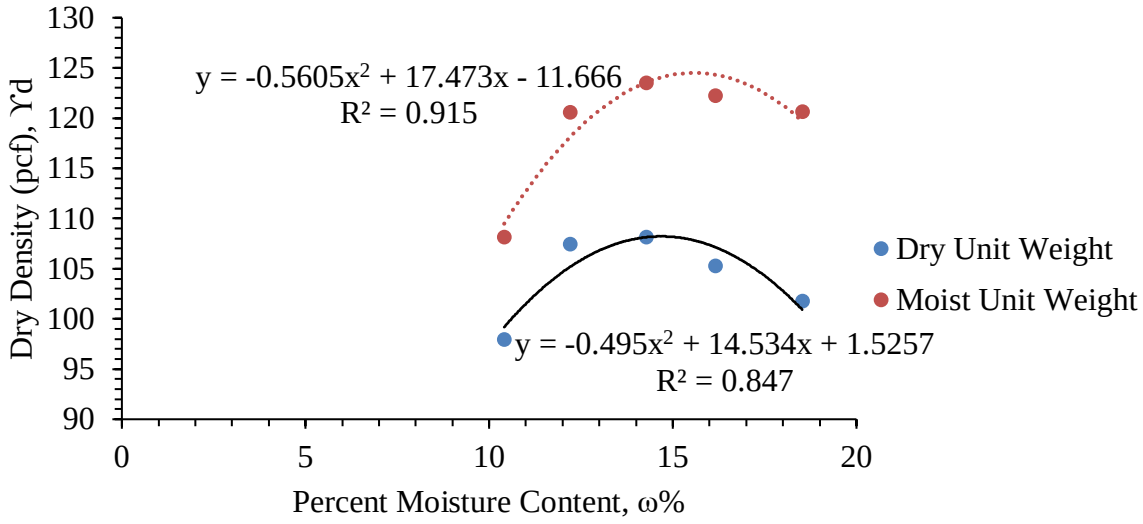

Figure B. 3 Westbound Soil MD Curve

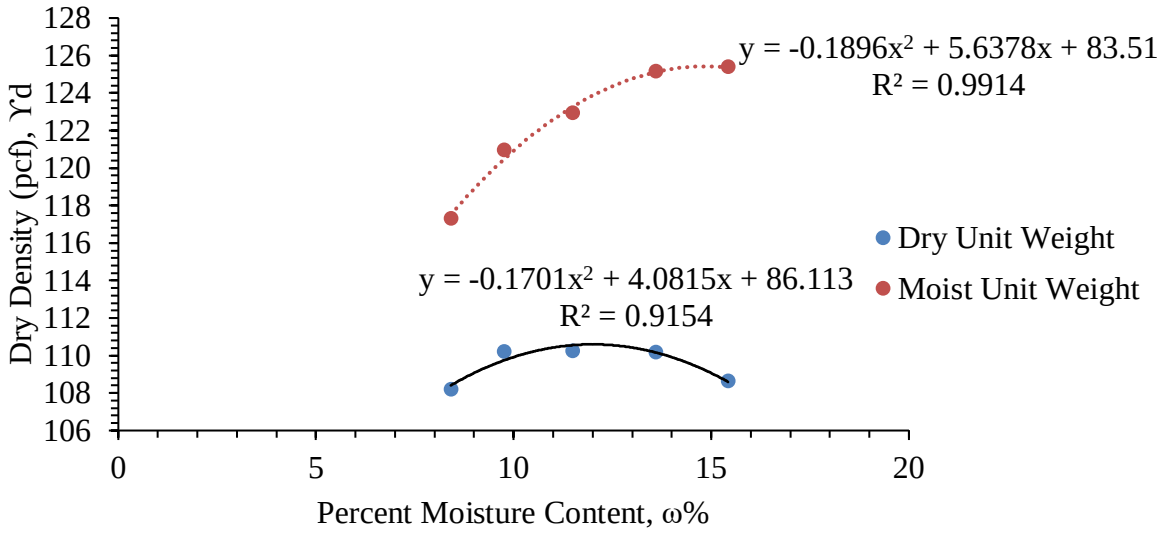

Figure B. 4 Site Soil MD Curve

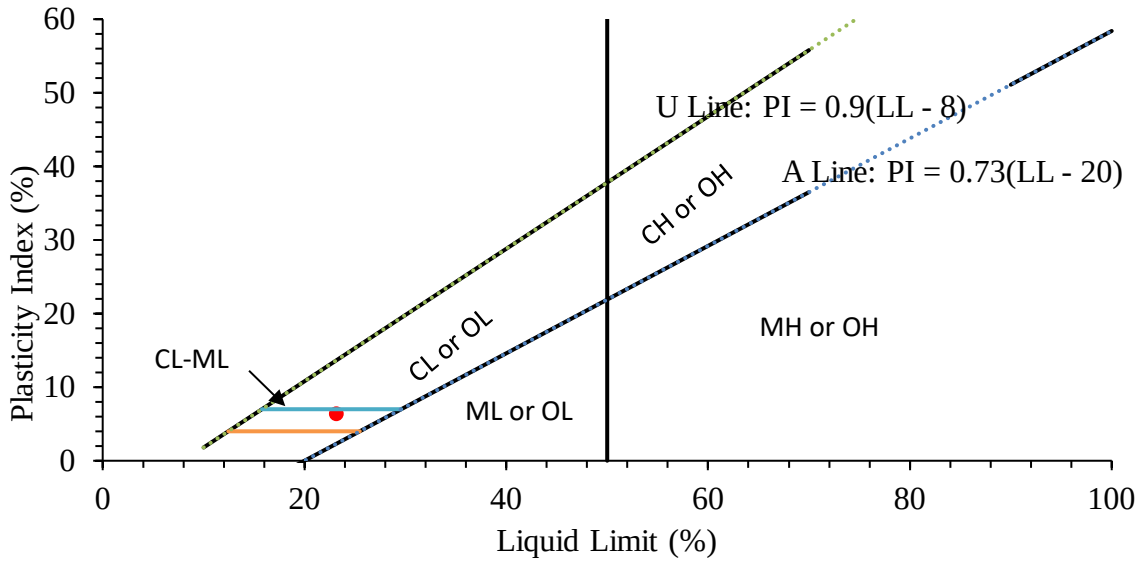

Figure B. 5 Upper Valley Soil Plasticity Chart

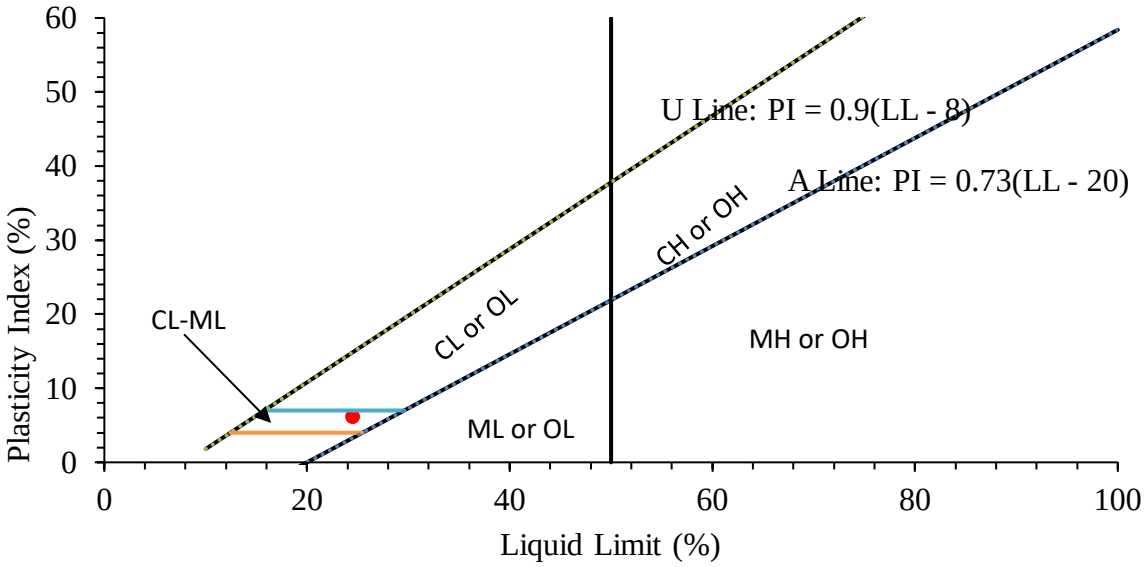

Figure B. 6 Interchange Soil Plasticity Chart

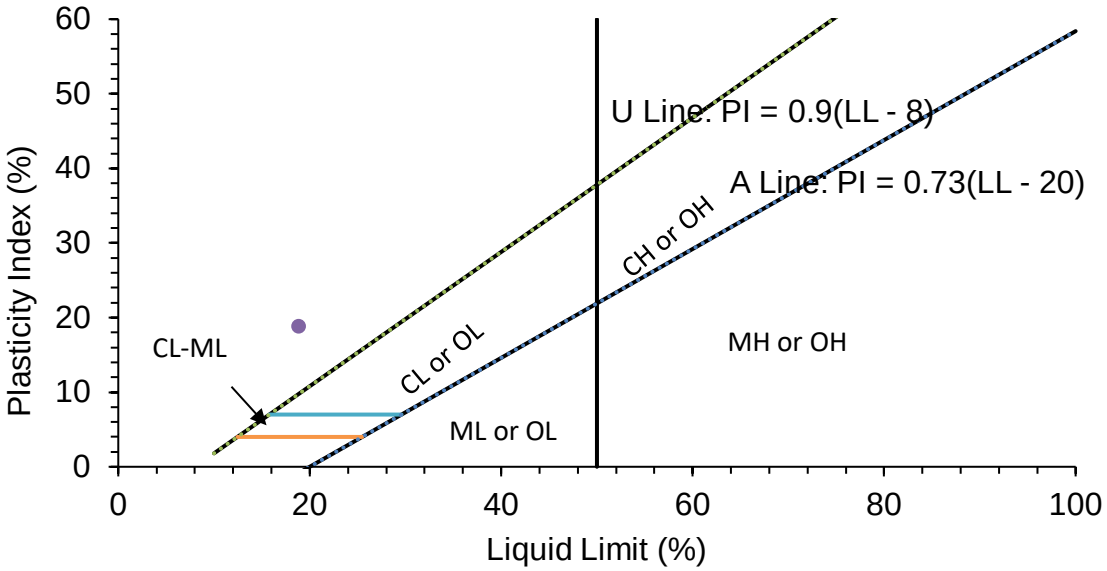

Figure B. 7 Westbound Soil Plasticity Chart

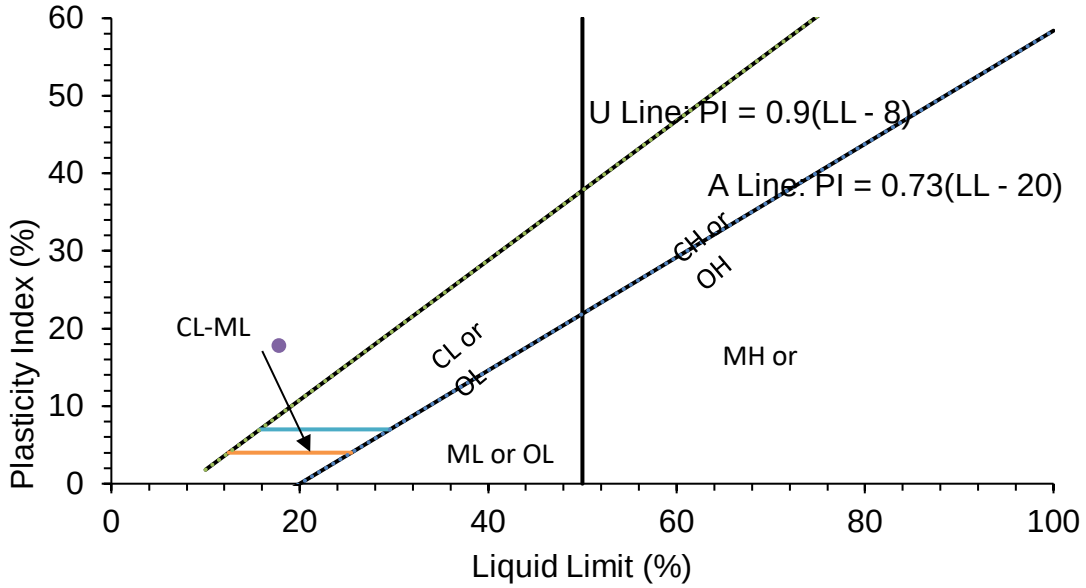

Figure B. 8 Site Soil Plasticity Chart

Table B. 1 Bound Cations in Selected Soils

Bound Cations				
	Interchange (mg/L)	Site Pond (mg/L)	Upper Valley (mg/L)	Westbound (mg/L)
Ca	17.38	201.88	415.15	17.04
K	5.25	8.29	20.08	9.02
Mg	1.90	1.91	21.36	1.90
Na	25.39	27.81	38.94	27.16
P	0.16	0.00	0.00	0.04
As	0.17	0.10	0.32	0.04
Ba	2.32	0.68	2.90	0.54
Cu	0.13	0.03	0.00	0.03
Hg	0.03	0.07	0.03	0.01
Li	0.10	0.10	0.12	0.10
Mn	0.10	0.87	0.15	0.58
Pb	0.20	0.09	0.07	0.07
Se	0.17	0.14	0.22	0.23
Sn	0.04	0.00	0.21	0.08
Sr	0.03	0.20	3.52	0.18
Zn	0.32	0.08	0.00	0.18
Si	1.91	1.13	2.91	1.44

Table B. 2 Soluble Cations in Selected Soils

Soluble Cations				
	Interchange (mg/L)	Site Pond (mg/L)	Upper Valley (mg/L)	Westbound (mg/L)
Ca	15.47	58.13	14.28	104.09
K	2.54	2.49	5.01	3.09
Mg	0.81	1.45	1.39	2.73
Na	22.36	23.39	30.43	22.59
As	0.00	0.07	0.00	0.07
Ba	0.00	0.05	0.03	0.06
Hg	0.05	0.03	0.22	0.13
Li	0.10	0.10	0.11	0.10
Pb	0.05	0.03	0.00	0.03
Sn	0.00	0.00	0.03	0.00
Sr	0.02	0.16	0.13	0.40
Si	1.97	0.88	2.71	1.40

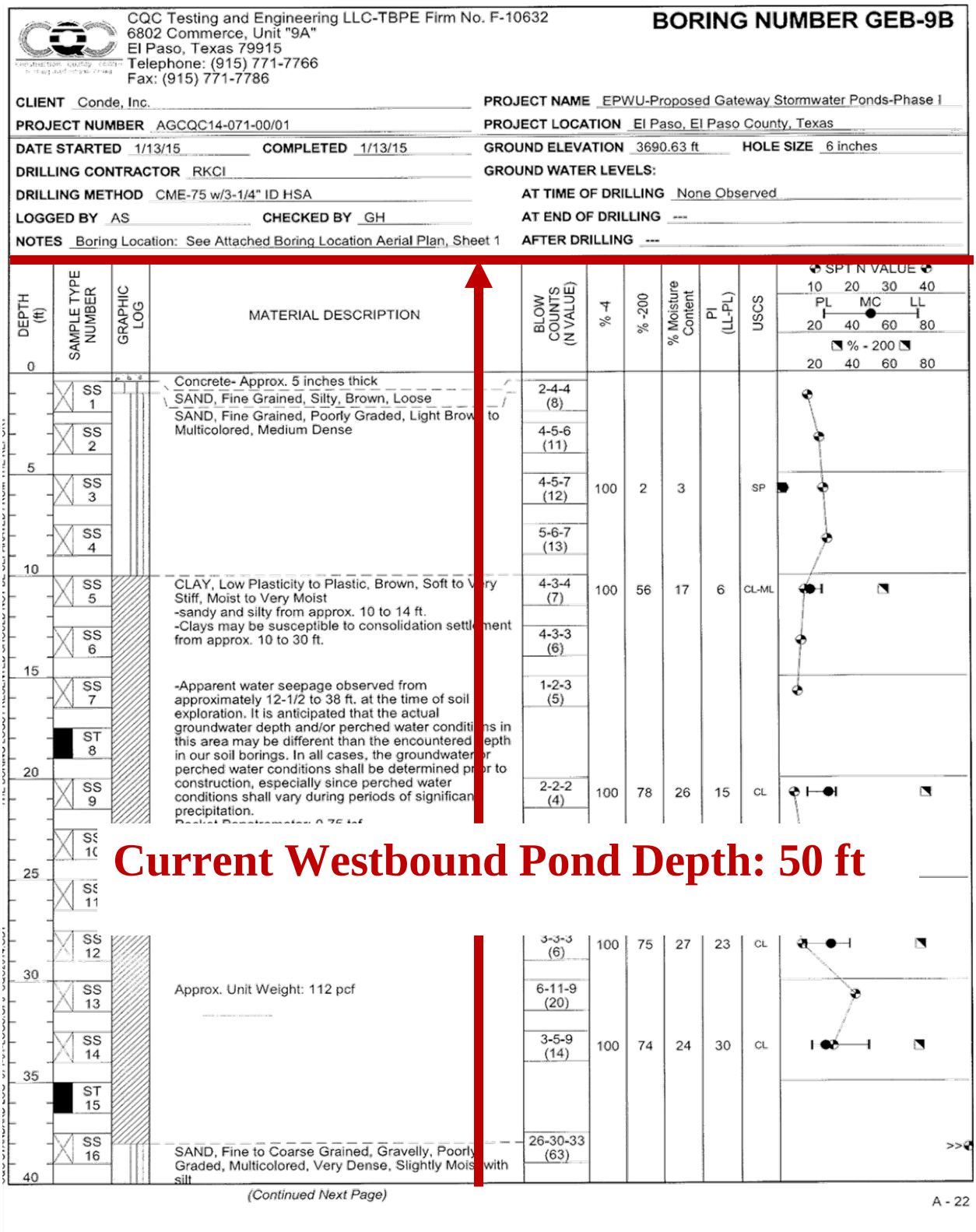

Current Westbound Pond Depth: 50 ft

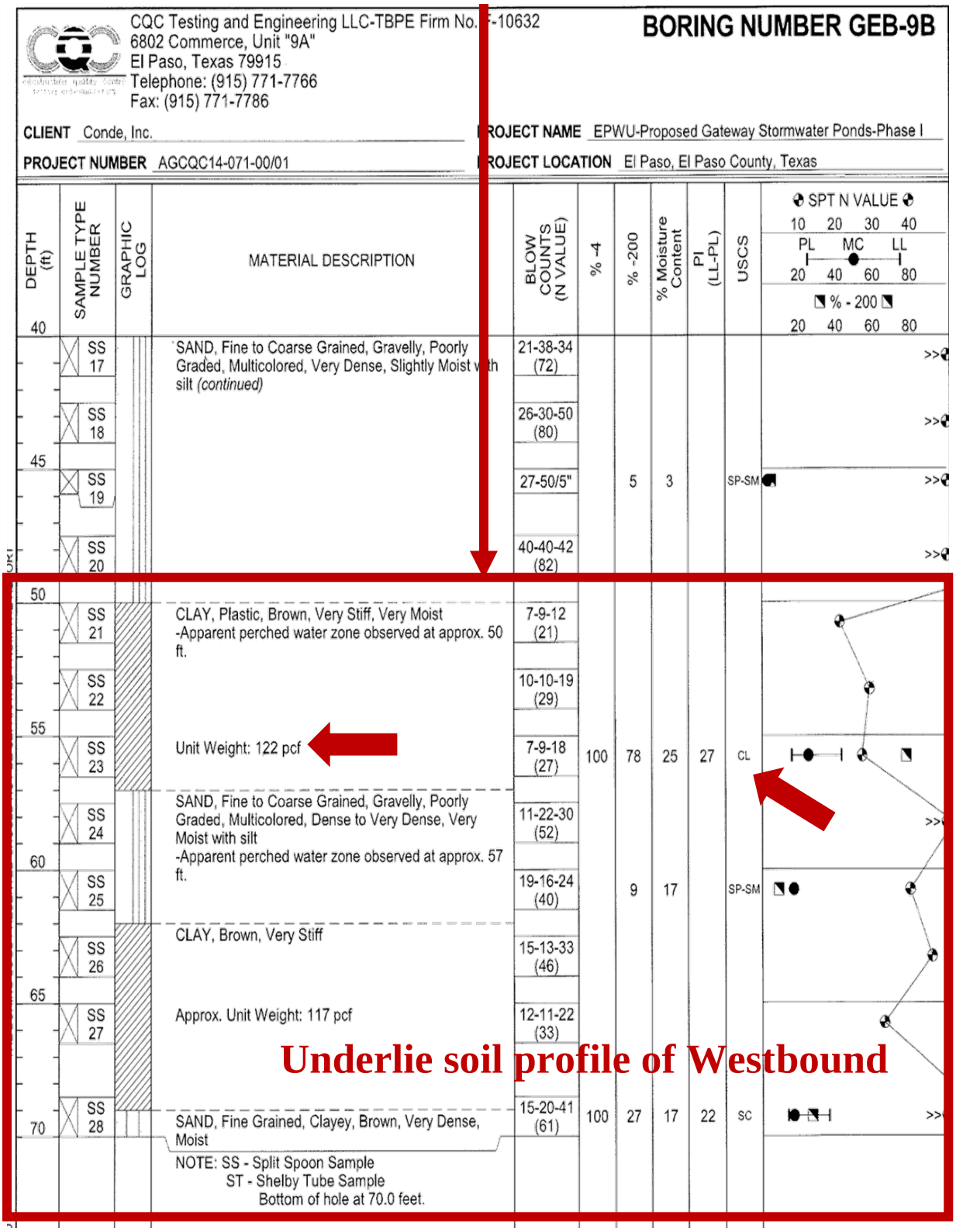

Figure B. 9 CQC Boring Log for Westbound pond

APPENDIX C: GYPSUM ANALYTICAL RESULTS

Table C.1 Major, Minor and Trace Constituents of RG

Major and minor Constituent:	mg/kg
Calcium, Ca	250518.40
Iron, Fe	576.99
Magnesium, Mg	1416.00
Phosphorous, P	106.60
Potassium, K	7782.84
Sodium, Na	5816.00
Trace Constituent:	**mg/kg**
Arsenic, As	31.98
Cadmium, Cd	1.33
Chromium, Cr	4.00
Copper, Cu	4.00
Iron, Fe	576.99
Lithium, Li	4.00
Manganese, Mn	27.98
Nickel, Ni	6.66
Lead, Pb	6.66
Selenium, Se	4.00
Zinc, Zn	5.46
Chloride, Cl	1200.00
Nitrate, NO3	458.00
Sulfate, SO4	595978.40

ANALYTICAL REPORT

March 27, 2014

Work Order: 94B0021

Report To
Gilbert Garcia El Paso C & D Recycling 12520 Pellicano El Paso, TX 79996

Project : Gypsum

Project Number : Gypsum

PO :

RECYCLED WALLBOARD Gypsum

Analyte	Result	Method	Limits
ID:Gypsum	Matrix:Solid	Collected: 02/11/14 00:00	
Determination of Conventional Chemistry Parameters			
Nitrogen, Kjeldahl, total	142 mg/kg	EPA 351.2	
Determination of Inorganic Anions			
Chloride	791 mg/kg	EPA 9056	
Determination of Total Metals			
Aluminum, total	550 mg/kg	EPA 6010B	
Arsenic, total	<25.0 mg/kg	EPA 6010B	
Boron, total	84.1 mg/kg	EPA 6010B	
Cadmium, total	<1.0 mg/kg	EPA 6010B	
Calcium, total	188000 mg/kg	EPA 6010B	
Chromium, total	<3.0 mg/kg	EPA 6010B	
Cobalt, total	<1.0 mg/kg	EPA 6010B	
Copper, total	<3.0 mg/kg	EPA 6010B	
Iron, total	433 mg/kg	EPA 6010B	
Lead, total	<5.00 mg/kg	EPA 6010B	
Lithium, total	3 mg/kg	EPA 6010B	
Magnesium, total	713 mg/kg	EPA 6010B	
Manganese, total	20.9 mg/kg	EPA 6010B	
Molybdenum, total	<1.0 mg/kg	EPA 6010B	
Nickel, total	<5.0 mg/kg	EPA 6010B	
Phosphorus, total	<100 mg/kg	EPA 6010B	
Potassium, total	247 mg/kg	EPA 6010B	
Selenium, total	<3.0 mg/kg	EPA 6010B	
Sulfur, total	129000 mg/kg	EPA 6010B	
Zinc, total	4.1 mg/kg	EPA 6010B	

Figure C. 1 RG Analytical Results

APPENDIX D: XRD RESULTS AND SEM IMAGES

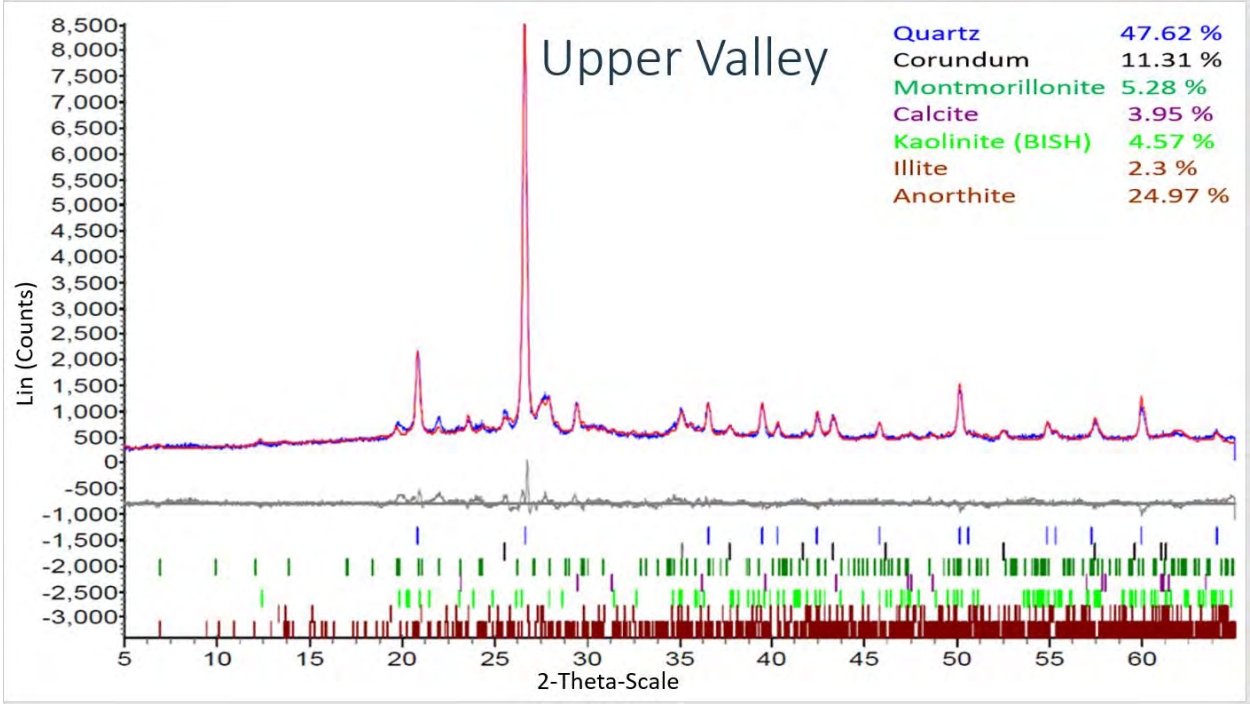

Figure D. 1 XRD Pattern for Upper Valley Soil Identified at Particles <0.42 mm

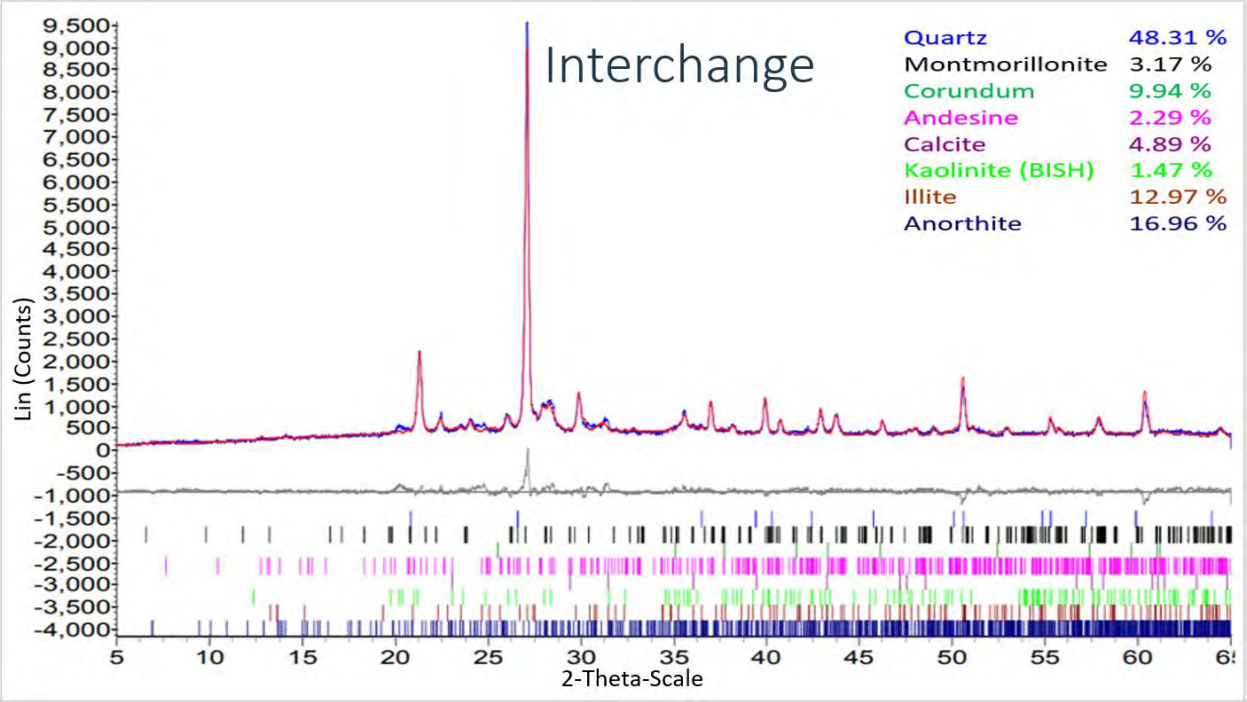

Figure D. 2 XRD Pattern for Interchange Soil Identified at Particles <0.42 mm

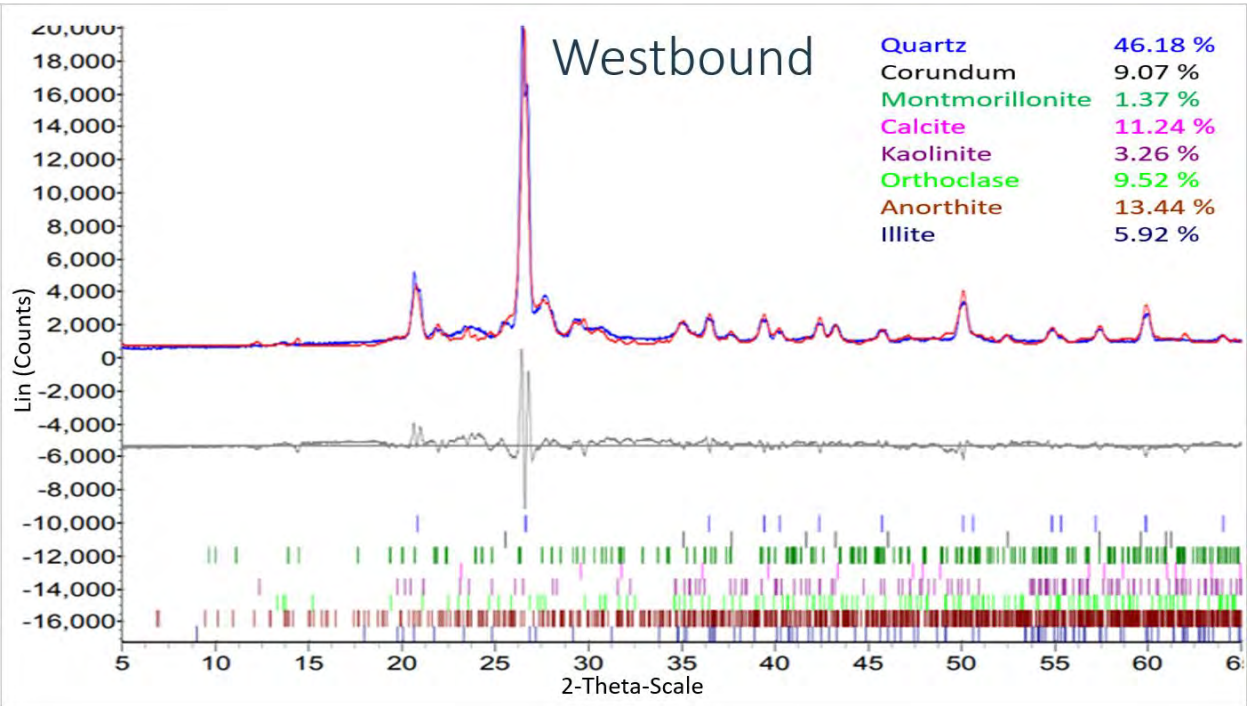

Figure D. 3 XRD Pattern for Westbound Soil Identified at Particles <0.42 mm

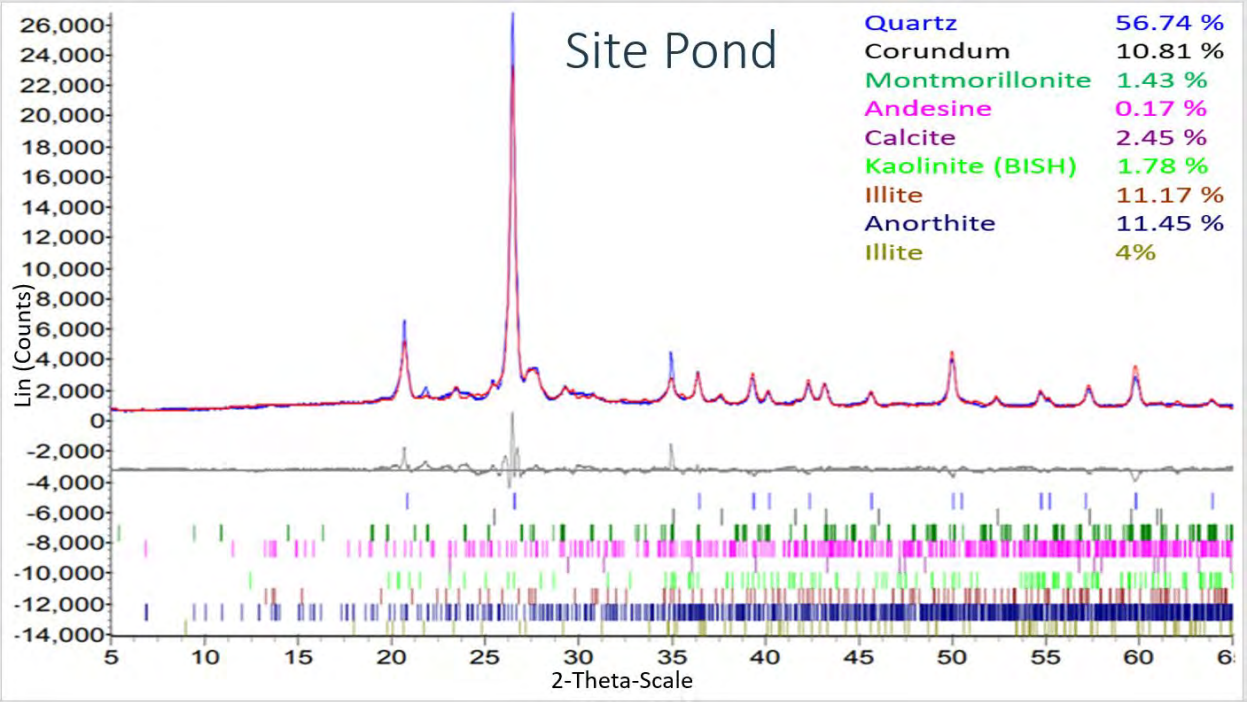

Figure D. 4 XRD Pattern for Site Pond Soil Identified at Particles <0.42 mm

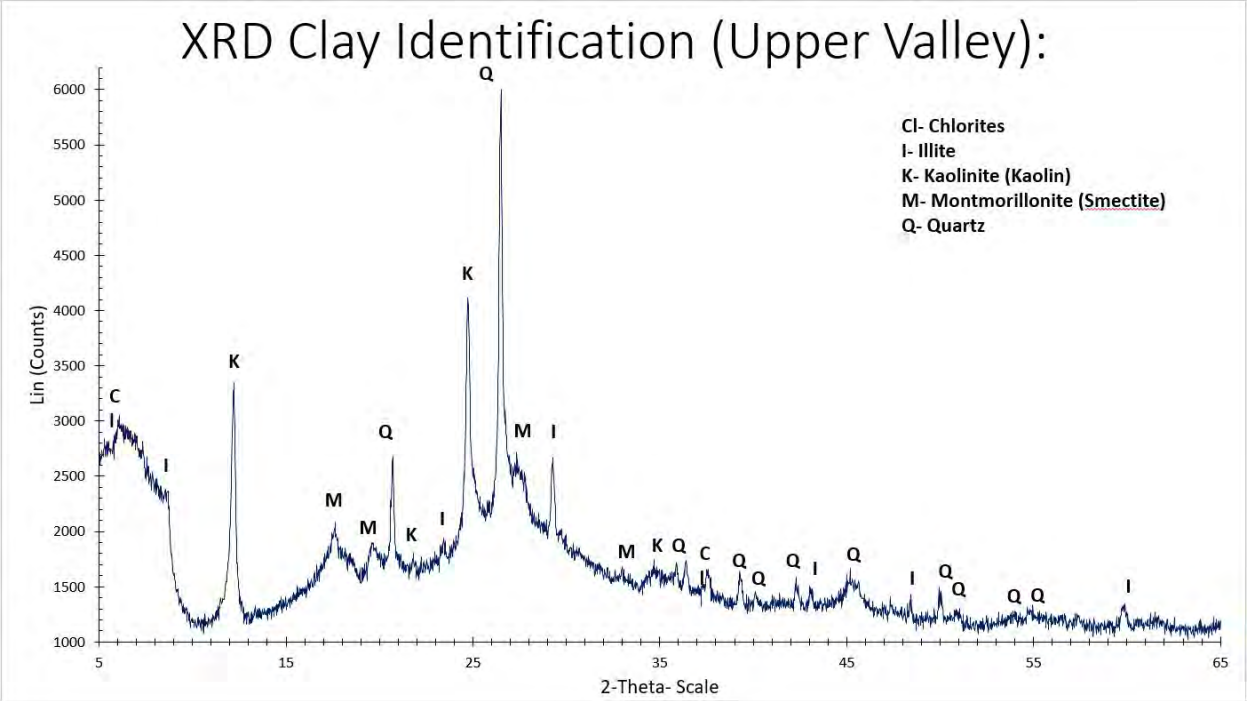

Figure D. 5 XRD Pattern Identification for Upper Valley Soil at Particles < 0.074 mm

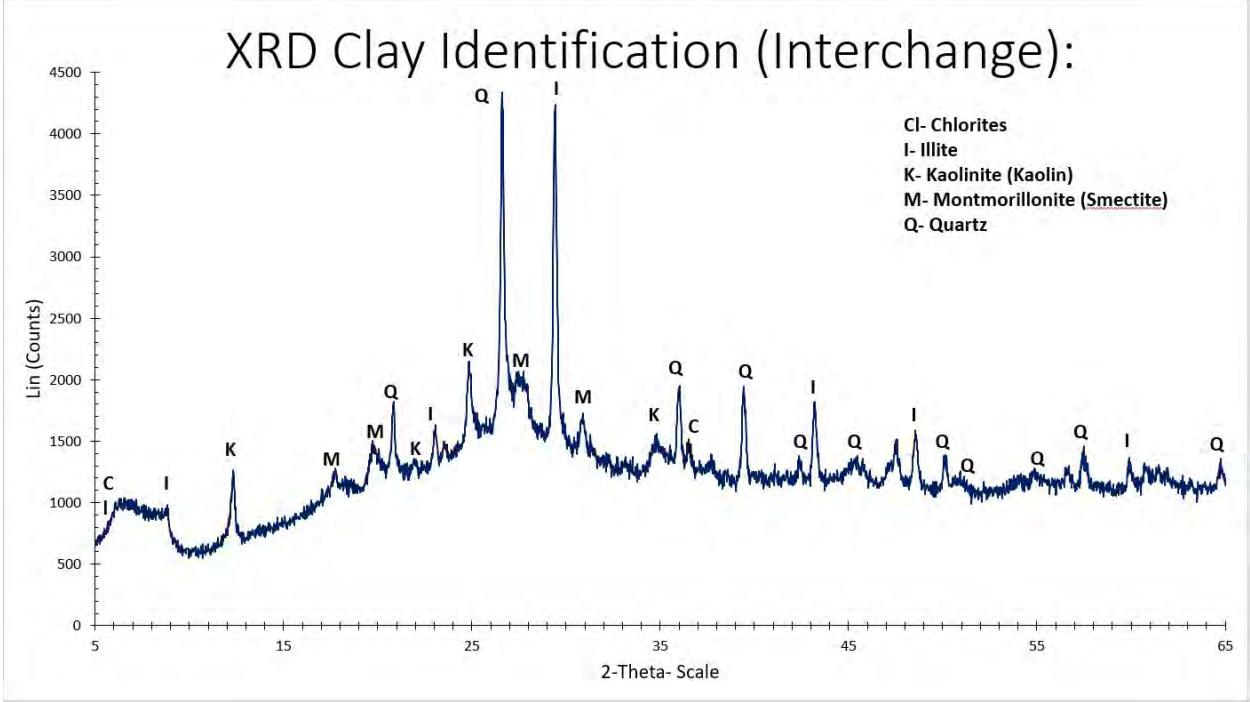

Figure D. 6 XRD Pattern Identification for Interchange Soil at Particles < 0.074 mm

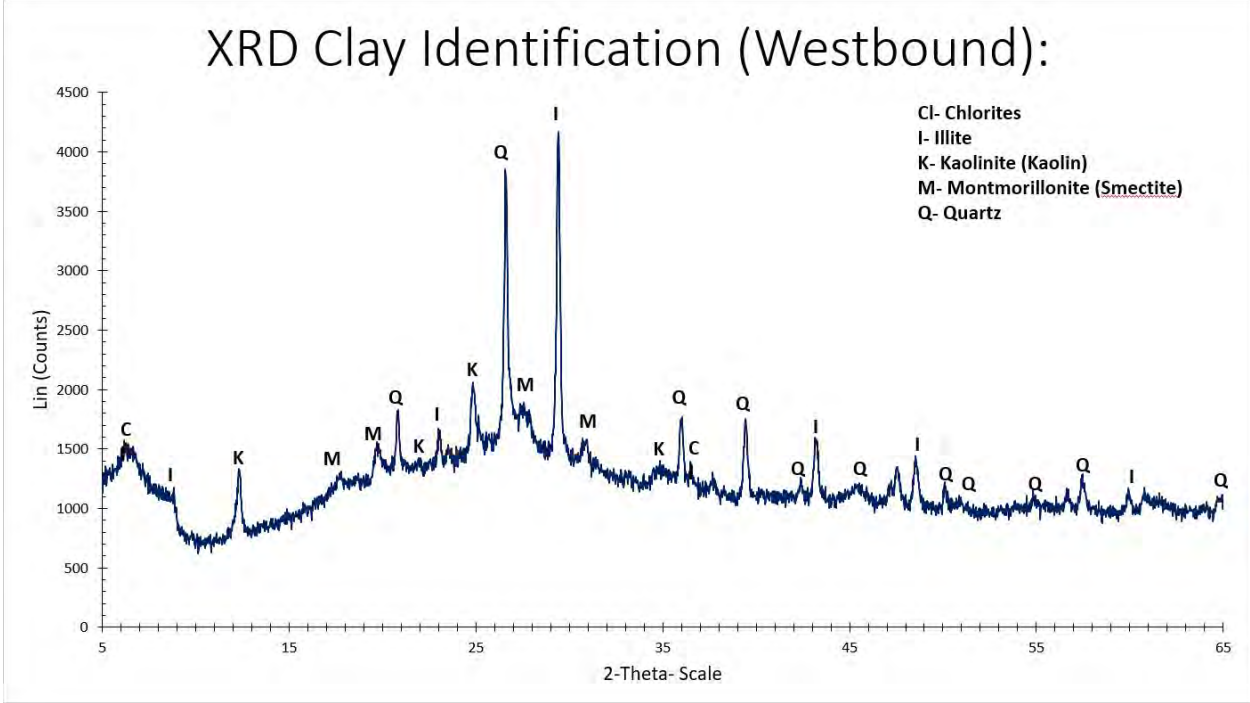

Figure D. 7 XRD Pattern Identification for Westbound Soil at Particles < 0.074 mm

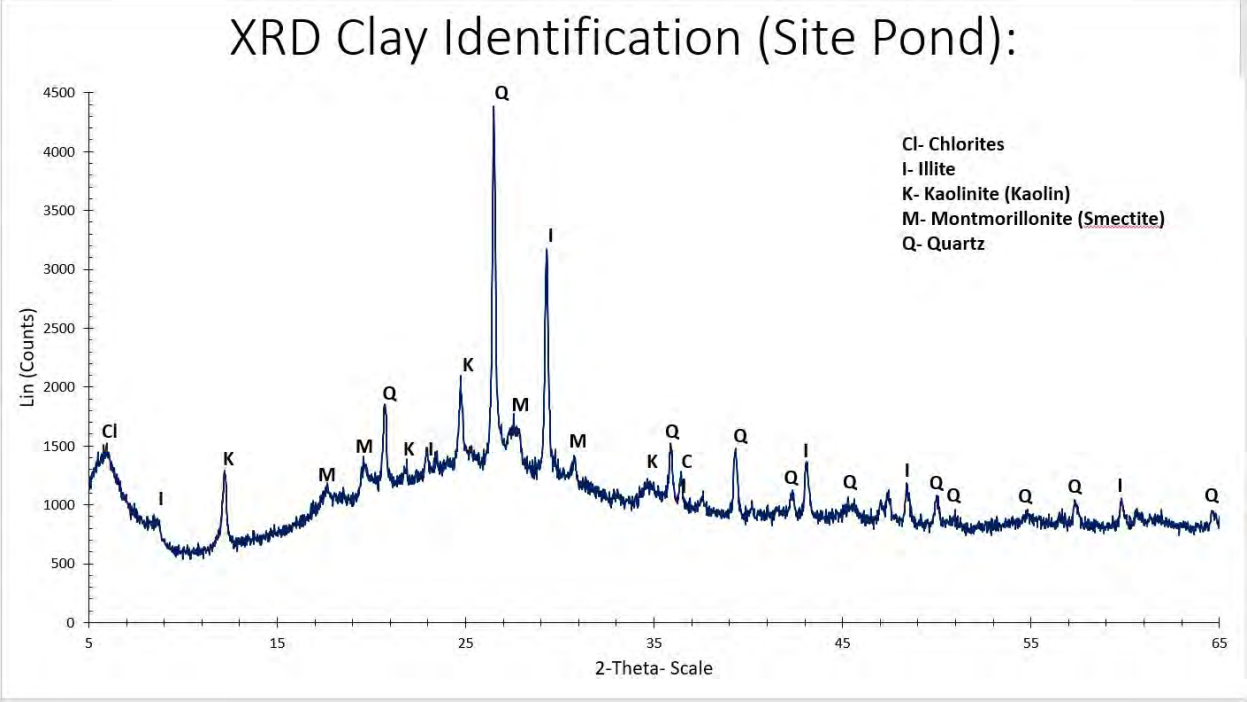

Figure D. 8 XRD Pattern Identification for Site Pond Soil at Particles < 0.074 mm

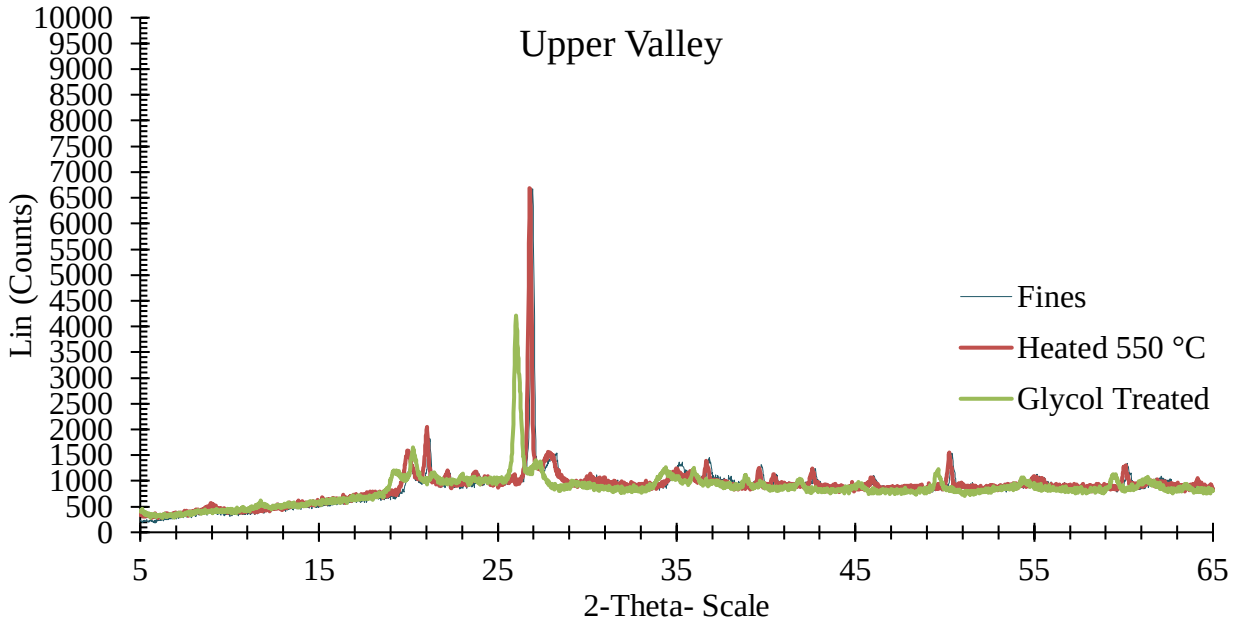

Figure D. 9 Upper Valley XRD Fines Pattern Shiftiness in Response to Treatments

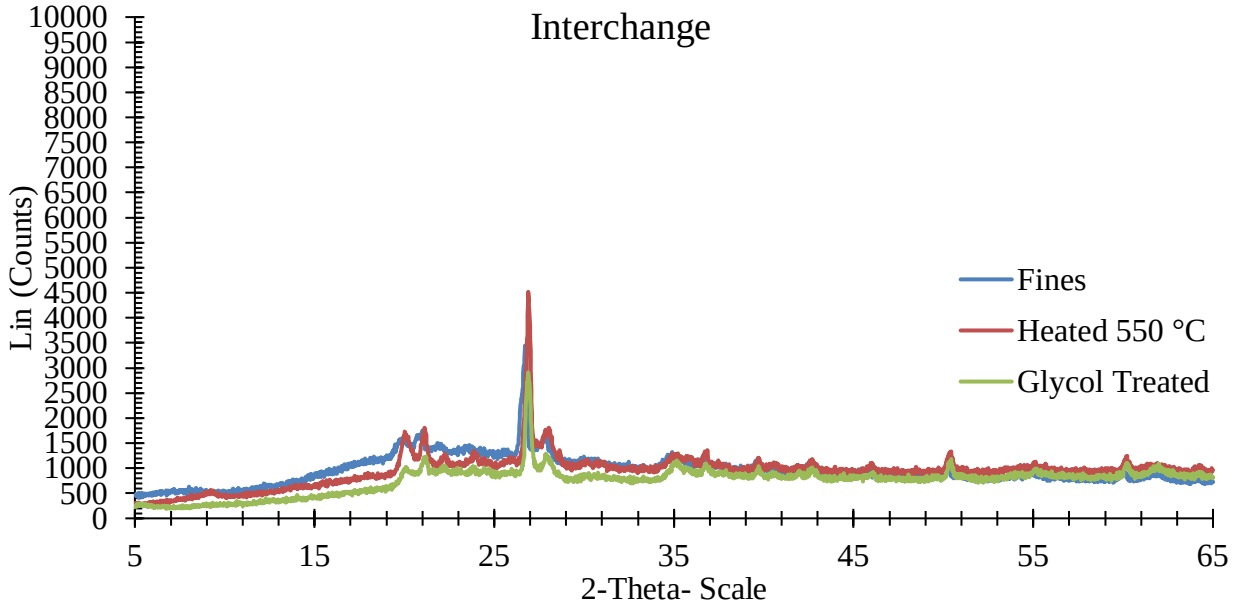

Figure D. 10 Interchange XRD Fines Pattern Shiftiness in Response to Treatments

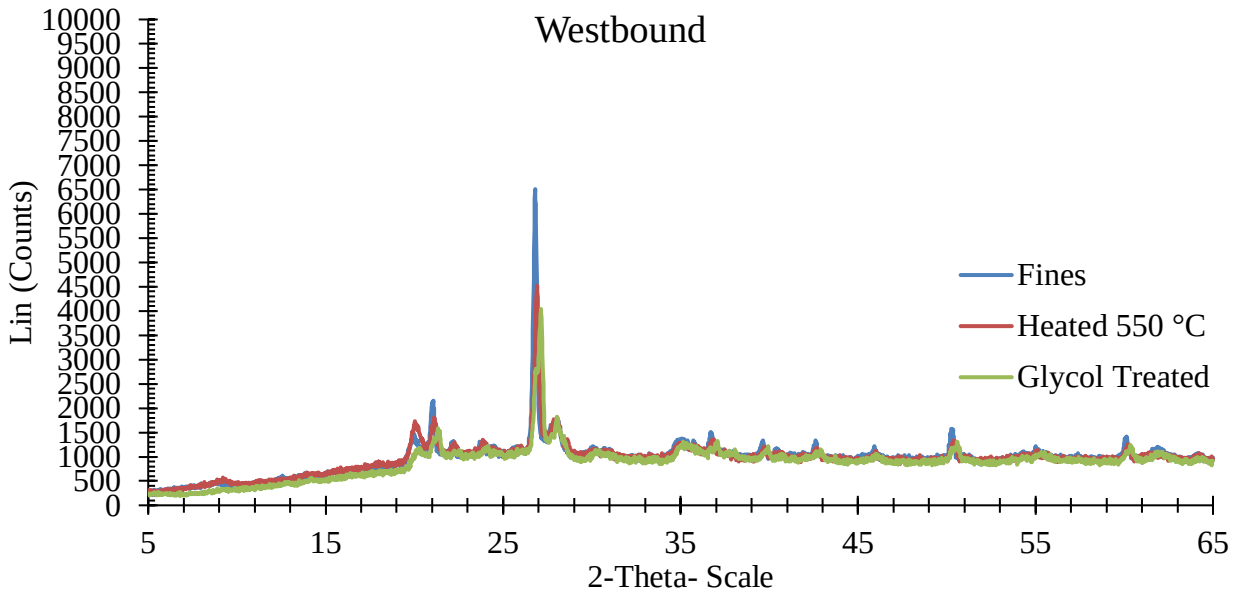

Figure D. 11 Westbound XRD Fines Pattern Shiftiness in Response to Treatments

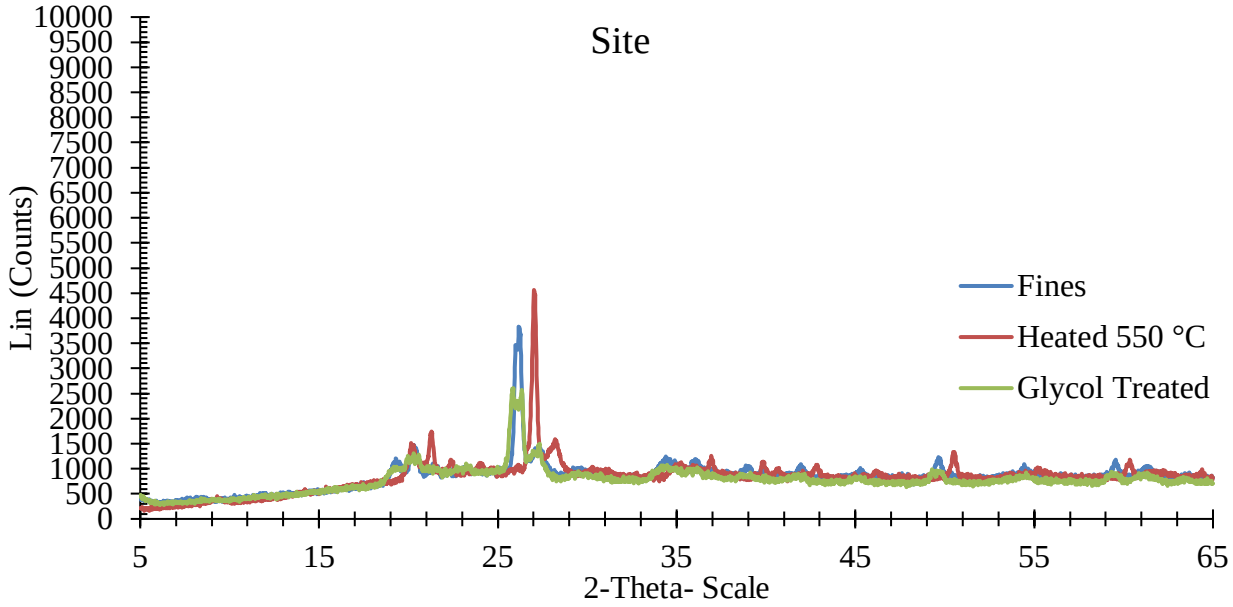

Figure D. 12 Site XRD Fines Pattern Shiftiness in Response to Treatments

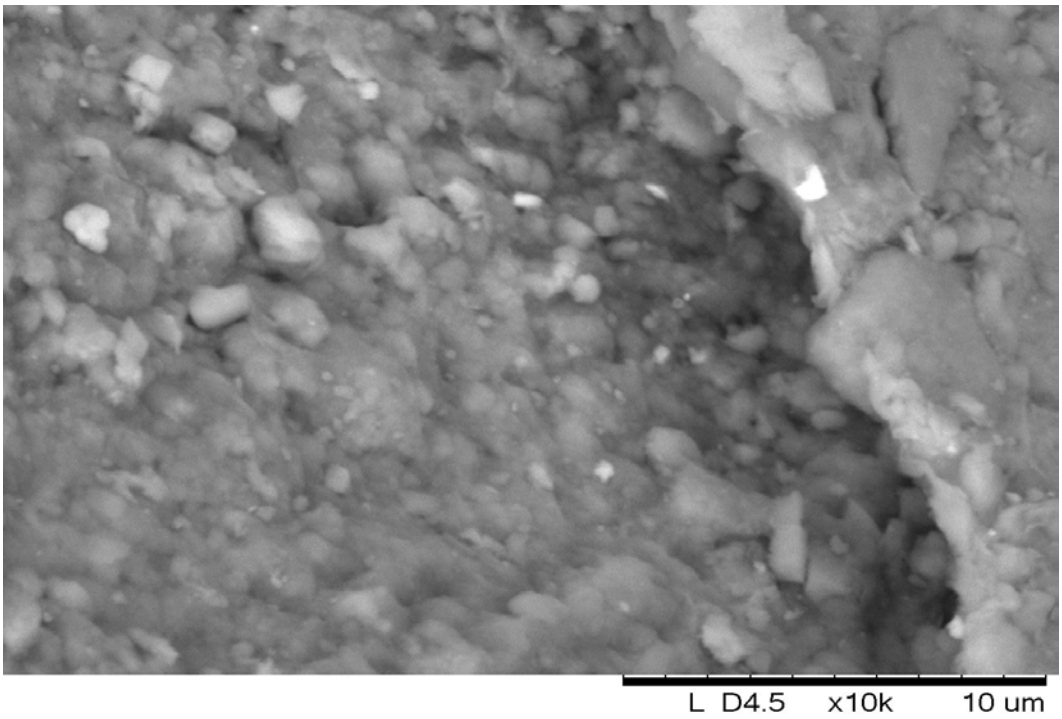

Figure D. 13 Upper Valley Soil under SEM

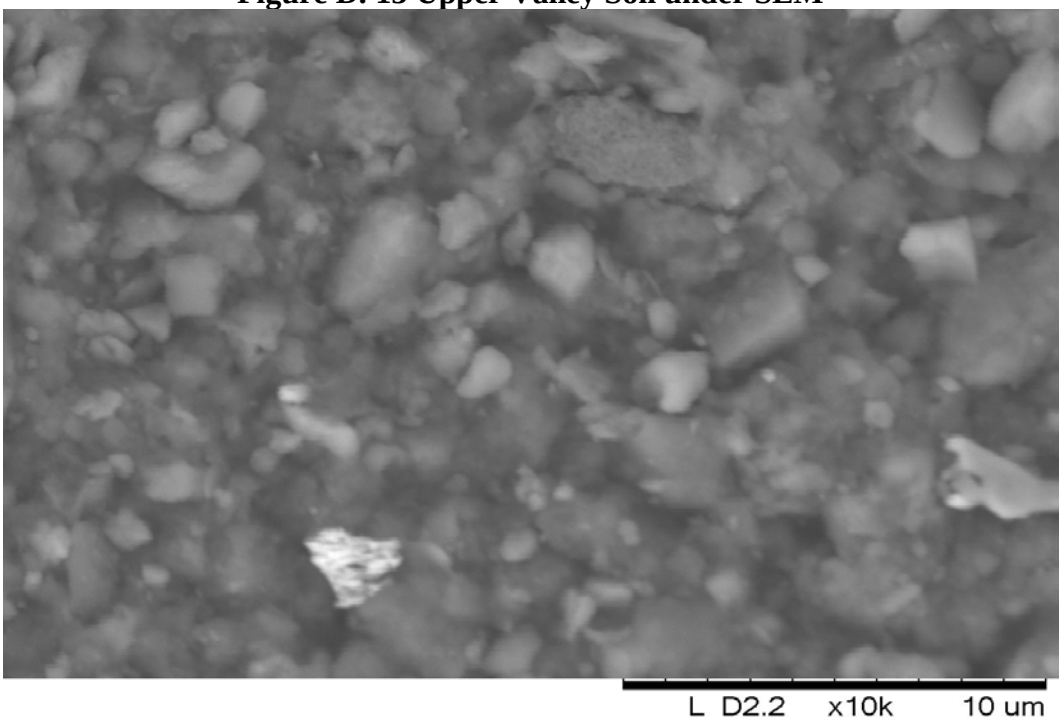

Figure D. 14 Interchange Soil under SEM

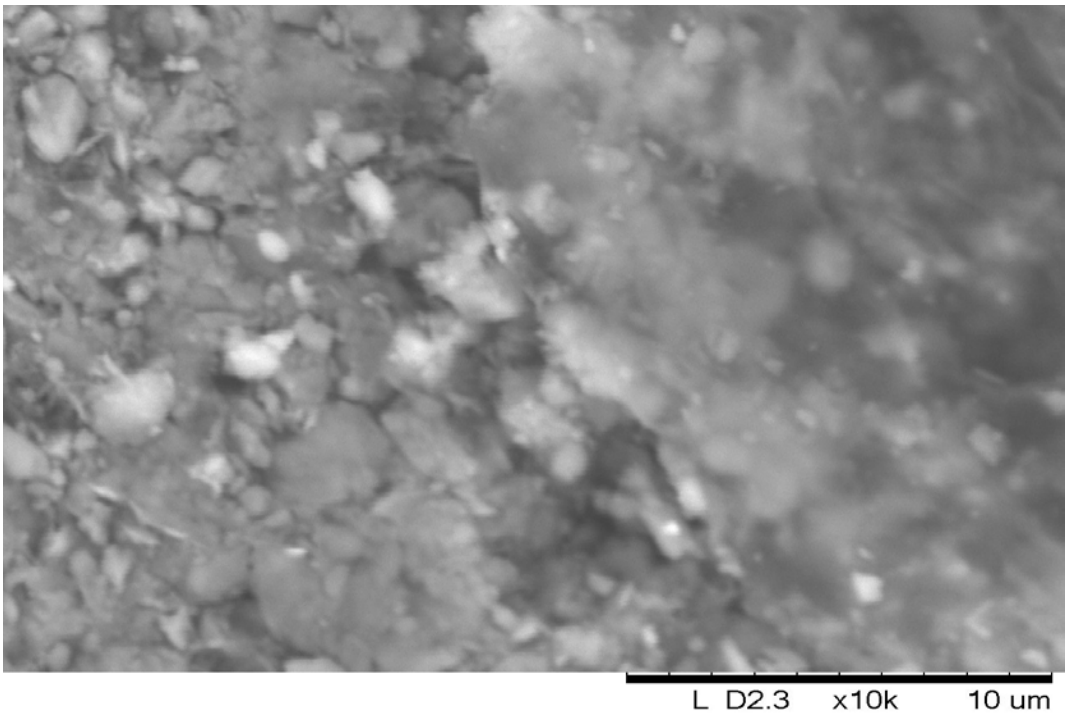

Figure D. 15 Westbound Soil under SEM

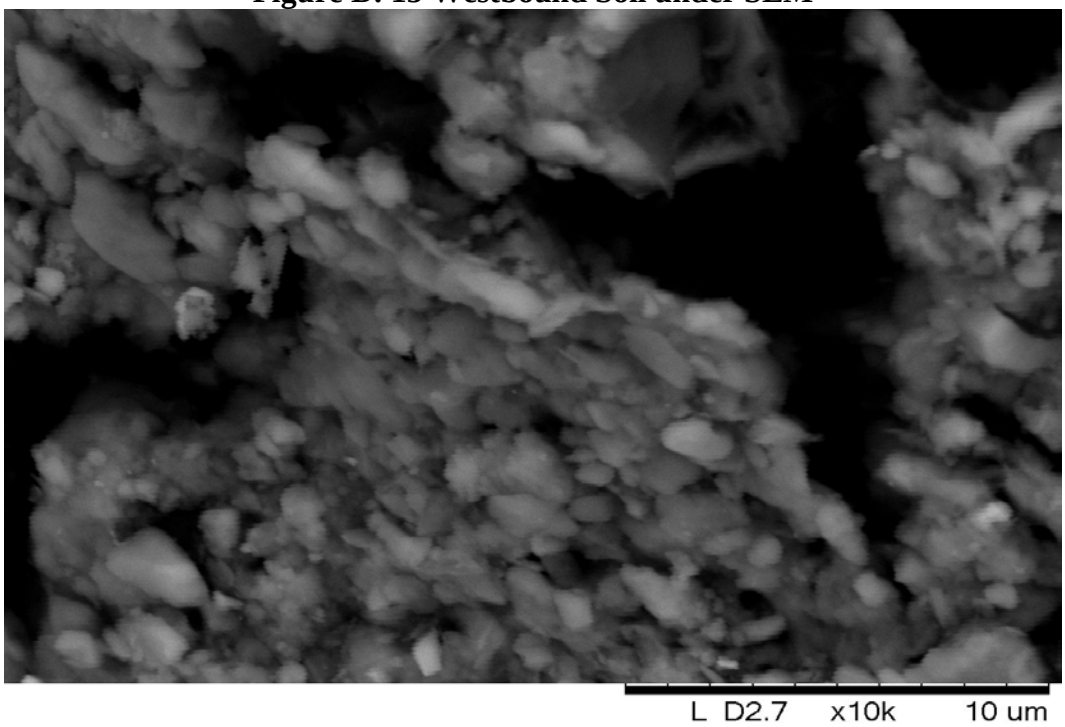

Figure D. 16 Site Soil under SEM

APPENDIX E: RBCA TOOLKIT (INPUT PARAMETERS AND LEACHING RESULTS)

RBCA SITE ASSESSMENT — Input Parameter Summary

Site Name: Westbound
Site Location: El Paso, TX

Completed By: Jorge Navarrete
Date Completed: NA

Exposure Parameters		Residential				Commercial/Industrial		User Defined
		Child*	Adolescent	Adult	Age-Adjusted**	Adult	Construct.	
ATc	Averaging time for carcinogens (yr)	70	70	70	NA	70	70	-
ATn	Averaging time for non-carcinogens (yr)	6	12	30	NA	25	1	-
BW	Body weight (kg)	15	35	70	NA	70	70	-
ED	Exposure duration (yr)	6	12	30	NA	25	1	-
	Averaging time for vapor flux (yr)	30	30	30	NA	30	30	-
EF	Exposure frequency (days/yr)	350	350	350	NA	250	180	-
EFD	Exposure frequency for dermal exposure	350	350	350	NA	250	180	-
IRw	Ingestion rate of water (L/day)	1	1	2	2.5	1	NA	-
IRs	Ingestion rate of soil (mg/day)	200	200	100	387	50	100	-
SA	Skin surface area (dermal) (cm^2)	2023	2023	3160	4771	3160	3160	-
M	Soil to skin adherence factor	0.5	0.5	0.5	NA	0.5	0.5	-
ETswim	Swimming exposure time (hr/event)	1	3	3	NA	NA	NA	NA
EVswim	Swimming event frequency (events/yr)	12	12	12	NA	NA	NA	NA
IRswim	Water ingestion while swimming (L/hr)	0.5	0.5	0.05	0.3	NA	NA	NA
SAswim	Skin surface area for swimming (cm^2)	3500	8100	23000	15680	NA	NA	NA
IRfish	Ingestion rate of fish (kg/yr)	0.025	0.025	0.025	0.053	NA	NA	NA
fish	Contaminated fish fraction (unitless)	1	1	1	NA	NA	NA	NA
IRbg	Below-ground vegetable ingestion	0.002	0.002	0.006	2.053	NA	NA	NA
IRabg	Above-ground vegetable ingestion	0.001	0.001	0.002	0.887	NA	NA	NA
VGbg	Above-ground Veg. Ingest. Correction Factor	0.01	0.01	0.01	NA	NA	NA	NA
VGabg	Below-ground Veg. Ingest. Correction Factor	0.01	0.01	0.01	NA	NA	NA	NA

* = Child Receptor used for Non-Carcinogens

** = Age-adjusted rate is effective value corresponding to adult exposure factors.

Complete Exposure Pathways and Receptors	On-site	Off-site 1	Off-site 2
Groundwater:			
Groundwater Ingestion	None	None	None
Soil Leaching to Groundwater Ingestion	None	MCL	MCL
Apply MCL Values	No	Yes	Yes
Applicable Surface Water Exposure Routes:			
Swimming	NA	NA	None
Fish Consumption	NA	NA	None
Aquatic Life Protection	NA	NA	None
Soil:			
Direct Contact: direct combined pathways	None	NA	NA
Apply CLEA- UK SGV levels		No	
Outdoor Air:			
Particulates from Surface Soils	None	None	None
Volatilization from Soils	None	None	None
Volatilization from Groundwater	None	None	None
Indoor Air:			
Volatilization from Soils	None	NA	NA
Volatilization from Groundwater	None	None	None
Soil Leaching to Groundwater Volatilization	None	None	None

Receptor Distance from Source Media	On-site	Off-site 1	Off-site 2	(Units)
Groundwater receptor	NA	NA	NA	(ft)
Outdoor air inhalation receptor	NA	NA	NA	(ft)
Indoor air inhalation receptor	NA	NA	NA	(ft)

Target Health Risk Values		Individual	Cumulative
TR	Target Risk (carcinogens)	1.0E-5	1.0E-5
THQ	Target Hazard Quotient (non-carcinogenic risk)	1.0E+0	1.0E+0

Modeling Options	
RBCA tier	Tier 2
Outdoor air volatilization model	NA
Indoor air volatilization model	NA
Soil leaching model	ASTM leaching model
Use soil attenuation model (SAM) for leachate?	Yes
Use dual-equilibrium desorption model?	Yes
Apply Mass Balance Limit for Soil Volatilization?	No
Apply UK (CLEA) SVG as soil concentration limit	No
Vegetable calculation options	NA
Air dilution factor	NA
Groundwater dilution-attenuation factor	Domenico model

Figure E. 1 RBCA Tool Kit Chemical Releases Input Summary I

Site Name: Westbound
Site Location: El Paso, TX

Completed By: Jorge Navarrete
Date Completed: NA

Surface Soil Column Parameters		Value			(Units)
h_{cap}	Capillary zone thickness	NA			(ft)
h_v	Vadose zone thickness	NA			(ft)
ρ_b	Soil bulk density	1.7			(g/cm^3)
f_{oc}	Fraction organic carbon	0.01			(-)
n	Soil total porosity	***0.36***			(-)
		capillary	**vadose**	**foundation**	
θ_w	Volumetric water content	***0.35***	***0.34***	0.12	(-)
θ_a	Volumetric air content	***0.01***	***0.02***	0.26	(-)
K_{vs}	Vertical hydraulic conductivity	***0.1***			(ft/d)
k_v	Vapor permeability	***1.08E-16***			(ft^2)
L_{gw}	Depth to groundwater	***25***			(ft)
pH	Soil/groundwater pH	***7.65***			(-)
W	Length of source-zone area parallel to wind	NA			(ft)
W_{gw}	Length of source-zone area parallel to GW flow	***168***			(ft)
L_{ss}	Thickness of affected surface soils	NA			(ft)
A	Source zone area	NA			(ft^2)
L_s	Depth to top of affected soils	0			(ft)
L_{base}	Depth to base of affected soils	***20***			(ft)
L_{subs}	Thickness of affected soils	***20***			(ft)

Groundwater Parameters		Value	(Units)
h_{gw}	Groundwater mixing zone depth	***20***	(ft)
I	Net groundwater infiltration rate	***200***	(in/yr)
U_{gw}	Groundwater Darcy velocity	***0.33***	(ft/d)
v_{gw}	Groundwater seepage velocity	***0.868421053***	(ft/d)
K_s	Saturated hydraulic conductivity	***33***	(ft/d)
	Groundwater gradient	0.01	(-)
S_w	Width of groundwater source zone	***168***	(ft)
S_d	Depth of groundwater source zone	***20***	(ft)
n_{eff}	Effective porosity in water-bearing unit	0.38	(-)
$f_{oc\text{-}sat}$	Fraction organic carbon in water-bearing unit	0.001	(-)
pH_{sat}	Groundwater pH	***7.64***	(-)
	Biodegradation considered?	No	

Transport Parameters		Off-site 1	Off-site 2	Off-site 1	Off-site 2	(Units)
Lateral Groundwater Transport		**Groundwater Ingestion**		**Groundwater to Indoor Air**		
x	Longitudinal dispersivity	2.0E+1	1.0E+2	NA	NA	(ft)
y	Transverse dispersivity	6.6E+0	3.3E+1	NA	NA	(ft)
z	Vertical dispersivity	1.0E+0	5.0E+0	NA	NA	(ft)
Lateral Outdoor Air Transport		**Soil to Outdoor Air Inhal.**		**GW to Outdoor Air Inhal.**		
y	Transverse dispersion coefficient	NA	NA	NA	NA	(ft)
z	Vertical dispersion coefficient	NA	NA	NA	NA	(ft)
ADF	Air dispersion factor	NA	NA	NA	NA	(-)

Figure E. 2 RBCA Tool Kit Chemical Releases Input Summary II

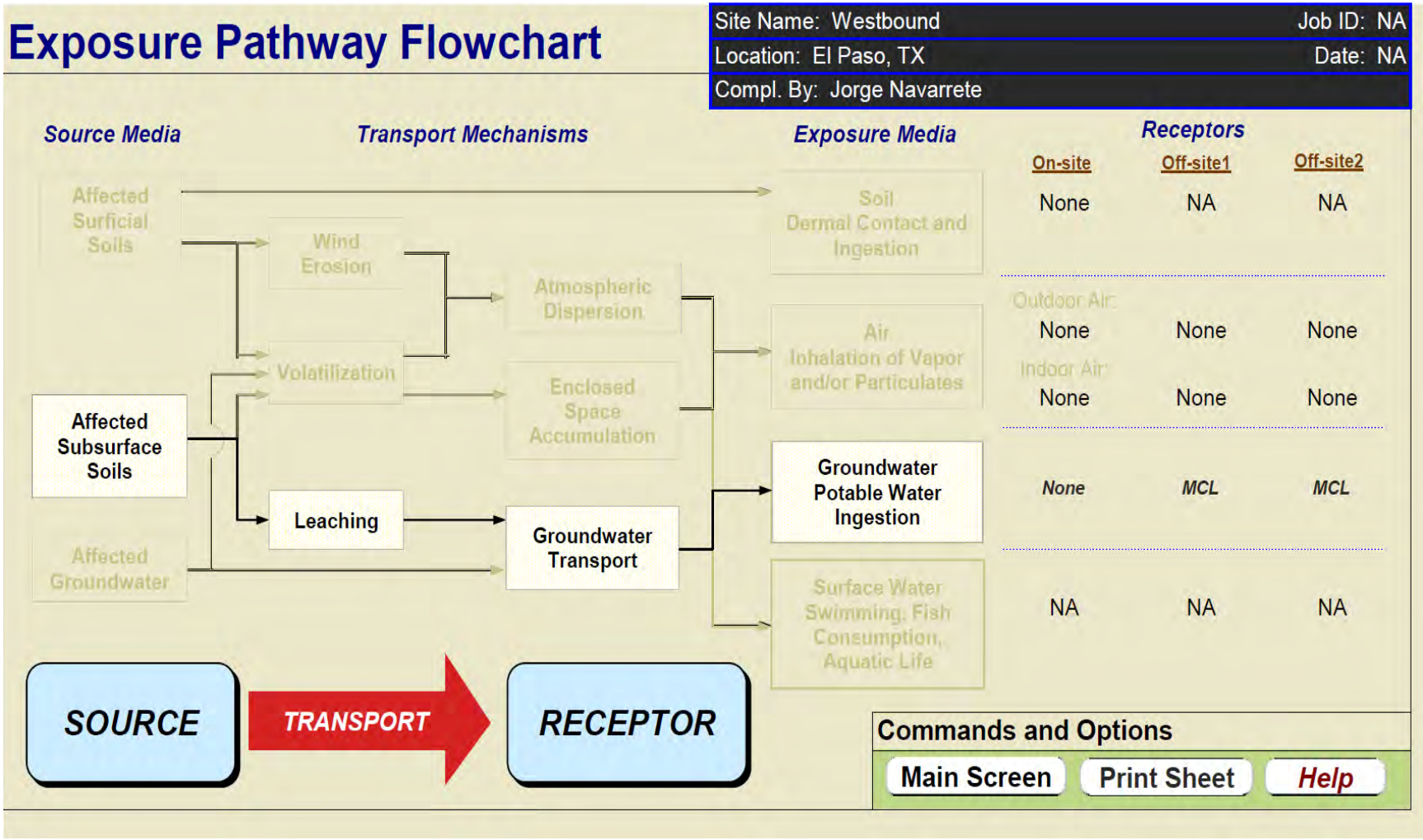

Figure E. 3 Exposure Pathway Flowchart

Constiuent: Arsenic
Source Medium: Affected Soils Leaching to Groundwater
Biodegredation: None

Concentration vs. Distance from Source
(for given time)

Time (yr) 1.0

Distance (ft)		0	120	240	360	480	600	720	840	960	1080	1200
t = 1.0 yr	Conc. (mg/L)	5.9E-4	0.0E+0	0.0E+0	0.0E+0	0.0E+0	0.0E+0	0.0E+0	0.0E+0	0.0E+0	0.0E+0	0.0E+0
Steady-state		5.9E-4	5.3E-4	2.9E-4	1.6E-4	9.7E-5	6.4E-5	4.6E-5	3.4E-5	2.6E-5	2.1E-5	1.7E-5

Off-site1	Off-site2
MCL	MCL
200	1000
0.0E+0	0.0E+0
3.6E-4	2.4E-5
1.0E-2	1.0E-2

POE Concentration Limit (mg/L)

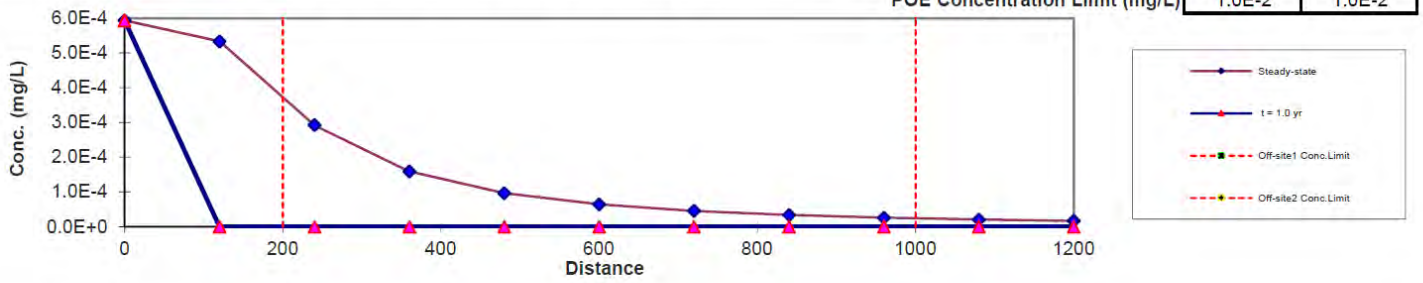

Concentration vs. Time
(for given distance from source)

Distance (ft) 0

Time (yr)		0	0.1	0.2	0.3	0.4	0.5	0.6	0.7	0.8	0.9	1
x = 0 ft	Conc. (mg/L)	3.0E-4	5.9E-4	5.9E-4	5.9E-4	5.9E-4	5.9E-4	5.9E-4	5.9E-4	5.9E-4	5.9E-4	5.9E-4
Off-site1 (200 ft)		0.0E+0	0.0E+0	0.0E+0	0.0E+0	0.0E+0	0.0E+0	0.0E+0	0.0E+0	0.0E+0	0.0E+0	0.0E+0
Off-site2 (1000 ft)		0.0E+0	0.0E+0	0.0E+0	0.0E+0	0.0E+0	0.0E+0	0.0E+0	0.0E+0	0.0E+0	0.0E+0	0.0E+0

Time to Reach Conc. Limit (yr)	
Off-site1	NA
Off-site2	NA

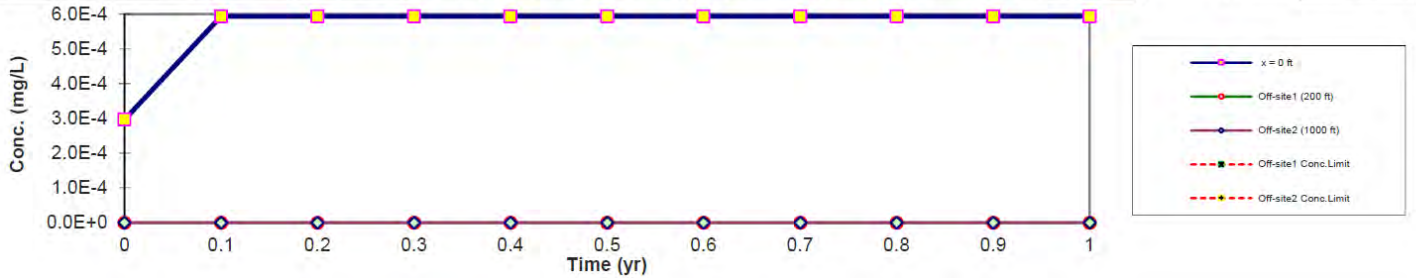

Figure E. 4 Arsenic Leaching Path in a One-Year Analysis

Constiuent: Cadmium
Source Medium: Affected Soils Leaching to Groundwater
Biodegredation: None

Concentration vs. Distance from Source
(for given time)

Time (yr) 1.0

Distance (ft)		0	120	240	360	480	600	720	840	960	1080	1200
t = 1.0 yr	Conc. (mg/L)	5.1E-5	0.0E+0	0.0E+0	0.0E+0	0.0E+0	0.0E+0	0.0E+0	0.0E+0	0.0E+0	0.0E+0	0.0E+0
Steady-state		5.1E-5	4.6E-5	2.5E-5	1.4E-5	8.4E-6	5.6E-6	3.9E-6	2.9E-6	2.3E-6	1.8E-6	1.5E-6

	Off-site1	Off-site2
	MCL	MCL
POE Concentration Limit (mg/L)	200	1000
	0.0E+0	0.0E+0
	3.1E-5	2.1E-6
	5.0E-3	5.0E-3

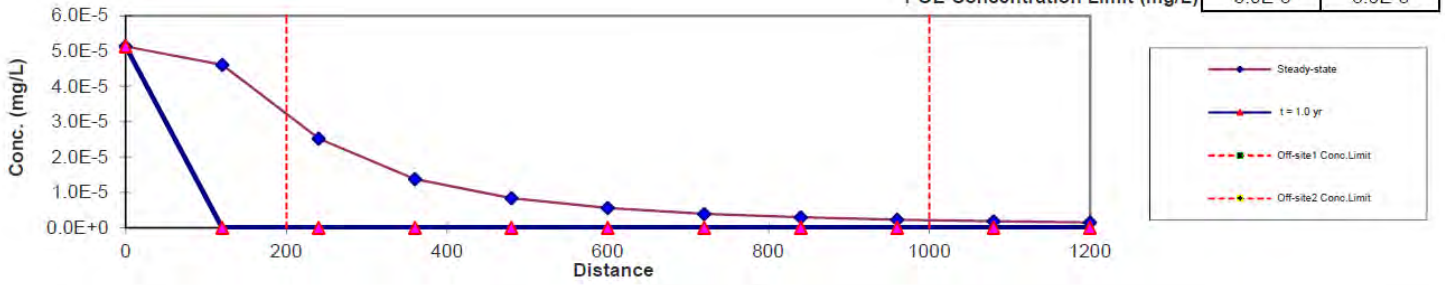

Concentration vs. Time
(for given distance from source)

Distance (ft) 0

Time (yr)		0	0.1	0.2	0.3	0.4	0.5	0.6	0.7	0.8	0.9	1
x = 0 ft	Conc. (mg/L)	2.6E-5	5.1E-5	5.1E-5	5.1E-5	5.1E-5	5.1E-5	5.1E-5	5.1E-5	5.1E-5	5.1E-5	5.1E-5
Off-site1 (200 ft)		0.0E+0	0.0E+0	0.0E+0	0.0E+0	0.0E+0	0.0E+0	0.0E+0	0.0E+0	0.0E+0	0.0E+0	0.0E+0
Off-site2 (1000 ft)		0.0E+0	0.0E+0	0.0E+0	0.0E+0	0.0E+0	0.0E+0	0.0E+0	0.0E+0	0.0E+0	0.0E+0	0.0E+0

Time to Reach Conc. Limit (yr)	
Off-site1	NA
Off-site2	NA

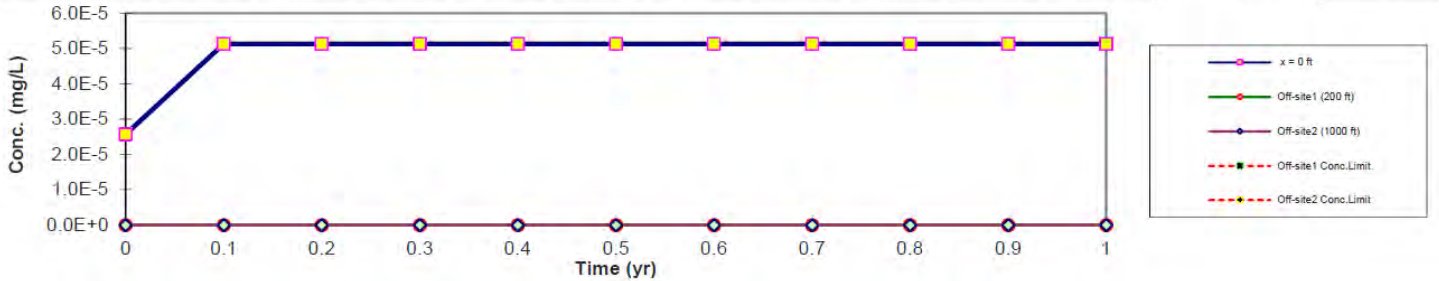

Figure E. 5 Cadmium Leaching Path in a One-Year Analysis

Constiuent: Chromium (total)
Source Medium: Affected Soils Leaching to Groundwater
Biodegredation: None

Concentration vs. Distance from Source
(for given time)

Time (yr) 1.0

Distance (ft)		0	120	240	360	480	600	720	840	960	1080	1200
t = 1.0 yr	Conc. (mg/L)	2.4E-4	0.0E+0	0.0E+0	0.0E+0	0.0E+0	0.0E+0	0.0E+0	0.0E+0	0.0E+0	0.0E+0	0.0E+0
Steady-state		2.4E-4	2.1E-4	1.2E-4	6.3E-5	3.8E-5	2.5E-5	1.8E-5	1.3E-5	1.0E-5	8.2E-6	6.7E-6

	Off-site1	Off-site2
	MCL	MCL
	200	1000
	0.0E+0	0.0E+0
	1.4E-4	9.6E-6
POE Concentration Limit (mg/L)	noMCL	no MCL

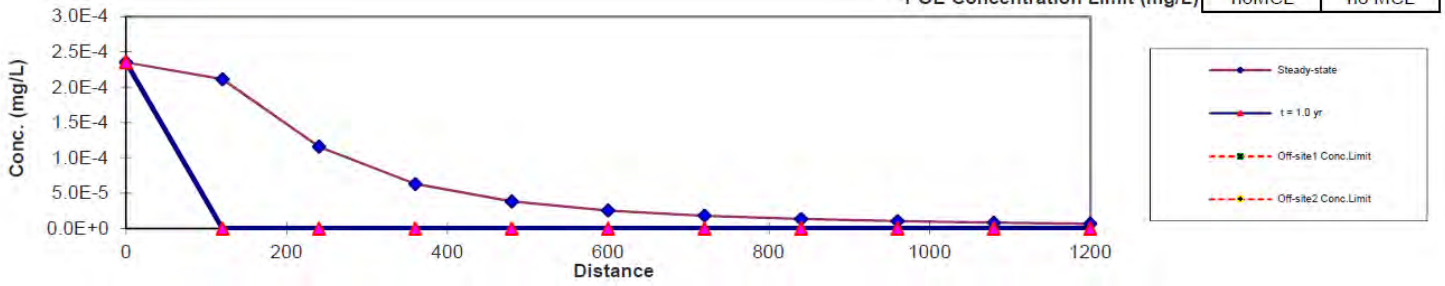

Concentration vs. Time
(for given distance from source)

Distance (ft) 0

Time (yr)		0	0.1	0.2	0.3	0.4	0.5	0.6	0.7	0.8	0.9	1
x = 0 ft	Conc. (mg/L)	1.2E-4	2.4E-4	2.4E-4	2.4E-4	2.4E-4	2.4E-4	2.4E-4	2.4E-4	2.4E-4	2.4E-4	2.4E-4
Off-site1 (200 ft)		0.0E+0	0.0E+0	0.0E+0	0.0E+0	0.0E+0	0.0E+0	0.0E+0	0.0E+0	0.0E+0	0.0E+0	0.0E+0
Off-site2 (1000 ft)		0.0E+0	0.0E+0	0.0E+0	0.0E+0	0.0E+0	0.0E+0	0.0E+0	0.0E+0	0.0E+0	0.0E+0	0.0E+0

Time to Reach Conc. Limit (yr)	
Off-site1	NA
Off-site2	NA

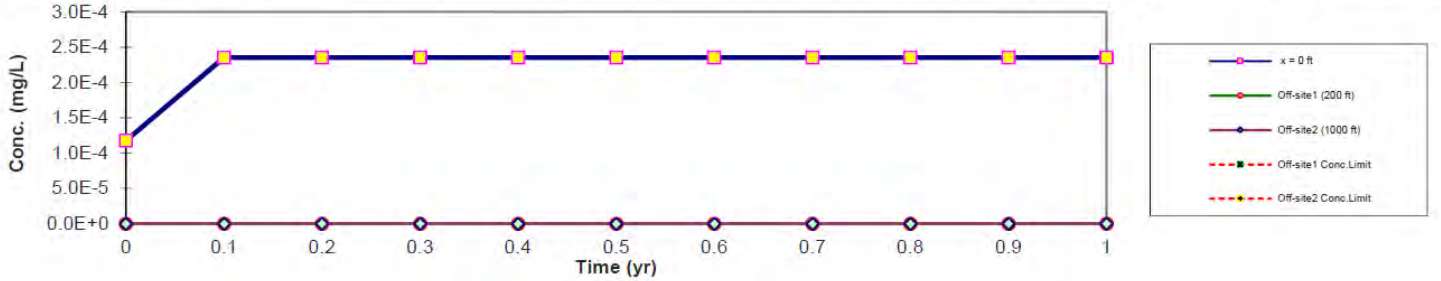

Figure E. 6 Chromium (Total) Leaching Path in a One-Year Analysis

Constiuent: Copper
Source Medium: Affected Soils Leaching to Groundwater
Biodegredation: None

Concentration vs. Distance from Source
(for given time)

Time (yr) 1.0

Distance (ft)		0	120	240	360	480	600	720	840	960	1080	1200
t = 1.0 yr	Conc. (mg/L)	1.6E-3	0.0E+0	0.0E+0	0.0E+0	0.0E+0	0.0E+0	0.0E+0	0.0E+0	0.0E+0	0.0E+0	0.0E+0
Steady-state		1.6E-3	1.5E-3	8.1E-4	4.4E-4	2.7E-4	1.8E-4	1.3E-4	9.4E-5	7.2E-5	5.8E-5	4.7E-5

	Off-site1	Off-site2
	MCL	MCL
POE Concentration Limit (mg/L)	200	1000
	0.0E+0	0.0E+0
	1.0E-3	6.7E-5
	1.3E+0	1.3E+0

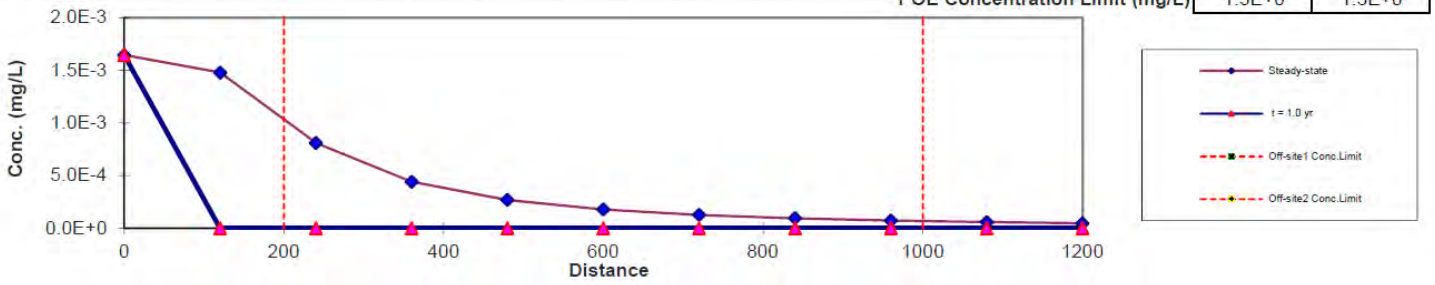

Concentration vs. Time
(for given distance from source)

Distance (ft) 0

Time (yr)		0	0.1	0.2	0.3	0.4	0.5	0.6	0.7	0.8	0.9	1
x = 0 ft	Conc. (mg/L)	8.2E-4	1.6E-3	1.6E-3	1.6E-3	1.6E-3	1.6E-3	1.6E-3	1.6E-3	1.6E-3	1.6E-3	1.6E-3
Off-site1 (200 ft)		0.0E+0	0.0E+0	0.0E+0	0.0E+0	0.0E+0	0.0E+0	0.0E+0	0.0E+0	0.0E+0	0.0E+0	0.0E+0
Off-site2 (1000 ft)		0.0E+0	0.0E+0	0.0E+0	0.0E+0	0.0E+0	0.0E+0	0.0E+0	0.0E+0	0.0E+0	0.0E+0	0.0E+0

Time to Reach Conc. Limit (yr)	
Off-site1	NA
Off-site2	NA

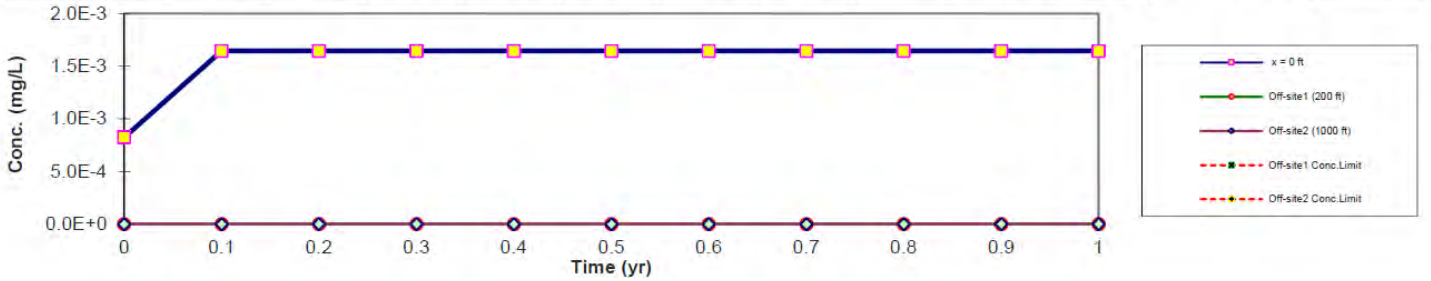

Figure E. 7 Copper Leaching Path in a One-Year Analysis

Constiuent: Lead (inorganic)
Source Medium: Affected Soils Leaching to Groundwater
Biodegredation: None

Concentration vs. Distance from Source
(for given time)

Time (yr) 1.0

Distance (ft)		0	120	240	360	480	600	720	840	960	1080	1200
t = 1.0 yr	Conc. (mg/L)	1.0E-4	0.0E+0	0.0E+0	0.0E+0	0.0E+0	0.0E+0	0.0E+0	0.0E+0	0.0E+0	0.0E+0	0.0E+0
Steady-state		1.0E-4	9.3E-5	5.1E-5	2.8E-5	1.7E-5	1.1E-5	7.9E-6	5.9E-6	4.5E-6	3.6E-6	2.9E-6

	Off-site1	Off-site2
	MCL	MCL
POE Concentration Limit (mg/L)	200	1000
t = 1.0 yr	0.0E+0	0.0E+0
Steady-state	6.3E-5	4.2E-6
	NA	NA

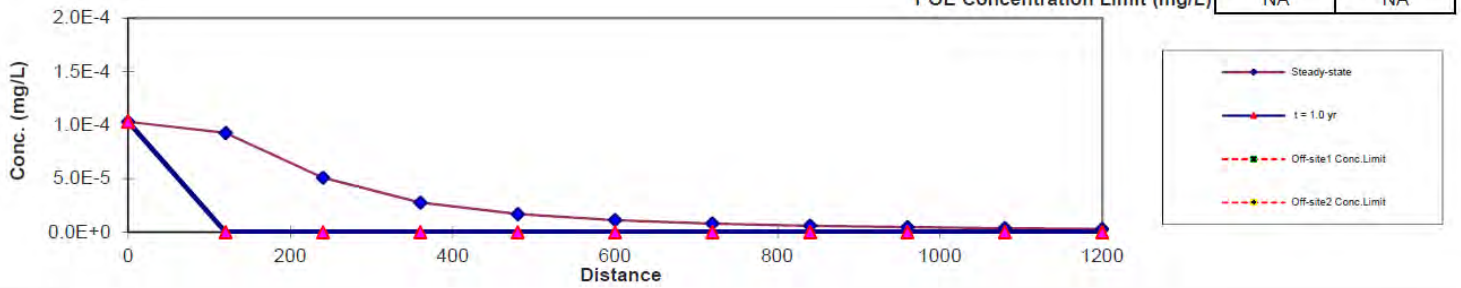

Concentration vs. Time
(for given distance from source)

Distance (ft) 0

Time (yr)		0	0.1	0.2	0.3	0.4	0.5	0.6	0.7	0.8	0.9	1
x = 0 ft	Conc. (mg/L)	5.2E-5	1.0E-4	1.0E-4	1.0E-4	1.0E-4	1.0E-4	1.0E-4	1.0E-4	1.0E-4	1.0E-4	1.0E-4
Off-site1 (200 ft)		0.0E+0	0.0E+0	0.0E+0	0.0E+0	0.0E+0	0.0E+0	0.0E+0	0.0E+0	0.0E+0	0.0E+0	0.0E+0
Off-site2 (1000 ft)		0.0E+0	0.0E+0	0.0E+0	0.0E+0	0.0E+0	0.0E+0	0.0E+0	0.0E+0	0.0E+0	0.0E+0	0.0E+0

Time to Reach Conc. Limit (yr)	
Off-site1	NA
Off-site2	NA

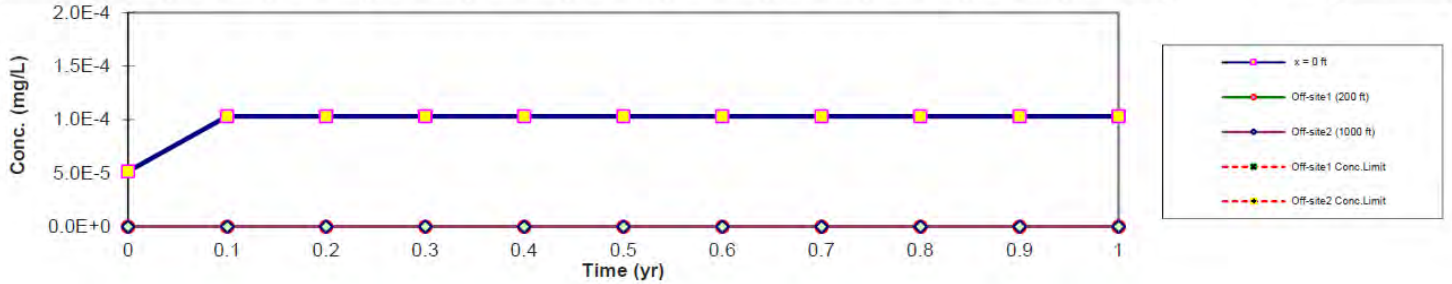

Figure E. 8 Lead Leaching Path in a One-Year Analysis

Constiuent: Manganese
Source Medium: Affected Soils Leaching to Groundwater
Biodegredation: None

Concentration vs. Distance from Source
(for given time)

Time (yr) 1.0

Distance (ft)		0	120	240	360	480	600	720	840	960	1080	1200
t = 1.0 yr	Conc. (mg/L)	4.8E-1	0.0E+0	0.0E+0	0.0E+0	0.0E+0	0.0E+0	0.0E+0	0.0E+0	0.0E+0	0.0E+0	0.0E+0
Steady-state		4.8E-1	4.3E-1	2.4E-1	1.3E-1	7.8E-2	5.2E-2	3.7E-2	2.7E-2	2.1E-2	1.7E-2	1.4E-2

POE Concentration Limit (mg/L)	Off-site1	Off-site2
	MCL	MCL
	200	1000
	0.0E+0	0.0E+0
	2.9E-1	1.9E-2
	noMCL	no MCL

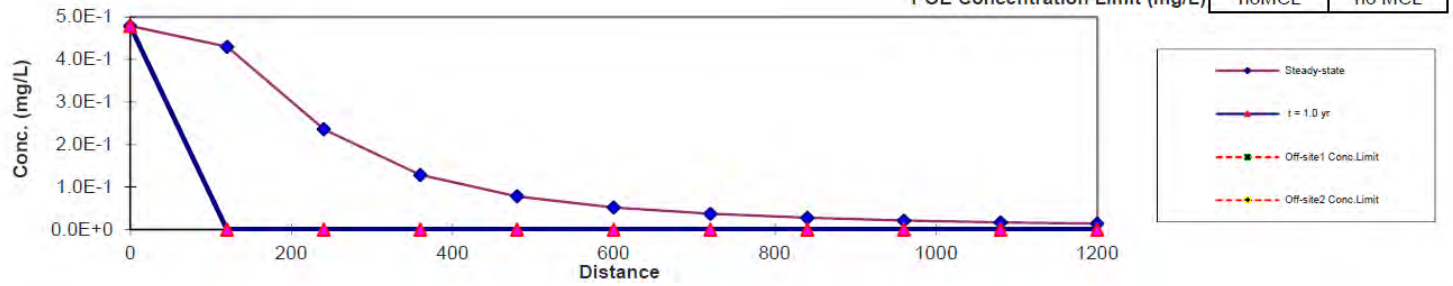

Concentration vs. Time
(for given distance from source)

Distance (ft) 0

Time (yr)		0	0.1	0.2	0.3	0.4	0.5	0.6	0.7	0.8	0.9	1
x = 0 ft	Conc. (mg/L)	2.4E-1	4.8E-1	4.8E-1	4.8E-1	4.8E-1	4.8E-1	4.8E-1	4.8E-1	4.8E-1	4.8E-1	4.8E-1
Off-site1 (200 ft)		0.0E+0	0.0E+0	0.0E+0	0.0E+0	0.0E+0	0.0E+0	0.0E+0	0.0E+0	0.0E+0	0.0E+0	0.0E+0
Off-site2 (1000 ft)		0.0E+0	0.0E+0	0.0E+0	0.0E+0	0.0E+0	0.0E+0	0.0E+0	0.0E+0	0.0E+0	0.0E+0	0.0E+0

Time to Reach Conc. Limit (yr)	
Off-site1	NA
Off-site2	NA

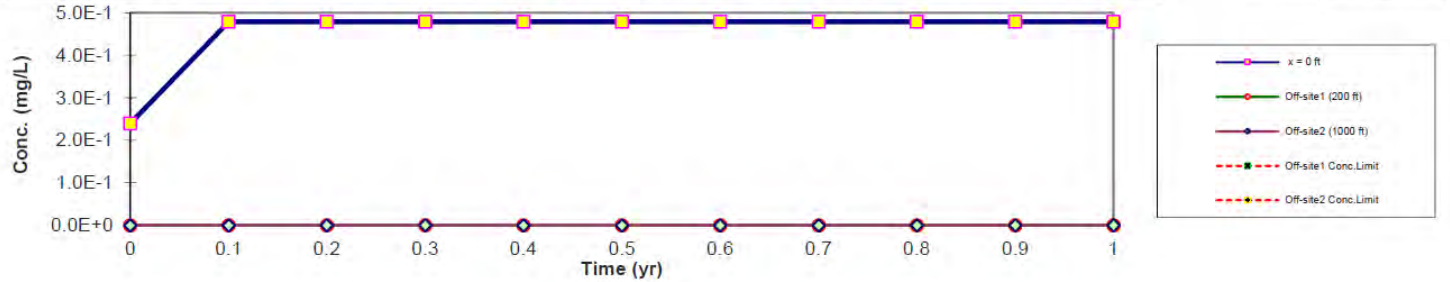

Figure E. 9 Manganese Leaching Path in a One-Year Analysis

Constiuent: Nickel
Source Medium: Affected Soils Leaching to Groundwater
Biodegredation: None

Concentration vs. Distance from Source
(for given time)

Time (yr) 1.0

Distance (ft)		0	120	240	360	480	600	720	840	960	1080	1200
t = 1.0 yr	Conc. (mg/L)	7.7E-5	0.0E+0	0.0E+0	0.0E+0	0.0E+0	0.0E+0	0.0E+0	0.0E+0	0.0E+0	0.0E+0	0.0E+0
Steady-state		7.7E-5	7.0E-5	3.8E-5	2.1E-5	1.3E-5	8.4E-6	5.9E-6	4.4E-6	3.4E-6	2.7E-6	2.2E-6

Off-site1	Off-site2
MCL	MCL
200	1000
0.0E+0	0.0E+0
4.7E-5	3.1E-6
1.0E-1	1.0E-1

POE Concentration Limit (mg/L)

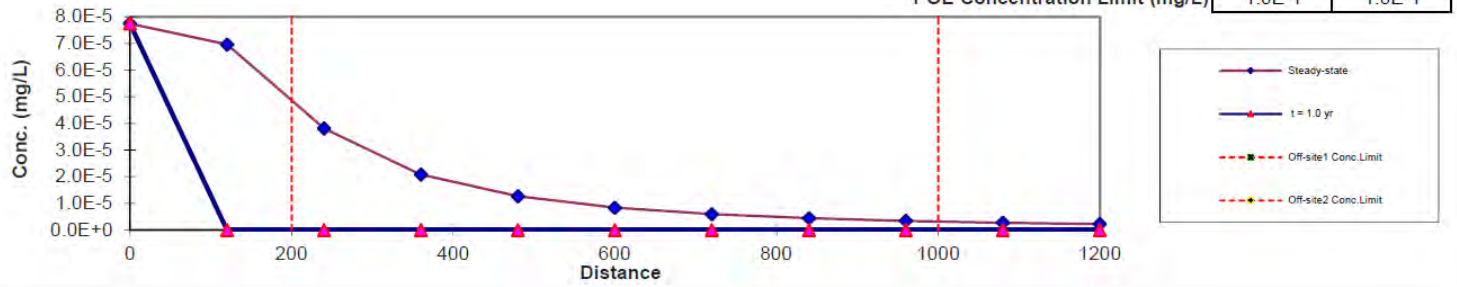

Concentration vs. Time
(for given distance from source)

Distance (ft) 0

Time (yr)		0	0.1	0.2	0.3	0.4	0.5	0.6	0.7	0.8	0.9	1
x = 0 ft	Conc. (mg/L)	3.9E-5	7.7E-5	7.7E-5	7.7E-5	7.7E-5	7.7E-5	7.7E-5	7.7E-5	7.7E-5	7.7E-5	7.7E-5
Off-site1 (200 ft)		0.0E+0	0.0E+0	0.0E+0	0.0E+0	0.0E+0	0.0E+0	0.0E+0	0.0E+0	0.0E+0	0.0E+0	0.0E+0
Off-site2 (1000 ft)		0.0E+0	0.0E+0	0.0E+0	0.0E+0	0.0E+0	0.0E+0	0.0E+0	0.0E+0	0.0E+0	0.0E+0	0.0E+0

Time to Reach Conc. Limit (yr)	
Off-site1	NA
Off-site2	NA

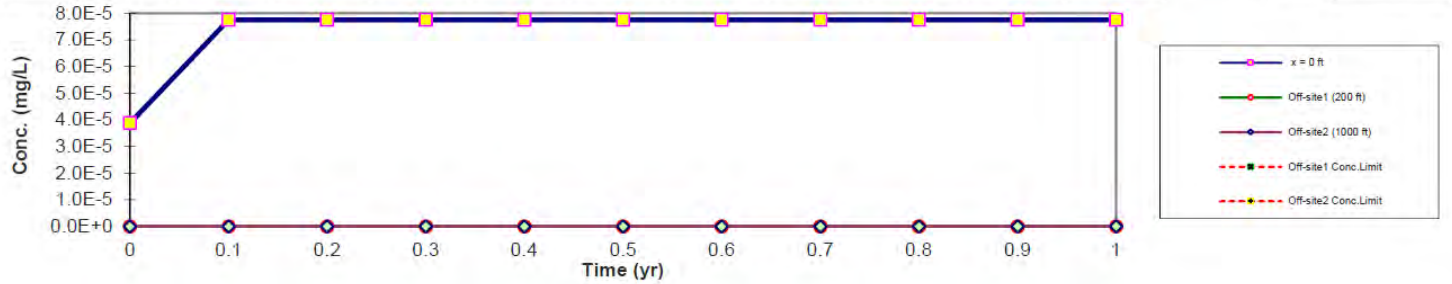

Figure E. 10 Nickel Leaching Path in a One-Year Analysis

Constiuent: Zinc
Source Medium: Affected Soils Leaching to Groundwater
Biodegredation: None

Concentration vs. Distance from Source
(for given time)

Time (yr) 1.0

Distance (ft)		0	120	240	360	480	600	720	840	960	1080	1200
t = 1.0 yr	Conc. (mg/L)	4.0E-2	0.0E+0	0.0E+0	0.0E+0	0.0E+0	0.0E+0	0.0E+0	0.0E+0	0.0E+0	0.0E+0	0.0E+0
Steady-state		4.0E-2	3.6E-2	2.0E-2	1.1E-2	6.5E-3	4.3E-3	3.0E-3	2.3E-3	1.7E-3	1.4E-3	1.1E-3

Off-site1	Off-site2
MCL	MCL
200	1000
0.0E+0	0.0E+0
2.4E-2	1.6E-3
noMCL	no MCL

POE Concentration Limit (mg/L)

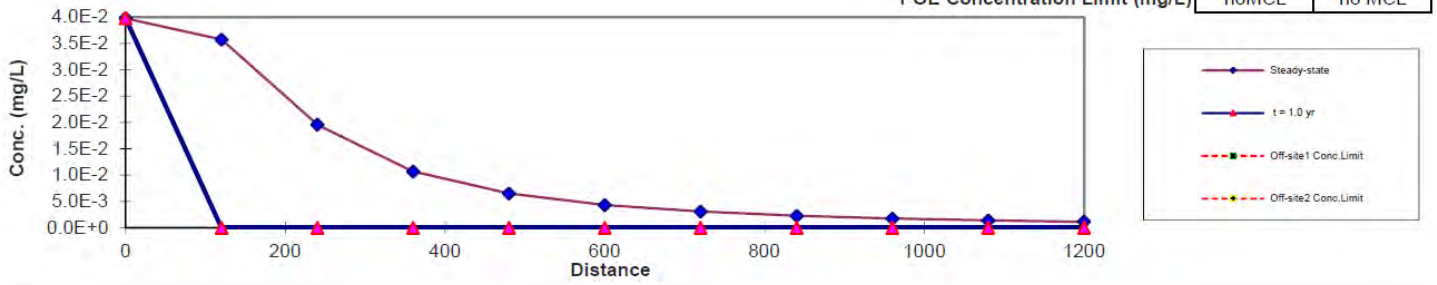

Concentration vs. Time
(for given distance from source)

Distance (ft) 0

Time (yr)		0	0.1	0.2	0.3	0.4	0.5	0.6	0.7	0.8	0.9	1
x = 0 ft	Conc. (mg/L)	2.0E-2	4.0E-2	4.0E-2	4.0E-2	4.0E-2	4.0E-2	4.0E-2	4.0E-2	4.0E-2	4.0E-2	4.0E-2
Off-site1 (200 ft)		0.0E+0	0.0E+0	0.0E+0	0.0E+0	0.0E+0	0.0E+0	0.0E+0	0.0E+0	0.0E+0	0.0E+0	0.0E+0
Off-site2 (1000 ft)		0.0E+0	0.0E+0	0.0E+0	0.0E+0	0.0E+0	0.0E+0	0.0E+0	0.0E+0	0.0E+0	0.0E+0	0.0E+0

Time to Reach Conc. Limit (yr)

Off-site1	NA
Off-site2	NA

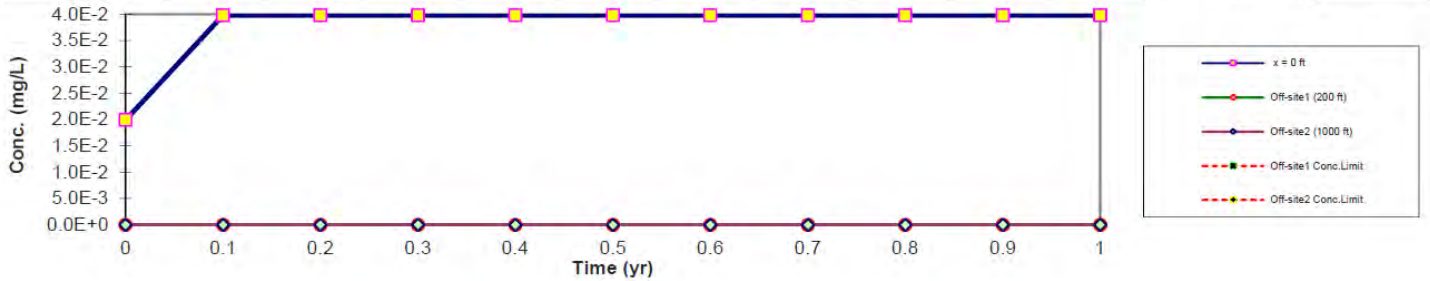

Figure E. 11 Zinc Leaching Path in a One-Year Analysis

APPENDIX F: 3D PRINTED DIMENSION DETAILS

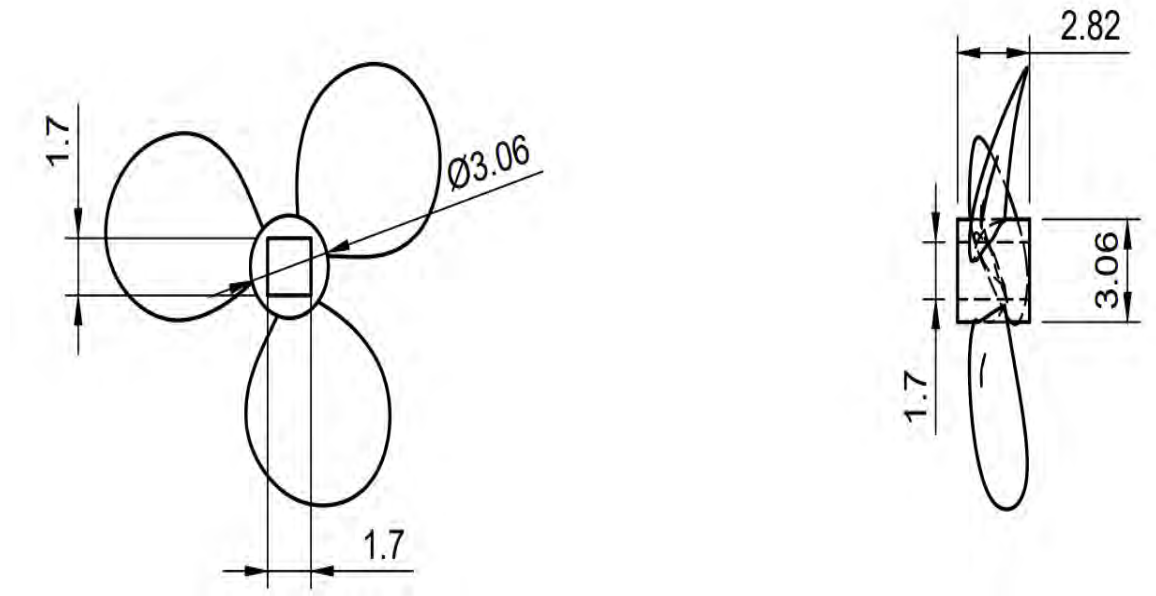

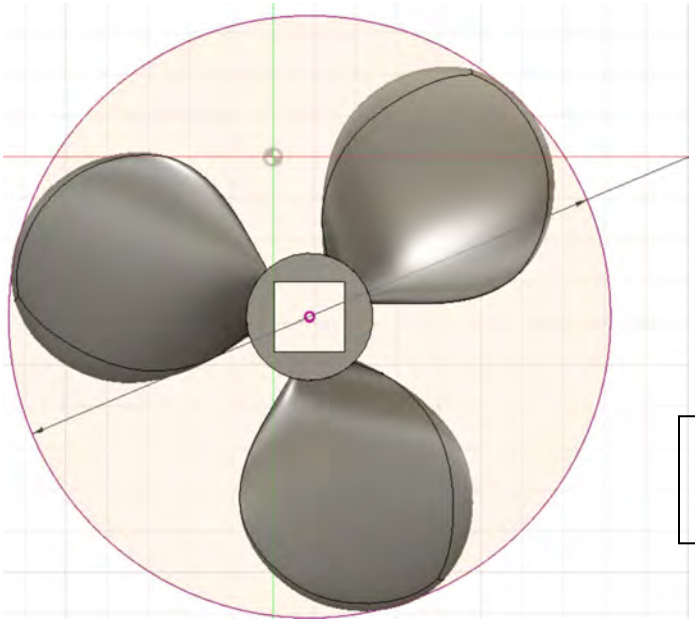

1.452 cm

NOTE: Dimensions are in cm.

Figure F. 1 Fan 1 Dimensions in cm

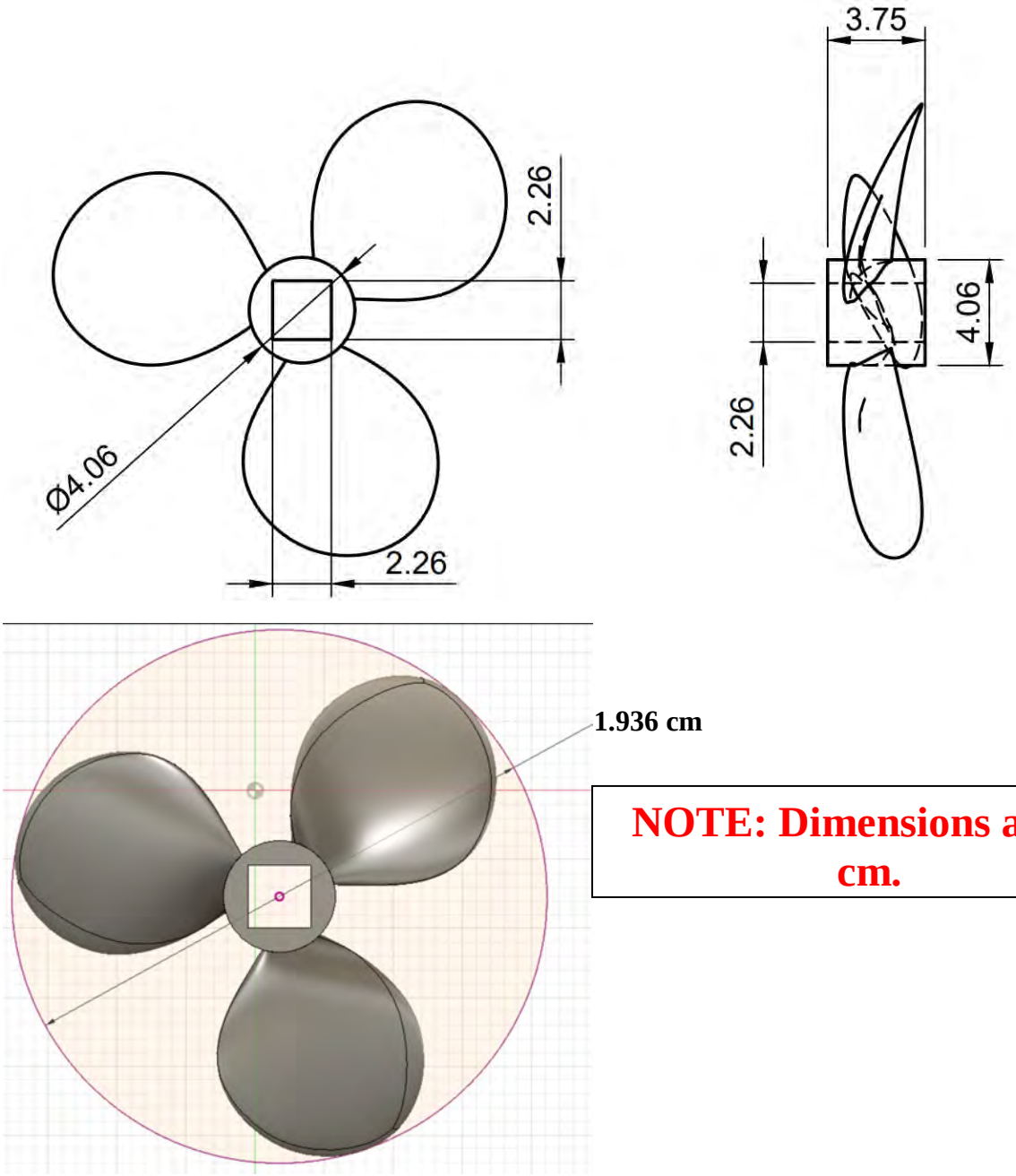

NOTE: Dimensions are in cm.

Figure F. 2 Fan 2 Dimensions in cm

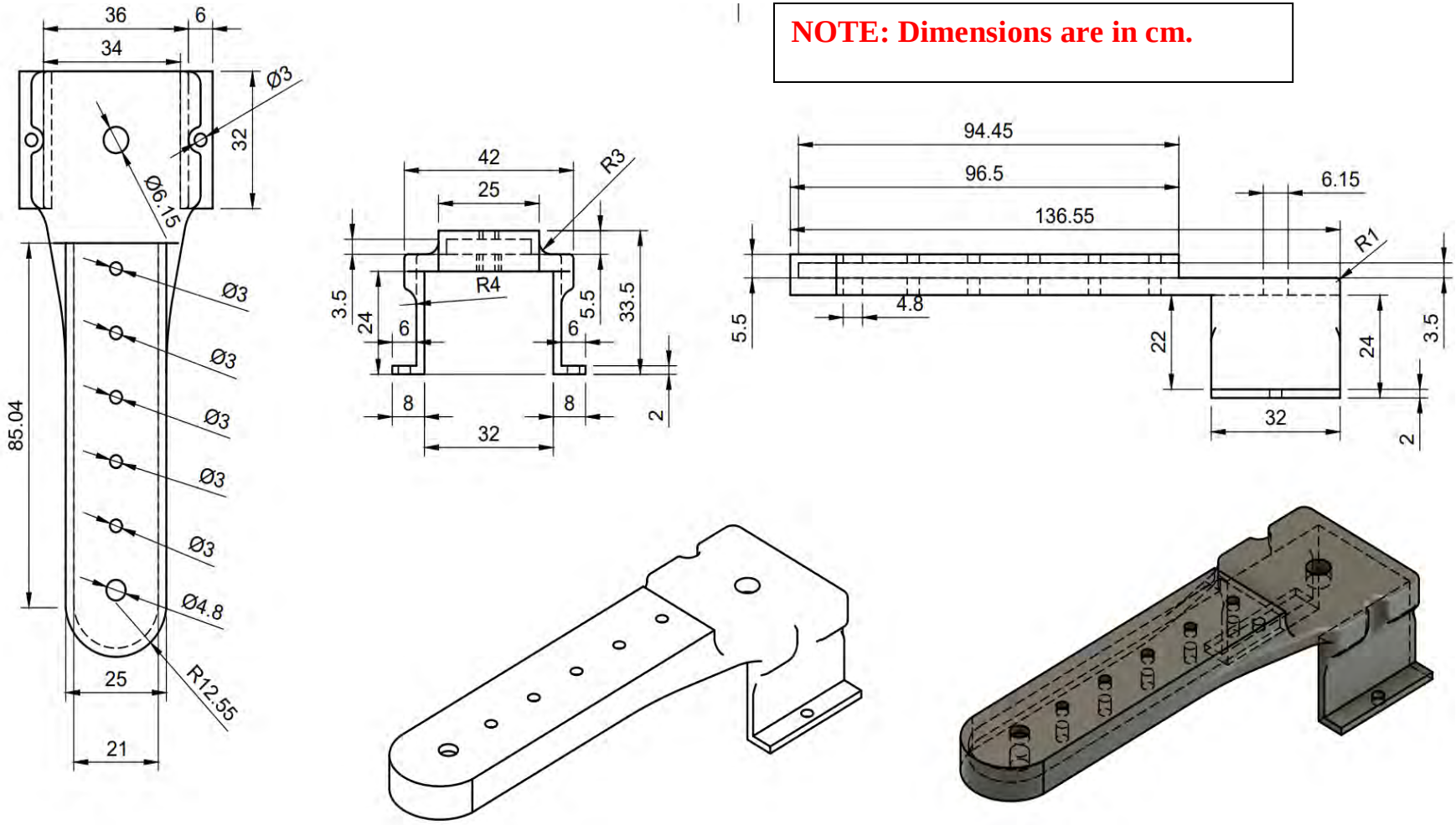

Figure F. 3 Gearbox Dimensions

APPENDIX G: LEACHING RESULTS

Table G. 1 Upper Valley Sample Characteristics Prior/After Leaching Cycles

Test #	Sample	RG Application Method	Amount (mL)	pH	Conductivity (mS/cm)	Dry Density (pcf)
1	Collected Water	DI	80	7.94	2.80	186.3
	Top			8.83	115.00	
	Bottom			8.91	116.10	
2	Collected Water	DI	130	8.17	2.09	221.7
	Top			8.99	116.10	
	Bottom			8.88	115.10	
3	Collected Water	DI	30	7.53	2.80	221.7
	Top			8.93	114.70	
	Bottom			9.04	114.90	
4	Collected Water	DPW	80	8.02	3.94	221.7
	Top			8.81	114.40	
	Bottom			8.81	116.00	
5	Collected Water	DPW	30	7.58	4.01	222.4
	Top			8.97	116.50	
	Bottom			8.61	113.60	
6	Collected Water	DPW	130	7.98	3.64	187.2
	Top			8.68	116.20	
	Bottom			8.76	117.80	
7	Collected Water	DDI	30	7.56	4.76	187.2
	Top			8.95	115.70	
	Bottom			8.83	114.90	
8	Collected Water	DDI	80	7.86	4.60	187.2
	Top			8.93	114.20	
	Bottom			8.8	113.90	
9	Collected Water	DDI	130	7.91	4.15	186
	Top			8.72	113.60	
	Bottom			8.77	116.70	

Table G. 2 Upper Valley Top Sections Leaching Analysis Results

Upper Valley									
Concentration of Elements in mg/L									
Test No.	1	2	3	4	5	6	7	8	9
Ca	330.07	323.60	318.74	349.90	329.00	357.87	353.31	343.69	335.76
K	22.49	22.04	24.46	23.66	23.26	24.03	24.25	23.86	22.97
Mg	22.76	21.87	21.36	24.14	21.81	24.06	23.11	22.02	21.57
Na	138.06	138.10	134.13	142.94	142.16	144.70	146.88	143.42	136.71
P	0.00	0.00	0.02	0.00	0.00	0.00	0.00	0.00	0.00
As	0.01	0.02	0.14	0.08	0.09	0.04	0.00	0.04	0.09
Ba	2.54	2.79	2.02	3.02	2.52	2.87	2.77	2.72	2.67
Cd	0.02	0.01	0.00	0.01	0.00	0.01	0.00	0.00	0.01
Cr	0.00	0.00	0.01	0.01	0.01	0.00	0.00	0.00	0.00
Cu	0.00	0.00	0.00	0.00	0.02	0.00	0.01	0.01	0.01
Fe	0.00	0.00	0.00	0.00	0.00	0.00	0.00	0.00	0.00
Hg	0.05	0.04	0.02	0.03	0.01	0.01	0.06	0.04	0.04
Li	0.14	0.13	0.13	0.14	0.14	0.14	0.14	0.14	0.14
Mn	0.56	0.39	0.17	0.30	0.24	0.11	0.44	0.30	0.32
Ni	0.01	0.00	0.00	0.00	0.00	0.00	0.01	0.00	0.01
Pb	0.00	0.00	0.03	0.06	0.09	0.03	0.02	0.03	0.03
Se	0.01	0.00	0.01	0.00	0.11	0.07	0.04	0.02	0.00
Sn	0.12	0.15	0.11	0.15	0.12	0.13	0.11	0.12	0.09
Sr	3.15	3.02	2.96	3.26	2.95	3.26	3.26	3.18	3.04
U	0.00	0.00	0.00	0.00	0.00	0.00	0.00	0.00	0.00
V	0.00	0.00	0.00	0.00	0.00	0.00	0.00	0.00	0.00
W	0.02	0.02	0.02	0.00	0.00	0.00	0.00	0.00	0.00
Zn	0.00	0.02	0.00	0.00	0.00	0.00	0.00	0.00	0.00
Si	1.91	2.02	1.94	2.38	1.96	2.46	2.39	2.33	2.35

Table G. 3 Upper Valley Bottom Sections Leaching Analysis Results

Upper Valley									
Concentration of Elements in mg/L									
Test No.	1	2	3	4	5	6	7	8	9
Ca	301.33	328.25	339.12	364.37	367.96	361.96	370.90	378.48	367.11
K	19.78	20.36	21.79	21.06	23.16	22.07	23.06	22.65	20.70
Mg	19.46	21.17	21.51	19.06	20.18	19.60	20.29	19.20	16.05
Na	125.00	134.45	132.37	124.49	128.90	124.55	124.00	123.96	123.48
P	0.00	0.00	0.00	0.00	0.00	0.00	0.00	0.00	0.00
As	0.07	0.03	0.00	0.17	0.07	0.08	0.00	0.00	0.00
Ba	2.18	2.71	2.86	2.52	2.24	2.32	2.61	2.66	2.45
Cd	0.02	0.04	0.00	0.00	0.00	0.01	0.00	0.00	0.00
Cr	0.01	0.01	0.01	0.01	0.00	0.01	0.01	0.01	0.01
Cu	0.01	0.01	0.00	0.00	0.01	0.00	0.02	0.00	0.01
Fe	0.00	0.00	0.00	0.00	0.00	0.00	0.00	0.00	0.00
Hg	0.04	0.05	0.03	0.02	0.04	0.00	0.03	0.03	0.05
Li	0.13	0.13	0.13	0.13	0.13	0.13	0.13	0.13	0.13
Mn	0.32	0.43	0.19	0.08	0.06	0.07	0.19	0.12	0.17
Ni	0.00	0.00	0.00	0.01	0.00	0.01	0.00	0.01	0.00
Pb	0.03	0.04	0.03	0.02	0.06	0.02	0.01	0.03	0.02
Se	0.00	0.00	0.01	0.09	0.01	0.07	0.00	0.00	0.11
Sn	0.11	0.09	0.15	0.10	0.09	0.11	0.08	0.11	0.03
Sr	2.79	2.96	3.10	2.89	2.99	3.02	3.22	3.20	2.92
U	0.00	0.00	0.00	0.00	0.00	0.00	0.00	0.00	0.00
V	0.00	0.00	0.00	0.00	0.00	0.00	0.00	0.00	0.00
W	0.00	0.00	0.00	0.00	0.00	0.01	0.00	0.00	0.01
Zn	0.00	0.00	0.00	0.00	0.00	0.00	0.00	0.04	0.00
Si	1.67	1.86	2.18	2.19	2.08	2.09	2.34	2.39	2.12

Table G. 4 Upper Valley Collected Solutions Results

Upper Valley									
Concentration of Elements in mg/L									
Test No.	1	2	3	4	5	6	7	8	9
Ca	177.78	124.17	135.18	283.08	347.51	302.88	427.10	403.13	343.31
K	39.83	31.18	42.85	47.96	52.11	48.40	58.32	59.20	51.75
Mg	36.13	24.22	38.93	39.59	47.71	42.21	53.10	52.18	47.72
Na	501.61	352.94	567.53	621.41	726.45	636.16	874.97	895.77	785.21
P	0.11	0.06	0.09	0.04	0.04	0.10	0.14	0.18	0.08
As	0.02	0.03	0.03	0.03	0.03	0.03	0.04	0.03	0.03
Ba	0.04	0.07	0.05	0.19	0.11	0.14	0.10	0.08	0.06
Cd	0.00	0.00	0.00	0.00	0.00	0.00	0.00	0.00	0.00
Cr	0.00	0.00	0.00	0.00	0.00	0.00	0.00	0.00	0.00
Cu	0.13	0.08	0.11	0.05	0.05	0.12	0.17	0.22	0.10
Fe	0.40	0.93	0.70	0.00	0.01	0.01	0.37	0.01	0.35
Hg	0.02	0.01	0.00	0.00	0.00	0.00	0.00	0.00	0.00
Li	0.20	0.16	0.25	0.24	0.28	0.25	0.37	0.38	0.35
Mn	0.00	0.14	0.00	0.11	0.01	0.19	0.28	0.03	0.00
Ni	0.01	0.01	0.01	0.01	0.00	0.01	0.01	0.01	0.01
Pb	0.01	0.00	0.00	0.00	0.00	0.00	0.01	0.00	0.00
Se	0.03	0.03	0.04	0.01	0.04	0.02	0.04	0.02	0.03
Sn	0.36	0.21	0.29	0.23	0.26	0.23	0.27	0.25	0.25
Sr	2.49	1.63	2.53	3.50	4.17	3.77	5.04	4.88	4.17
U	0.47	1.03	0.81	0.00	0.02	0.01	0.47	0.02	0.44
V	0.02	0.01	0.02	0.02	0.02	0.02	0.02	0.03	0.02
W	0.01	0.01	0.00	0.00	0.00	0.00	0.00	0.00	0.00
Zn	0.00	0.25	0.02	0.03	0.02	0.01	0.04	0.00	0.01
Si	5.98	5.72	5.62	5.47	6.45	5.60	5.88	6.09	6.93

Table G. 5 Interchange Sample Characteristics Prior/After Leaching Cycles

Test #	Sample	RG Application Method	Amount (mL)	pH	Conductivity (mS/cm)	Dry Density (pcf)
1	Collected Water	DI	30	7.40	1.240	186
	Top			8.39	116.7	
	Bottom			8.36	113.6	
2	Collected Water	DPW	30	7.40	1.620	221.5
	Top			8.62	117.9	
	Bottom			8.51	114.6	
3	Collected Water	DDI	80	7.89	2.540	186.1
	Top			8.51	118.3	
	Bottom			8.63	116.0	
4	Collected Water	DI	80	7.90	0.892	221.7
	Top			8.63	116.0	
	Bottom			8.66	117.7	
5	Collected Water	DDI	30	7.25	2.750	186.2
	Top			8.65	113.7	
	Bottom			8.72	113.8	
6	Collected Water	DPW	80	7.84	1.760	222.2
	Top			8.81	115.2	
	Bottom			8.71	115.2	
7	Collected Water	DI	130	7.94	1.073	238.3
	Top			8.64	116.6	
	Bottom			8.71	114.1	
8	Collected Water	DPW	130	7.83	1.615	221.6
	Top			8.38	116.5	
	Bottom			8.45	115.8	
9	Collected Water	DDI	130	7.97	2.610	186
	Top			8.11	113.9	
	Bottom			8.18	113.4	

Table G. 6 Interchange Top Sections Leaching Analysis

Interchange									
Concentration of Elements in mg/L									
Test No.	1	2	3	4	5	6	7	8	9
Ca	292.21	309.44	327.51	296.14	300.53	297.86	269.88	311.05	283.17
K	13.08	14.69	14.33	12.76	13.16	12.86	12.00	14.50	12.79
Mg	12.24	14.08	16.46	13.52	13.71	14.13	12.09	16.27	13.54
Na	34.06	34.22	35.39	33.62	34.72	33.99	33.72	34.50	34.27
P	0.26	0.13	0.11	0.08	0.08	0.05	0.07	0.09	0.10
As	0.05	0.02	0.05	0.02	0.06	0.00	0.07	0.00	0.03
Ba	0.67	0.76	0.75	0.59	0.67	0.72	0.54	0.78	0.58
Cd	0.01	0.02	0.02	0.02	0.02	0.02	0.02	0.03	0.02
Cr	0.01	0.01	0.01	0.01	0.01	0.01	0.00	0.00	0.00
Cu	0.24	0.13	0.14	0.12	0.14	0.11	0.11	0.12	0.13
Fe	0.00	0.00	0.00	0.00	0.00	0.00	0.00	0.00	0.00
Hg	0.05	0.04	0.03	0.02	0.03	0.03	0.05	0.04	0.02
Li	0.12	0.13	0.13	0.12	0.12	0.13	0.12	0.13	0.12
Mn	1.07	0.93	0.95	1.03	1.16	1.26	1.08	1.26	1.21
Ni	0.00	0.00	0.00	0.00	0.01	0.02	0.00	0.00	0.00
Pb	0.06	0.05	0.03	0.00	0.03	0.06	0.02	0.03	0.02
Se	0.07	0.00	0.03	0.00	0.00	0.00	0.00	0.01	0.10
Sn	0.02	0.04	0.04	0.06	0.07	0.02	0.02	0.08	0.08
Sr	1.27	1.38	1.56	1.32	1.29	1.36	1.22	1.50	1.25
U	0.00	0.00	0.00	0.00	0.00	0.01	0.01	0.02	0.04
V	0.00	0.00	0.00	0.00	0.00	0.00	0.00	0.03	0.00
W	0.00	0.03	0.00	0.00	0.00	0.00	0.00	0.00	0.00
Zn	0.09	0.10	0.23	0.10	0.13	0.17	0.11	0.10	0.10
Si	1.56	1.66	1.88	1.57	1.68	1.45	1.43	1.76	1.42

Table G. 7 Interchange Bottom Sections Leaching Analysis

Interchange									
Concentration of Elements in mg/L									
Test No.	1	2	3	4	5	6	7	8	9
Ca	291.55	327.76	303.07	280.59	284.65	273.34	261.72	280.28	301.36
K	12.31	13.46	11.94	11.45	11.42	12.09	10.43	11.83	12.07
Mg	12.60	13.69	10.96	12.04	10.70	11.98	10.81	11.88	10.23
Na	33.74	33.22	34.39	33.03	33.75	33.41	33.07	33.00	34.47
P	0.09	0.10	0.08	0.08	0.11	0.12	0.08	0.12	0.08
As	0.02	0.00	0.00	0.09	0.12	0.00	0.00	0.00	0.00
Ba	0.68	0.78	0.62	0.51	0.56	0.57	0.49	0.65	0.54
Cd	0.02	0.02	0.02	0.01	0.02	0.02	0.01	0.02	0.02
Cr	0.01	0.01	0.01	0.00	0.00	0.00	0.00	0.00	0.01
Cu	0.13	0.13	0.12	0.11	0.11	0.11	0.10	0.11	0.12
Fe	0.00	0.00	0.00	0.00	0.00	0.00	0.00	0.00	0.00
Hg	0.03	0.01	0.02	0.02	0.02	0.03	0.01	0.04	0.04
Li	0.12	0.12	0.12	0.12	0.12	0.12	0.12	0.12	0.12
Mn	0.86	0.91	0.74	0.76	1.04	1.14	0.82	0.95	0.97
Ni	0.01	0.00	0.01	0.00	0.01	0.00	0.01	0.01	0.00
Pb	0.04	0.04	0.06	0.03	0.00	0.07	0.04	0.00	0.05
Se	0.00	0.00	0.00	0.05	0.00	0.00	0.04	0.00	0.00
Sn	0.06	0.04	0.01	0.03	0.00	0.03	0.06	0.01	0.00
Sr	1.25	1.43	1.29	1.22	1.17	1.29	1.12	1.29	1.24
U	0.00	0.00	0.00	0.00	0.00	0.02	0.01	0.03	0.04
V	0.00	0.00	0.00	0.00	0.00	0.00	0.00	0.01	0.00
W	0.02	0.00	0.00	0.00	0.00	0.00	0.00	0.01	0.00
Zn	0.11	0.22	0.11	0.11	0.15	0.12	0.15	0.11	0.11
Si	1.46	1.63	1.56	1.40	1.35	1.43	1.13	1.38	1.45

Table G. 8 Interchange Collected Solutions Results

Interchange									
Concentration of Elements in mg/L									
Test No.	1	2	3	4	5	6	7	8	9
Ca	190.16	306.16	508.22	145.00	557.36	333.14	189.01	287.10	501.00
K	20.19	24.37	31.42	14.55	31.40	23.76	17.57	24.02	31.41
Mg	19.50	27.09	42.71	14.10	44.36	28.27	16.86	25.45	43.38
Na	55.41	52.18	66.58	33.84	63.93	47.24	33.52	43.94	64.87
P	0.29	0.11	0.09	0.22	0.22	0.13	0.22	0.10	0.07
As	0.04	0.05	0.03	0.03	0.03	0.04	0.05	0.04	0.03
Ba	0.11	0.44	0.21	0.18	0.26	0.51	0.30	0.54	0.19
Cd	0.00	0.00	0.00	0.00	0.00	0.00	0.00	0.00	0.00
Cr	0.00	0.00	0.00	0.00	0.00	0.00	0.00	0.00	0.00
Cu	0.32	0.13	0.10	0.25	0.26	0.15	0.25	0.12	0.09
Fe	0.00	0.02	0.00	0.00	0.00	0.00	0.00	0.01	0.00
Hg	0.00	0.00	0.00	0.00	0.00	0.00	0.00	0.00	0.00
Li	0.09	0.10	0.15	0.07	0.14	0.11	0.08	0.10	0.15
Mn	0.01	0.03	0.00	0.00	0.04	0.00	0.00	0.03	0.01
Ni	0.01	0.01	0.00	0.01	0.01	0.01	0.00	0.01	0.02
Pb	0.00	0.00	0.00	0.00	0.00	0.00	0.00	0.00	0.00
Se	0.04	0.02	0.02	0.02	0.01	0.02	0.01	0.01	0.01
Sn	0.22	0.24	0.28	0.20	0.31	0.26	0.18	0.17	0.30
Sr	1.68	2.13	3.23	1.15	3.53	2.18	1.33	1.94	3.28
U	0.00	0.03	0.00	0.00	0.00	0.01	0.00	0.01	0.01
V	0.02	0.02	0.03	0.02	0.03	0.02	0.03	0.03	0.03
W	0.00	0.00	0.00	0.00	0.00	0.00	0.00	0.00	0.00
Zn	0.08	0.04	0.04	0.07	0.12	0.05	0.07	0.05	0.07
Si	5.10	5.87	4.64	4.80	5.06	4.86	5.07	4.92	5.02

Table G. 9 Westbound Sample Characteristics Prior/After Leaching Cycles

Test #	Sample	Water Type	Amount (mL)	pH	Conductivity (mS/cm)	Dry Density (pcf)
1	Collected Water	DI	30	7.24	3.67	187
	Top			8.83	115.00	
	Bottom			8.91	116.10	
2	Collected Water	DPW	30	6.61	3.29	220.5
	Top			8.99	116.10	
	Bottom			8.88	115.10	
3	Collected Water	DDI	80	7.73	3.74	186.8
	Top			8.93	114.70	
	Bottom			9.04	114.90	
4	Collected Water	DI	80	7.09	3.28	221
	Top			8.81	114.40	
	Bottom			8.81	116.00	
5	Collected Water	DDI	30	7.21	3.79	186.7
	Top			8.97	116.50	
	Bottom			8.61	113.60	
6	Collected Water	DPW	80	7.43	3.30	221.4
	Top			8.68	116.20	
	Bottom			8.76	117.80	
7	Collected Water	DI	130	7.25	3.38	186.6
	Top			8.95	115.70	
	Bottom			8.83	114.90	
8	Collected Water	DPW	130	7.36	3.21	221
	Top			8.93	114.20	
	Bottom			8.8	113.90	
9	Collected Water	DDI	130	7.35	3.55	186.7
	Top			8.72	113.60	
	Bottom			8.77	116.70	

Table G. 10 Westbound Top Sections Leaching Analysis

Westbound									
Concentration of Elements in mg/L									
Test No.	1	2	3	4	5	6	7	8	9
Ca	487.25	397.72	500.13	437.13	417.34	409.76	449.74	470.20	448.00
K	15.41	12.46	15.51	13.20	14.37	13.62	19.07	14.29	14.14
Mg	14.37	11.52	13.15	12.19	12.86	12.78	13.12	13.31	13.89
Na	35.51	35.14	36.07	34.92	36.36	35.16	34.85	34.30	35.22
P	0.05	0.05	0.04	0.04	0.06	0.04	0.03	0.06	0.03
As	0.09	0.08	0.00	0.09	0.01	0.01	0.02	0.00	0.00
Ba	0.38	0.39	0.37	0.36	0.33	0.36	0.40	0.45	0.43
Cd	0.01	0.01	0.01	0.01	0.01	0.01	0.00	0.01	0.01
Cr	0.01	0.01	0.01	0.01	0.01	0.01	0.01	0.01	0.01
Cu	0.07	0.06	0.05	0.05	0.08	0.07	0.07	0.10	0.05
Fe	0.00	0.00	0.00	0.00	0.00	0.00	0.00	0.00	0.00
Hg	0.04	0.04	0.04	0.03	0.06	0.04	0.08	0.04	0.04
Li	0.13	0.13	0.13	0.13	0.13	0.13	0.13	0.13	0.13
Mn	0.72	0.60	0.71	0.68	0.66	0.65	0.72	0.73	0.77
Ni	0.01	0.01	0.02	0.00	0.01	0.01	0.02	0.01	0.02
Pb	0.02	0.02	0.01	0.05	0.06	0.03	0.05	0.00	0.00
Se	0.00	0.00	0.00	0.00	0.00	0.00	0.05	0.02	0.00
Sn	0.00	0.00	0.00	0.00	0.01	0.02	0.05	0.00	0.04
Sr	2.06	1.64	1.94	1.73	1.77	1.79	1.74	1.81	1.79
U	0.05	0.07	0.08	0.06	0.04	0.06	0.00	0.00	0.00
V	0.13	0.12	0.11	0.11	0.08	0.10	0.00	0.00	0.00
W	0.00	0.01	0.00	0.00	0.01	0.01	0.07	0.02	0.00
Zn	0.11	0.09	0.12	0.10	0.12	0.12	0.10	0.08	0.14
Si	1.22	1.09	1.25	1.16	1.15	1.25	1.31	1.24	1.24

Table G. 11 Westbound Bottom Sections Leaching Analysis

Westbound									
Concentration of Elements in mg/L									
Test No.	1	2	3	4	5	6	7	8	9
Ca	359.87	383.52	453.41	406.85	468.34	414.66	443.78	424.74	404.48
K	11.04	11.08	13.01	11.99	13.32	13.07	14.20	13.10	10.78
Mg	7.53	7.49	8.16	8.30	8.71	8.08	9.37	7.75	6.20
Na	34.83	34.48	36.16	34.85	35.99	35.09	34.11	34.17	34.85
P	0.03	0.01	0.01	0.02	0.05	0.08	0.02	0.03	0.03
As	0.00	0.04	0.03	0.11	0.00	0.06	0.13	0.14	0.06
Ba	0.40	0.36	0.37	0.42	0.38	0.39	0.44	0.39	0.34
Cd	0.01	0.01	0.01	0.01	0.01	0.01	0.01	0.01	0.00
Cr	0.01	0.01	0.01	0.01	0.01	0.02	0.01	0.01	0.01
Cu	0.07	0.05	0.05	0.06	0.06	0.08	0.06	0.04	0.04
Fe	0.00	0.00	0.00	0.00	0.00	0.00	0.00	0.00	0.00
Hg	0.04	0.05	0.03	0.05	0.05	0.10	0.05	0.05	0.06
Li	0.12	0.12	0.13	0.12	0.13	0.13	0.13	0.13	0.12
Mn	0.62	0.62	0.68	0.62	0.67	0.66	0.78	0.69	0.69
Ni	0.01	0.00	0.01	0.00	0.02	0.02	0.00	0.00	0.01
Pb	0.03	0.04	0.00	0.00	0.00	0.04	0.01	0.01	0.03
Se	0.00	0.00	0.04	0.00	0.01	0.01	0.01	0.00	0.03
Sn	0.00	0.00	0.00	0.00	0.00	0.00	0.00	0.00	0.00
Sr	1.38	1.48	1.84	1.53	1.86	1.60	1.60	1.60	1.48
U	0.07	0.04	0.06	0.06	0.05	0.00	0.00	0.00	0.00
V	0.14	0.09	0.12	0.14	0.11	0.00	0.00	0.00	0.00
W	0.00	0.00	0.00	0.00	0.00	0.15	0.03	0.03	0.00
Zn	0.12	0.11	0.09	0.13	0.09	0.13	0.08	0.09	0.06
Si	1.13	1.19	1.25	1.24	1.26	1.08	1.22	1.16	1.02

Table G. 12 Westbound Collected Solutions Results

Westbound									
Concentration of Elements in mg/L									
Test No.	1	2	3	4	5	6	7	8	9
Ca	645.02	608.68	656.46	614.49	645.00	610.60	610.57	628.88	633.38
K	45.80	44.46	46.43	44.55	46.21	45.08	42.40	41.72	44.75
Mg	63.02	61.61	62.02	61.83	64.70	61.56	61.25	60.61	60.62
Na	80.25	73.38	79.73	64.38	81.14	64.95	58.91	55.61	75.36
P	0.12	0.06	0.11	0.05	0.10	0.05	0.10	0.04	0.10
As	0.01	0.00	0.02	0.01	0.02	0.02	0.02	0.00	0.00
Ba	0.08	0.10	0.09	0.10	0.08	0.10	0.08	0.09	0.09
Cd	0.00	0.00	0.00	0.00	0.00	0.00	0.00	0.00	0.00
Cr	0.00	0.00	0.00	0.00	0.00	0.00	0.00	0.00	0.00
Cu	0.14	0.06	0.12	0.05	0.12	0.05	0.11	0.04	0.11
Fe	0.01	0.02	0.00	0.00	0.01	0.00	0.00	0.00	0.00
Hg	0.00	0.00	0.00	0.00	0.00	0.00	0.00	0.00	0.00
Li	0.27	0.25	0.26	0.23	0.27	0.24	0.22	0.21	0.24
Mn	0.14	0.12	0.06	0.07	0.06	0.03	0.02	0.02	0.06
Ni	0.01	0.01	0.01	0.01	0.01	0.01	0.01	0.01	0.01
Pb	0.01	0.00	0.00	0.00	0.00	0.01	0.00	0.00	0.00
Se	0.00	0.01	0.02	0.00	0.01	0.00	0.00	0.01	0.00
Sn	0.30	0.30	0.27	0.28	0.28	0.27	0.28	0.27	0.27
Sr	4.42	4.17	4.55	4.20	4.51	4.24	4.21	4.09	4.47
U	0.01	0.02	0.00	0.00	0.01	0.00	0.00	0.00	0.00
V	0.02	0.03	0.02	0.02	0.03	0.02	0.02	0.01	0.02
W	0.00	0.00	0.00	0.00	0.00	0.00	0.00	0.00	0.00
Zn	0.13	0.09	0.10	0.07	0.10	0.07	0.10	0.06	0.11
Si	5.59	5.32	5.90	5.07	5.90	5.19	5.46	5.04	5.88

Table G. 13 Site Sample Characteristics Prior/After Leaching Cycles

Test #	Sample	Water Type	Amount (mL)	pH	Conductivity (mS/cm)	Dry Density (pcf)
1	Collected Water	DI	30	6.78	3.26	221.9
	Top			8.77	116.7	
	Bottom			8.53	114.4	
2	Collected Water	DPW	30	6.89	3.67	186.4
	Top			8.70	113.1	
	Bottom			8.83	113.2	
3	Collected Water	DDI	30	6.72	3.55	221.7
	Top			8.81	116.9	
	Bottom			8.66	113.0	
4	Collected Water	DI	80	7.67	3.62	186.7
	Top			8.77	114.8	
	Bottom			8.79	115.0	
5	Collected Water	DPW	80	7.25	3.36	221
	Top			9.00	116.6	
	Bottom			8.92	116.1	
6	Collected Water	DDI	130	7.62	3.61	186.7
	Top			8.94	116.4	
	Bottom			9.00	116.9	
7	Collected Water	DI	130	7.52	3.32	221.4
	Top			8.89	116.1	
	Bottom			8.92	115.5	
8	Collected Water	DDI	80	6.91	3.73	186.8
	Top			8.78	115.3	
	Bottom			8.67	116.1	
9	Collected Water	DPW	130	7.66	3.49	186.2
	Top			8.41	112.9	
	Bottom			8.48	114.1	

Table G. 14 Site Top Sections Leaching Analysis

Site Pond									
Concentration of Elements in mg/L									
Test No.	1	2	3	4	5	6	7	8	9
Ca	527.12	513.90	525.71	543.24	540.12	566.33	522.06	546.28	513.70
K	10.12	9.77	10.48	10.83	10.67	12.15	11.41	10.59	9.35
Mg	7.41	7.32	8.04	8.64	8.31	8.96	7.77	7.96	5.30
Na	36.07	35.41	36.88	36.14	35.71	36.76	34.83	36.47	34.12
P	0.02	0.01	0.05	0.01	0.05	0.05	0.05	0.06	0.03
As	0.09	0.04	0.03	0.02	0.06	0.04	0.07	0.09	0.01
Ba	0.30	0.31	0.38	0.44	0.41	0.36	0.33	0.34	0.41
Cd	0.00	0.00	0.01	0.00	0.00	0.01	0.01	0.01	0.00
Cr	0.04	0.03	0.02	0.02	0.02	0.01	0.01	0.01	0.01
Cu	0.05	0.04	0.06	0.06	0.05	0.05	0.04	0.05	0.05
Fe	0.15	0.09	0.04	0.02	0.01	0.00	0.00	0.00	0.00
Hg	0.07	0.06	0.07	0.06	0.05	0.05	0.05	0.03	0.06
Li	0.12	0.12	0.12	0.12	0.12	0.13	0.12	0.12	0.12
Mn	0.67	0.74	0.80	0.91	0.83	0.93	0.80	0.89	0.78
Ni	0.01	0.02	0.00	0.02	0.01	0.01	0.01	0.01	0.00
Pb	0.02	0.05	0.05	0.03	0.06	0.02	0.02	0.07	0.06
Se	0.00	0.07	0.00	0.00	0.00	0.00	0.00	0.06	0.00
Sn	0.00	0.00	0.00	0.00	0.00	0.00	0.00	0.00	0.00
Sr	1.68	1.68	1.76	1.86	1.83	1.91	1.72	1.76	1.71
U	0.26	0.19	0.14	0.11	0.11	0.09	0.08	0.07	0.06
V	0.17	0.16	0.17	0.15	0.11	0.16	0.13	0.13	0.12
W	0.00	0.04	0.00	0.01	0.02	0.00	0.02	0.01	0.03
Zn	0.08	0.11	0.10	0.16	0.09	0.10	0.09	0.09	0.09
Si	1.08	0.85	0.90	0.98	1.01	0.94	0.91	0.94	1.08

Table G. 15 Westbound Bottom Sections Leaching Analysis

Site Pond									
Concentration of Elements in mg/L									
Test No.	1	2	3	4	5	6	7	8	9
Ca	464.34	496.98	521.53	475.21	520.00	544.99	485.15	610.84	523.09
K	8.29	9.38	8.48	8.49	9.27	9.13	8.70	9.93	10.32
Mg	4.71	5.35	5.29	4.92	5.23	5.18	4.80	6.04	7.95
Na	34.21	34.56	35.67	34.43	34.61	35.26	34.11	35.92	35.65
P	0.04	0.02	0.04	0.06	0.02	0.05	0.05	0.06	0.03
As	0.06	0.00	0.07	0.07	0.00	0.02	0.05	0.17	0.04
Ba	0.33	0.35	0.37	0.38	0.37	0.33	0.35	0.45	0.41
Cd	0.00	0.01	0.00	0.00	0.01	0.00	0.00	0.00	0.01
Cr	0.03	0.03	0.02	0.02	0.01	0.02	0.01	0.01	0.01
Cu	0.04	0.05	0.05	0.05	0.04	0.05	0.04	0.05	0.05
Fe	0.09	0.06	0.03	0.02	0.00	0.00	0.00	0.00	0.00
Hg	0.04	0.04	0.02	0.06	0.05	0.05	0.03	0.03	0.05
Li	0.12	0.12	0.12	0.12	0.12	0.12	0.12	0.12	0.12
Mn	0.59	0.71	0.72	0.75	0.66	0.73	0.65	0.81	0.85
Ni	0.02	0.00	0.01	0.01	0.01	0.00	0.01	0.02	0.01
Pb	0.04	0.02	0.00	0.03	0.04	0.02	0.02	0.05	0.05
Se	0.09	0.00	0.05	0.00	0.11	0.00	0.10	0.04	0.01
Sn	0.00	0.00	0.00	0.00	0.00	0.00	0.00	0.00	0.00
Sr	1.38	1.64	1.65	1.44	1.69	1.75	1.51	2.00	1.76
U	0.17	0.16	0.13	0.12	0.09	0.07	0.08	0.07	0.08
V	0.18	0.21	0.10	0.10	0.13	0.15	0.14	0.14	0.14
W	0.00	0.02	0.00	0.02	0.00	0.00	0.00	0.02	0.00
Zn	0.16	0.11	0.12	0.08	0.07	0.07	0.07	0.13	0.10
Si	0.87	0.99	1.00	0.99	0.98	0.97	0.87	1.09	1.01

Table G. 16 Site Collected Solutions Results

Site Pond									
Concentration of Elements in mg/L									
Test No.	1	2	3	4	5	6	7	8	9
Ca	608.58	628.60	633.16	637.97	604.90	633.69	600.98	637.46	634.57
K	42.47	45.90	47.46	48.96	47.60	48.62	44.65	47.55	46.82
Mg	43.56	47.88	46.72	47.56	45.68	46.72	45.61	47.40	46.10
Na	159.34	206.39	196.67	193.41	173.67	182.62	166.61	207.54	168.80
P	0.08	0.27	0.09	0.17	0.08	0.14	0.08	0.16	0.14
As	0.02	0.02	0.01	0.03	0.04	0.03	0.02	0.01	0.02
Ba	0.14	0.13	0.18	0.11	0.13	0.11	0.12	0.11	0.11
Cd	0.00	0.00	0.00	0.00	0.00	0.00	0.00	0.00	0.00
Cr	0.00	0.00	0.00	0.00	0.00	0.00	0.00	0.00	0.00
Cu	0.09	0.32	0.10	0.20	0.10	0.17	0.10	0.19	0.17
Fe	0.03	0.01	0.00	0.00	0.01	0.00	0.00	0.00	0.00
Hg	0.00	0.00	0.00	0.00	0.00	0.00	0.00	0.00	0.00
Li	0.20	0.24	0.24	0.24	0.22	0.22	0.21	0.24	0.21
Mn	0.26	0.34	0.28	0.11	0.21	0.22	0.23	0.21	0.18
Ni	0.01	0.01	0.01	0.01	0.01	0.01	0.01	0.01	0.01
Pb	0.00	0.00	0.00	0.00	0.00	0.00	0.01	0.00	0.00
Se	0.01	0.01	0.02	0.02	0.01	0.01	0.00	0.00	0.01
Sn	0.24	0.25	0.23	0.23	0.24	0.23	0.23	0.22	0.22
Sr	3.48	3.83	3.83	3.88	3.73	3.86	3.68	3.90	3.88
U	0.04	0.01	0.01	0.00	0.01	0.00	0.01	0.00	0.01
V	0.02	0.02	0.02	0.03	0.03	0.03	0.03	0.03	0.03
W	0.00	-0.01	0.00	0.00	0.00	0.00	0.00	0.00	0.00
Zn	0.07	0.09	0.06	0.07	0.06	0.08	0.06	0.08	0.07
Si	3.31	3.26	3.60	3.35	3.50	3.82	3.28	3.93	3.51

Interchange compacted clay results

Table G. 17 Compacted Interchange Clay Top Section Leaching Analysis

Concentration of Elements in mg/L									
Test No.	1	2	3	4	5	6	7	8	9
Ca	312.89	304.02	294.27	294.25	320.39	308.39	310.32	321.57	319.74
K	15.79	13.44	14.80	15.25	15.78	15.27	15.29	15.14	13.63
Mg	17.37	15.19	15.90	16.78	17.20	16.68	16.34	16.63	15.63
Na	121.46	119.86	119.46	118.88	122.16	122.69	123.61	126.37	129.70
P	0.11	0.13	0.09	0.08	0.02	0.09	0.14	0.08	0.09
As	0.00	0.02	0.00	0.00	0.05	0.00	0.01	0.00	0.09
Ba	2.11	1.61	1.53	1.61	2.04	2.09	1.90	2.06	2.04
Cd	0.02	0.02	0.12	0.19	0.11	0.13	0.13	0.13	0.11
Cr	0.00	0.01	0.00	0.01	0.00	0.00	0.00	0.01	0.00
Cu	0.13	0.10	0.11	0.11	0.08	0.11	0.14	0.11	0.12
Fe	0.00	0.00	0.00	0.00	0.00	0.00	0.00	0.00	0.00
Hg	0.04	0.04	0.03	0.02	0.02	0.04	0.03	0.02	0.01
Li	0.13	0.12	0.13	0.13	0.13	0.13	0.12	0.13	0.12
Mn	0.48	0.41	0.58	0.42	0.16	0.28	0.58	0.30	0.46
Ni	0.00	0.01	0.00	0.01	0.00	0.01	0.02	0.01	0.02
Pb	0.04	0.06	0.02	0.06	0.04	0.00	0.00	0.01	0.01
Se	0.01	0.00	0.00	0.00	0.07	0.02	0.00	0.05	0.03
Sn	0.05	0.05	0.07	0.05	0.06	0.09	0.07	0.05	0.04
Sr	1.42	1.25	1.26	1.35	1.41	1.43	1.39	1.43	1.35
U	0.05	0.11	0.17	0.24	0.34	0.48	0.55	0.52	0.52
V	0.00	0.00	0.00	0.01	0.00	0.00	0.00	0.00	0.00
W	0.01	0.01	0.00	0.03	0.00	0.00	0.00	0.00	0.02
Zn	1.95	0.44	1.84	1.60	0.05	0.28	0.30	0.15	0.15
Si	1.58	1.11	1.35	1.47	1.55	1.69	1.33	1.60	1.52

Table G. 18 Compacted Interchange Clay Middle Section Leaching Analysis

Concentration of Elements in mg/L									
Test No.	1	2	3	4	5	6	7	8	9
Ca	332.66	302.06	297.89	354.87	314.50	297.83	317.09	304.41	312.11
K	17.65	14.64	15.26	17.58	15.79	13.48	15.20	13.71	13.41
Mg	18.10	15.70	15.94	19.44	17.31	14.25	16.22	15.03	15.43
Na	121.19	121.21	122.79	122.83	120.11	126.63	120.84	116.72	121.95
P	0.04	0.03	0.06	0.07	0.09	0.03	0.07	0.05	0.08
As	0.05	0.05	0.00	0.00	0.05	0.10	0.05	0.02	0.08
Ba	2.43	1.80	1.81	2.40	2.05	1.60	1.86	1.67	1.98
Cd	0.01	0.02	0.12	0.13	0.14	0.09	0.10	0.09	0.15
Cr	0.01	0.01	0.01	0.00	0.01	0.00	0.01	0.00	0.00
Cu	0.09	0.07	0.11	0.10	0.09	0.07	0.11	0.08	0.09
Fe	0.00	0.00	0.00	0.00	0.00	0.00	0.00	0.00	0.00
Hg	0.06	0.03	0.01	0.00	0.03	0.02	0.03	0.05	0.01
Li	0.13	0.13	0.13	0.13	0.13	0.12	0.12	0.12	0.12
Mn	0.29	0.23	0.25	0.21	0.23	0.48	0.73	0.50	0.41
Ni	0.01	0.01	0.01	0.02	0.01	0.00	0.01	0.00	0.00
Pb	0.02	0.08	0.00	0.02	0.02	0.04	0.02	0.05	0.04
Se	0.05	0.00	0.01	0.00	0.00	0.00	0.00	0.00	0.00
Sn	0.05	0.07	0.02	0.07	0.06	0.06	0.12	0.05	0.03
Sr	1.53	1.34	1.35	1.61	1.44	1.24	1.33	1.31	1.30
U	0.07	0.13	0.18	0.26	0.40	0.53	0.51	0.51	0.51
V	0.00	0.01	0.00	0.01	0.00	0.00	0.00	0.00	0.00
W	0.00	0.03	0.00	0.00	0.01	0.00	0.00	0.00	0.02
Zn	0.10	0.08	0.30	0.26	0.11	0.08	0.18	0.03	0.08
Si	1.78	1.28	1.42	1.89	1.41	1.31	1.32	1.41	1.54

Table G. 19 Compacted Interchange Clay Bottom Section Leaching Analysis

Concentration of Elements in mg/L									
Test No.	1	2	3	4	5	6	7	8	9
Ca	299.95	303.67	287.10	359.65	318.41	337.55	307.12	314.33	313.16
K	13.70	13.77	14.59	19.19	16.52	16.94	14.92	14.91	14.48
Mg	15.49	15.17	15.78	21.59	17.30	18.69	16.62	16.56	17.31
Na	125.04	119.62	119.84	115.22	122.42	127.61	124.29	120.04	124.99
P	0.10	0.07	0.08	0.10	0.06	0.09	0.26	0.11	0.17
As	0.00	0.04	0.00	0.03	0.15	0.09	0.06	0.02	0.06
Ba	2.00	1.71	1.87	2.36	1.69	2.62	2.20	2.05	2.10
Cd	0.02	0.02	0.11	0.18	0.11	0.12	0.13	0.11	0.15
Cr	0.00	0.00	0.01	0.01	0.01	0.00	0.01	0.01	0.01
Cu	0.11	0.09	0.10	0.13	0.06	0.12	0.27	0.13	0.17
Fe	0.00	0.00	0.00	0.00	0.00	0.00	0.00	0.00	0.00
Hg	0.01	0.04	0.00	0.02	0.04	0.03	0.01	0.00	0.02
Li	0.12	0.12	0.13	0.13	0.13	0.13	0.13	0.12	0.13
Mn	0.78	0.59	0.52	0.37	0.17	0.81	1.23	0.99	1.11
Ni	0.01	0.01	0.01	0.01	0.01	0.01	0.01	0.01	0.00
Pb	0.02	0.08	0.01	0.00	0.06	0.00	0.04	0.03	0.04
Se	0.00	0.00	0.00	0.00	0.00	0.00	0.02	0.00	0.00
Sn	0.05	0.05	0.09	0.10	0.06	0.07	0.05	0.07	0.09
Sr	1.28	1.29	1.28	1.71	1.43	1.55	1.40	1.40	1.42
U	0.17	0.14	0.22	0.28	0.45	0.53	0.50	0.50	0.51
V	0.00	0.00	0.01	0.03	0.00	0.00	0.00	0.00	0.00
W	0.01	0.00	0.00	0.00	0.00	0.00	0.00	0.00	0.00
Zn	0.39	0.10	0.87	1.69	0.03	0.10	1.30	0.14	0.14
Si	1.37	1.06	1.50	1.95	1.40	1.82	1.53	1.29	1.46

Table G. 20 Compacted Interchange Clay Collected Solution in Leaching Analysis

Concentration of Elements in mg/L									
Test No.	1	2	3	4	5	6	7	8	9
Ca	138.58	90.12	82.33	91.49	114.11	54.94	56.31	68.29	76.37
K	16.32	7.60	10.53	18.45	22.51	12.97	10.80	8.30	10.14
Mg	32.94	10.37	21.24	26.78	45.83	28.98	21.57	18.46	26.08
Na	55.23	37.52	45.13	56.26	174.25	62.74	83.42	44.16	51.65
P	0.02	0.02	0.01	0.04	0.49	0.02	0.08	0.02	0.02
As	0.01	0.02	0.03	0.00	0.16	0.02	0.04	0.00	0.01
Ba	0.15	0.23	0.18	0.16	0.12	0.11	0.10	0.15	0.14
Cd	0.00	0.00	0.00	0.00	0.00	0.00	0.00	0.00	0.00
Cr	0.00	0.00	0.00	1.13	35.36	0.01	2.32	0.02	0.01
Cu	0.02	0.02	0.03	0.06	0.50	0.03	0.07	0.03	0.03
Fe	0.02	0.00	0.00	3.08	73.72	0.04	6.01	0.08	0.02
Hg	0.00	0.00	0.01	0.01	0.13	0.01	0.03	0.01	0.00
Li	0.11	0.05	0.08	0.11	0.53	0.08	0.15	0.07	0.07
Mn	0.01	0.72	0.01	0.01	0.27	0.04	0.05	0.02	0.25
Ni	0.08	0.11	0.15	0.39	8.23	0.37	0.89	0.63	0.98
Pb	0.01	0.00	0.03	0.00	0.00	0.00	0.00	0.01	0.01
Se	0.00	0.00	0.00	0.00	0.35	0.02	0.02	0.00	0.01
Sn	0.24	0.10	0.19	0.25	0.47	0.25	0.20	0.19	0.22
Sr	1.47	0.78	1.15	1.31	1.63	0.98	0.84	0.86	1.09
U	0.04	0.00	0.03	2.65	62.85	0.07	5.52	0.12	0.05
V	0.03	0.03	0.08	0.10	0.87	0.05	0.00	0.00	0.05
W	0.00	0.00	0.00	0.00	0.05	0.00	0.00	0.00	0.00
Zn	0.09	0.60	0.08	0.06	0.00	0.14	0.08	0.03	0.11
Si	9.47	6.87	11.19	9.66	14.20	15.19	8.55	8.71	14.40

APPENDIX H: PROPOSED FANS IN THE MARKET

Platform:
Length..... ..9"
Width..... 4' 9"
Height..... 4' 5"
Total Weight.....1069 lbs
Draft..... 8 inches
Pontoons: Ultra High Molecular Polyethylene
Modular/Foam Filled
Excavation:
Excavation Depth: 25 feet max
Excavation Speed: 0-50 feet
Pump:
Type: Severe Duty Submersible Slurry
With High Chrome Iron Wear Parts
Motor: 10 hp, 1750 RPM, 460v.
1.35 Service Factor

Max. Spherical Solids: 1 inch
Percent solids by weight: 70% Maximum
Control Panel (Automation Optional):
Power: 460v, 3 phase, 60 hz
Manual push button w/indicator lights
Main pump on/off, hoist up/down, traverse fwd/off/rev.
Main circuit breaker
Separate breakers for each branched circuit
Magnetic contactors w/overloads & reset push buttons
Fused 120v control circuit
NEMA 3R enclosure
Urethane powder coated finish
Hoist Winch:
1 hp, TEFC, 230/460 VAC
Speed: 11 feet per minute
Load rating: 2000 lbs
Miscellaneous:
Four corner lifting eyes & single point pickup
Oven baked urethane powder coated finish
304 stainless steel fasteners
Special tools: none required

www.piranhapump.com

Equipment Specialties Co.
Solids Removal Systems
(505) 822-0449

P-10M Piranha Dredge

Remote Controlled Solids Removal Pumping System
Manual & Automated Controls

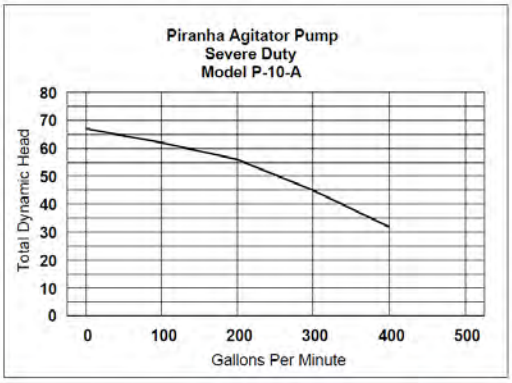

Figure H. 1 Piranha Remote Controlled Dredge Model Pump

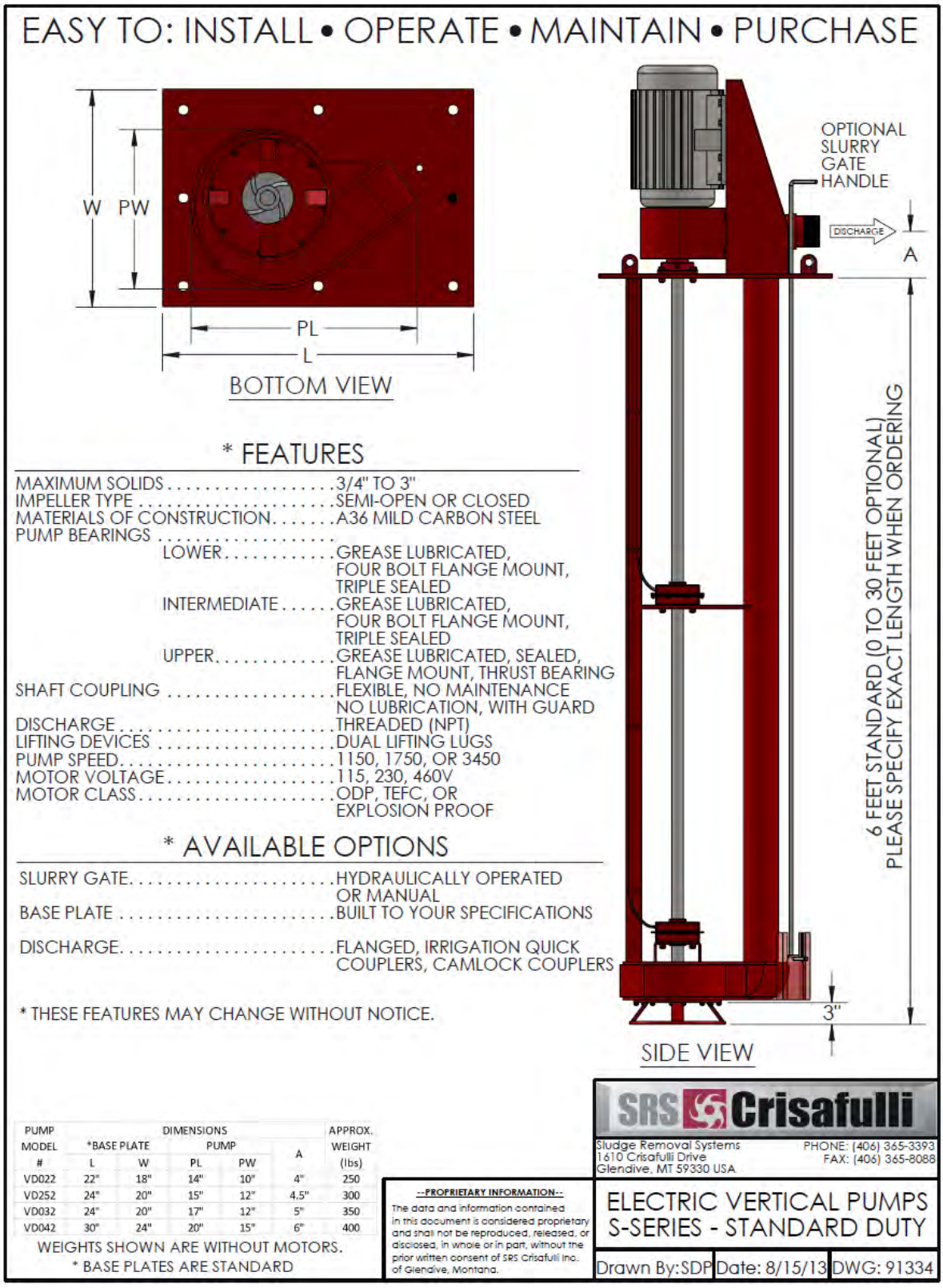

Figure H. 2: Vertical Pump S-Series

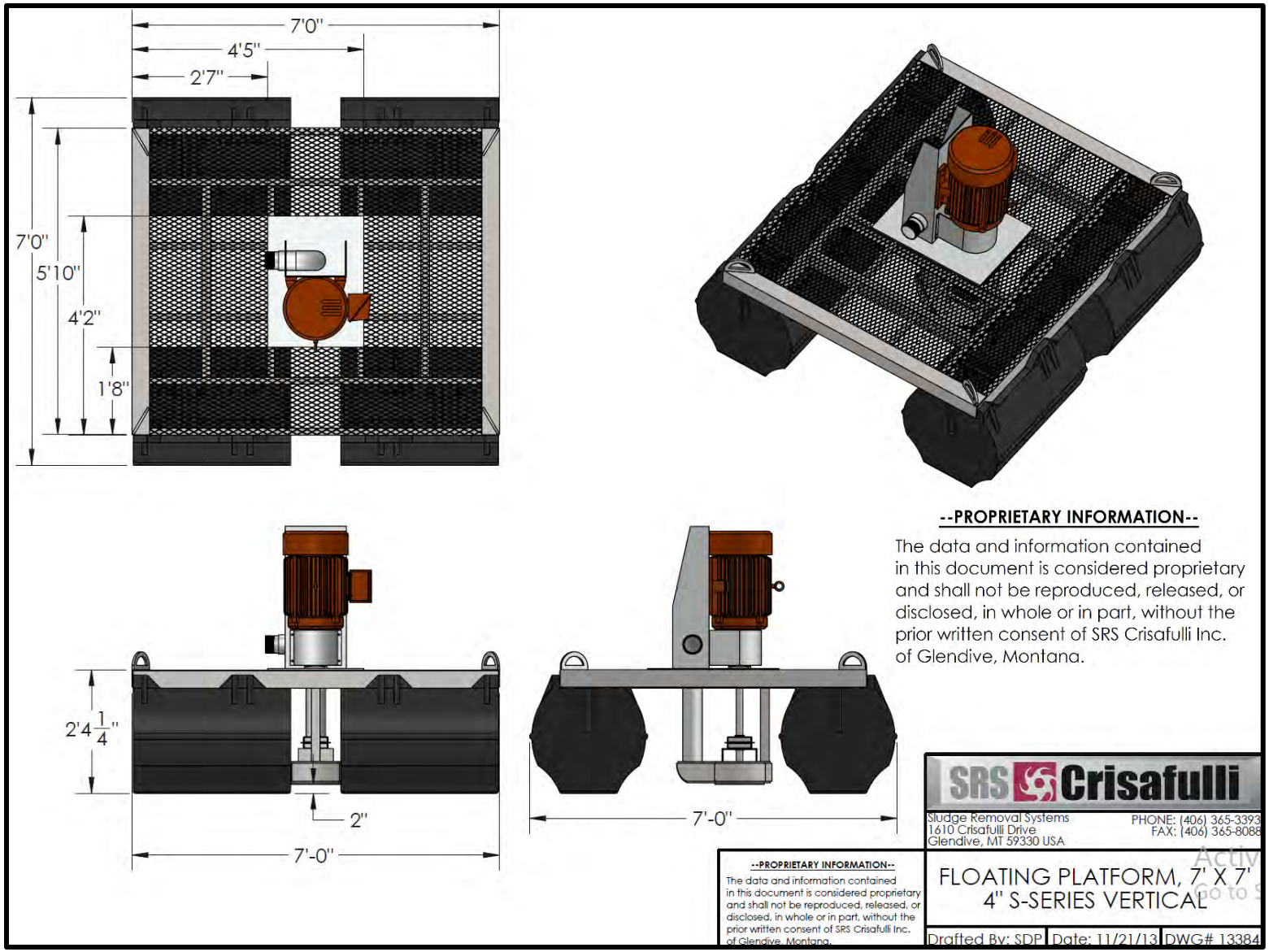

Figure H. 3 Floating Platform for Vertical Pumps-Series

CURRICULUM VITA

Jorge Navarrete earned his Bachelor of Science in Civil Engineering from The University of Texas at El Paso in Spring 2016. Immediately after that, Jorge joined the master's graduate program in Civil Engineering at UTEP. He worked as a Teaching Assistance two courses, twice for Civil Engineering Materials course and once for Reinforced Concrete Design.

As part of his graduate career, Jorge was the recipient of Dwight David Eisenhower Transportation Fellowship that granted him the ability to attend the Transportation Research Board (TRB) annual meeting in 2016 and 2017.

Jorge's thesis entitled, "Evaluation of Recycled Gypsum Application Dosages to Enhance the Water Infiltration Rate at Water Retention Ponds" and was supervised by Dr. Vivek Tandon. This research project worked was financed by El Paso Water.

Permanent address: P.O. BOX 204
FORT HANCOCK, TX 79839

This thesis was typed by Jorge Luis Navarrete.